Prognostic and Diagnostic Markers in the Renal (Transplant) Biopsy

Malou Snijders

Prognostic and Diagnostic Markers

in the Renal (Transplant) Biopsy

Cover design: J.F.B. Snijders & GVO drukkers en vormgevers B.V.

Printed by: GVO drukkers en vormgevers B.V.

The work of this thesis was conducted at the Department of Pathology of the Erasmus MC University Medical Center, Rotterdam, The Netherlands.

Prognostic and Diagnostic Markers
in the Renal (Transplant) Biopsy

Prognostische en diagnostische markers

in nier (transplantaat) biopten

PROEFSCHRIFT

ter verkrijging van de graad van doctor aan de

Erasmus Universiteit Rotterdam

op gezag van de rector magnificus

Prof. dr. R.C.M.E. Engels

en volgens besluit van het College voor Promoties.

De openbare verdediging zal plaatsvinden op

donderdag 29 oktober 2020 om 13.30 uur

door

Marina Louise Helena Snijders

geboren te 's-Gravenhage

Erasmus University Rotterdam

Promotiecommissie

Promotor: Prof. dr. F.J. van Kemenade

Overige leden: Prof. dr. C.C. Baan
Prof. dr. S.P. Berger
Dr. J.J.T.H. Roelofs

Co-promotoren: Dr. M.C. Clahsen-van Groningen
Dr. D.A. Hesselink

Cogito ergo sum

-René Descartes

Contents

CHAPTER 1

General Introduction

The kidneys' main function is to maintain the body's homeostasis. They maintain fluid, acid-base and electrolyte balance and produce several hormones, including erythropoietin. In patients with chronic kidney disease (CKD), the kidneys have lost (part of) their filtering capacity.[1] End-stage renal disease (ESRD; CKD stage 5, defined by an estimated glomerular filtration rate (eGFR) of less than 15 mL/min per 1.73 m^2 or the need for renal replacement therapy) is a life-threatening condition as patients are at risk of imminent death from fluid overload or electrolyte and pH disturbances.[2, 3] Patients with ESRD can be treated with either dialysis (hemodialysis or peritoneal dialysis) or kidney transplantation. Kidney transplantation is the preferred treatment, as it provides longer patient survival and better quality of life for most patients when compared to dialysis.[4]

The first successful kidney transplantation was performed in Boston in 1954 by the team of Joseph Murray.[5] This procedure was performed between identical twins and therefore there was no need to suppress the recipient's immune system in order to prevent rejection of the graft. As most renal transplant candidates will not have a genetically identical kidney donor, prevention of rejection is essential. Under such conditions, the immune system of the recipient will recognize the transplanted organ as foreign which will lead to an immune response directed against the cells of the donor kidney (the so-called alloimmune response) causing destruction of the graft. Allograft recognition and rejection is mediated by complex immunologic pathways which can generally be subdivided into cellular (T cell-mediated) and humoral (antibody/B cell-mediated) pathways.[6, 7] The discovery of the first immunosuppressive drugs in the 1960's and the subsequent evolution of pharmacological immunosuppression ever since, have significantly increased allograft survival. However, it is the short-term graft survival that has improved most, whereas the long-term kidney transplantation results have not improved to a similar degree.[8-10] Acute rejection remains an important problem in kidney transplantation with significant effects on long-term graft outcomes.

Although kidney transplantation has become an accepted therapy with good results, there remains room for further improvement. There is a need to better understand the pathophysiology of renal transplant failure and to improve transplant injury diagnostics. Accurately determining risk factors associated with both short- and long-term renal allograft failure is essential to develop effective interventions that can either prevent, treat or slow the progression of kidney transplant failure. A core renal biopsy for histological evaluation is considered the gold standard to analyze renal function impairment after renal transplantation and is an important

tool in the identification of possible risk factors for graft failure.[11, 12] The aim of this thesis is to identify potential important pathologic variables in kidney biopsies and their association with the risk of impaired renal transplant function.

1. Renal transplantation

In the Netherlands, 998 patients received a kidney transplant in 2018.[13] The diseases most commonly leading to renal failure and treated by kidney transplantation are diabetes mellitus, hypertension and glomerulonephritis.[14, 15] Donor kidneys can be derived from deceased donors (either donation after brain death or donation after circulatory death) and living donors (either related or non-related). Living donation provides a better allograft survival when compared to deceased-donor transplantation.[16]

An important factor influencing graft function is the extent of ischemic injury during kidney transplant surgery. The warm ischemia time describes ischemia of cells under normothermic conditions: the time between circulatory arrest and cold perfusion (first warm ischemia time) and the time from removal of the donor kidney from ice until reperfusion (second warm ischemia time).[17] The cold ischemia time is the storage time of the donor kidney in cold solution to preserve the viability of its cells. Optimal function of donor kidneys is achieved when the cold ischemia time is kept as short as possible.[18, 19] In most cases the native kidneys are not removed during surgery and the donor kidney is usually placed in the iliac fossa. The renal artery and vein are anastomosed to the iliac vessels and the ureter is anastomosed to the bladder.[20]

2. The renal biopsy

Kidney function after transplantation is evaluated by serum creatinine, urinary sediment and protein concentration, and core renal biopsy.[21] A core renal biopsy is an important diagnostic tool for nephrologists and can aid in diagnosing the cause of renal function loss and may also guide treatment.[22] Renal transplant biopsies can be used to diagnose the type and severity of rejection, but also to reveal other causes of renal inflammation and injury, like BK virus nephropathy, pyelonephritis, interstitial nephritis or recurrence of the primary kidney disease. It has been shown that a core renal biopsy alters the clinical diagnosis in 24-47% of the

patients.[23, 24] For example, IgA nephropathy, thin basement membrane nephropathy and C3 glomerulopathy can only be diagnosed by renal biopsy. Also, unexpected findings can be observed in renal biopsies from patients with diabetes mellitus and in patients with acute kidney injury (AKI).[25] Furthermore, with the help of renal biopsies new disease classifications have been generated and specific pathological features, like the degree of irreversible kidney damage, have prognostic value in both native and allograft biopsies.[25] Histological evaluation of pre-implantation renal transplant biopsies provides information on the organ quality and may be an important tool in the prediction of recipient outcome.[26-28]

Renal core biopsies are performed under real-time ultrasound guidance using a 14- to 18-gauge needle. Ideally, 2 renal core biopsies are obtained which are divided into a portion for light microscopy (LM), electron microscopy (EM) and immunofluorescence (IF). Figure 1 demonstrates the method used at the Pathology Department of the Erasmus MC, Rotterdam, for dividing 2 cores obtained from a transplant kidney. The biopsy cores should contain predominantly cortical tissue because this is the location of glomeruli and should be divided in a manner to maximize the number of glomeruli in each of the renal samples.[29]

The tissue sample for LM is placed into formalin which allows rapid fixation, after which the sample is infiltrated with melted paraffin wax. After solidification, 2-4 μm sections are cut and stained according to routine diagnostic practice for hematoxylin and eosin (H&E), periodic acid–Schiff (PAS), Jones and Masson's trichrome. The tissue sample for IF is frozen and stored at −80°C until cryosectioning. IF is performed using antibodies directed against IgA, IgG, IgM, C3c, C1q, kappa and lambda. A tissue sample of circa 4 mm is fixated in a glutaraldehyde solution and processed for EM. One or 2 glomeruli are usually selected for ultrastructural evaluation of the glomerular basement membrane, podocytes and endothelium, and for the presence of depositions.[30]
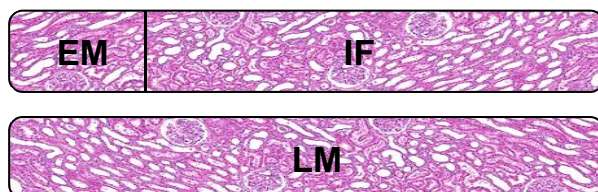

Figure 1. Two renal cores biopsies are generally taken and divided into a portion for light microscopy (LM), electron microscopy (EM) and immunofluorescence (IF).

The histological diagnosis of rejection is based on the Banff Classification.[31] The Banff Foundation for Organ Transplantation originated during a meeting in Banff, Canada, held in August 1991. The Banff meeting is a consensus meeting regarding allograft pathology that has been held every two years.[32] The Banff Classification of Kidney Allograft Pathology consists of the following six categories: (1) normal, (2) antibody-mediated rejection (ABMR), (3) borderline changes, (4) T cell-mediated rejection (TCMR), (5) interstitial fibrosis and tubular atrophy (IFTA), and (6) other.

Despite the standardization of the diagnostic features of these 6 categories in the Banff Classification, limited reproducibility and differential diagnostic dilemmas remain a problem using histological evaluation. First of all, adequate biopsy interpretation requires an experienced nephropathologist, who is not always readily available. In addition, histology of rejection can show a wide range of features and subjective interpretations of lesions may cause interobserver variation. The scoring system uses arbitrary thresholds and the interobserver agreement is poor, with most lesions having k-values of 0.4 or less.[33-35] Furthermore, renal biopsy findings currently do not provide sufficient insight into which transplant patients are at risk of future rejection episodes and allograft loss.

Therefore, alternative methods of diagnosing rejection, such as mass spectrometry (MS) and molecular analysis of renal tissue, are under investigation. Several publications have stressed the importance of combining current diagnostic practice with molecular analysis.[36-39] Gene expression analysis on the mRNA level in renal transplant biopsies can give novel insights into the underlying pathophysiology of rejection and could lead to the identification of diagnostic and prognostic markers and new therapeutic interventions. Naesens *et al.* reported that the examination of kidney biopsies at the molecular level can reveal abnormalities in the innate and adaptive immune response long before those abnormalities appear on histology.[40] The Banff Foundation is encouraging molecular research on renal allograft biopsies and also urges to incorporate molecular analysis in the diagnostic classification of kidney transplant rejection.[31] However, the implementation of molecular analysis into standard clinical practice remains challenging due to the requirement of large scale, multi-center validation in clinical trials.

3.   The immune system in renal transplantation

The current success of renal transplantation is the result of advances in our understanding of the alloimmune response. The two main classes of the immune system are the innate immune system and the adaptive immune system and both play an important role in rejection.

3.1   The innate immune system

The innate immune system provides a non-specific first line of defense against viruses, bacteria, parasites, and other foreign particles. Tissue stress experienced during the transplantation procedure is sufficient to trigger the innate immune response.[41] Immunological events in the donor kidney at the time of transplantation are caused by ischemia-reperfusion injury (IRI). IRI is initiated by oxygen deprivation causing ischemia and is further exacerbated once restoration of the blood flow is completed (reperfusion). Reperfusion of the ischemic tissue causes microvascular injury and the resupply of oxygen will lead to generation of reactive oxygen species.[42] This may eventually result in lysis of kidney cells which then release their intracellular contents. The first responders to IRI are components of the innate immune system, such as the complement system and toll-like receptors (TLRs), resulting in activation of dendritic cells, natural killer (NK) cells and macrophages which induce an inflammatory response.[43]

Toll-like receptors

TLRs are a family of transmembrane proteins expressed on inflammatory cells (*e.g.* dendritic cells, macrophages, NK cells) and non-inflammatory cells (epithelial and endothelial cells).[44] To date, 11 different TLRs have been identified in humans.[45] TLRs recognize so-called pathogen-associated molecular patterns (PAMPs), molecules unique to groups of related micro-organisms which are not associated with human cells. When exposed to PAMPs, the TLRs on macrophages and dendritic cells induce signaling events which promote the activation of the innate immune system.[46] All TLRs, except TLR3, require the adaptor MyD88 for signal transduction. TLR3 utilizes the adaptor Trif. TLR4 can signal via both MyD88 and Trif.[47] TLRs are also known to have an important role in the setting of kidney transplantation through the recognition of danger signals or damage-associated molecular patterns (DAMPs).[43, 48] These DAMPs are cells and cell contents displayed on stress

or injury like that caused by IRI. Recognition of DAMPs by TLRs cause activation of the innate immune system in the absence of infection and the response is characterized by an inflammatory cell infiltrate, production of proinflammatory cytokines and chemokines, and activation of the complement system.[48]

The complement system

Activation of the complement system can occur through three different pathways: the classical, alternative and the lectin pathway. All three pathways are triggered by distinct stimuli. When the complement system is activated, a cascade reaction is initiated resulting in the creation of complement components which have pro-inflammatory, chemo-attractant and cell-damaging effects.[49]

The **classical pathway** is initiated by the binding of IgM or IgG antibody-antigen complexes to C1q. C1q is part of the C1 complex, a multimeric complex consisting of a C1q molecule bound to two C1r and two C1s molecules. The binding of C1q to the Fc portion of an IgM or IgG immune complex induces a conformational change in the C1 complex leading to activation of C1r and C1s. Once activated, C1s cleaves C4 into C4a and C4b, and C2 into C2a and C2b, leading to the formation of C3 convertase.[50] The **lectin pathway** is very similar to the classical pathway. Mannose-binding lectin (MBL) binds to mannose proteins which are present on many pathogens. MBL forms a complex with mannose-associated serine protease (MASP)-1 and MASP-2 (which are comparable to C1r and C1s) leading to the cleavage of C4 and C2, initiating the formation of C3 convertase.[50] The **alternative pathway** is activated by the spontaneous hydrolysis of C3 which changes the structure of C3. The formed C3b covalently binds to the cell wall of a pathogen. Factor B then binds to C3b, which is cleaved by factor D, forming C3 convertase.[50]

All three pathways lead to the formation of homologous variants of C3 convertase which cleaves C3 to form C3a and C3b. C3a acts as a recruiter of inflammatory cells. C3b opsonizes foreign antigens and apoptotic cells which promotes phagocytosis. Furthermore, C3b is part of C5 convertase which cleaves C5 that leads to the activation of the final common pathway, the Membrane Attack Complex (MAC). MAC is composed of different complement proteins (C5b, C6, C7, C8 and several C9 molecules) that are able to form a cytolytic complex which promotes the removal of pathogens and cell debris (Figure 2).[51]
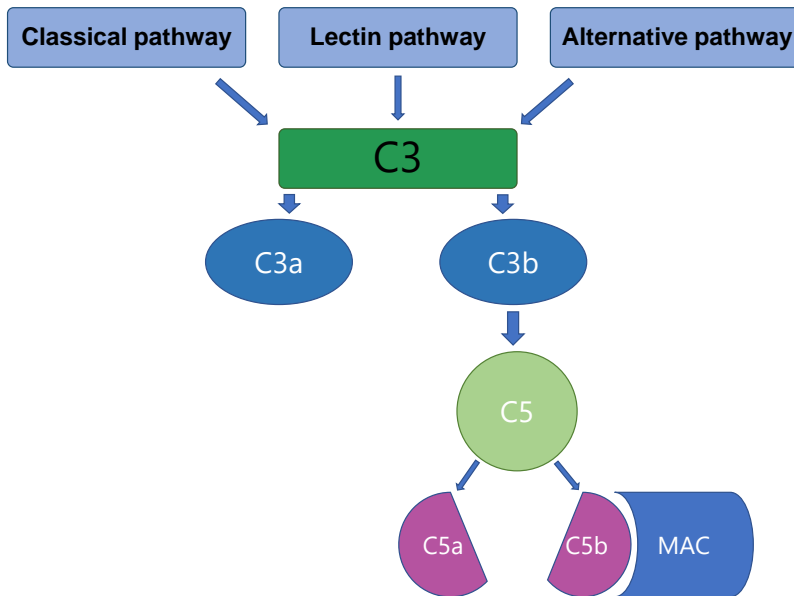
Figure 2. The complement system can be activated by the classical pathway, lectin pathway and the alternative pathway. All pathways lead to the cleavage of C3 by homologous variants of C3 convertase forming C3a and C3b. C3b opsonizes foreign antigens and apoptotic cells, promoting phagocytosis. C3b is also part of C5 convertase which cleaves C5 into C5a and C5b, leading to the activation the Membrane Attack Complex (MAC). C3a and C5a are anaphylatoxins that have multiple immune regulatory roles. MAC can directly kill pathogens or cells or can promote inflammation.

Apoptosis-related markers

IRI eventually causes cell death by necrosis (unregulated cell death) and apoptosis (programmed cell death). The major B-cell lymphoma 2 (BCL2) family members act to promote or suppress cell death and are the key regulators of apoptosis. Structurally, the BCL2 family members share one or more of the four characteristic domains entitled the BCL2 homology domains (named BH1, BH2, BH3 and BH4).[52] They are predominantly located on the mitochondria where the release of cytochrome c is regulated.[53] BCL2 family members are divided into two major sub-groups: the anti-apoptotic proteins (*e.g.* BCL2) and the pro-apoptotic proteins (*e.g.* BAX). The overexpression of BCL2 enhances cell survival by suppressing apoptosis as BCL2 stabilizes the mitochondrial membrane and prevents the release of cytochrome c into the cytosol.[54, 55] Cell death signals activate BH3 which results in inactivation of

BCL2 and conformational changes of BAX.[56] Oligomerization of BAX on the outer mitochondrial membrane leads to mitochondrial outer membrane permeabilization and cytochrome c release. This triggers the activation of a cascade leading to cell death (Figure 3).[56] The balance between cell death and survival upon stimulation is therefore regulated by the BAX:BCL ratio.[57, 58]
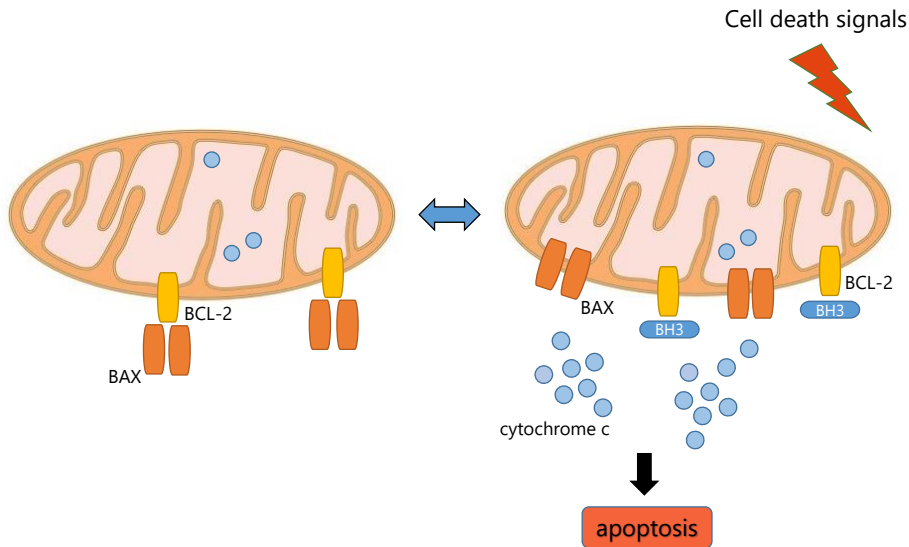
Figure 3. BAX and BCL-2 have opposing roles in apoptosis. When uninhibited, BCL-2 blocks BAX thereby suppressing apoptosis. Cell death signals cause activation of BH3 which results in the inactivation of BCL-2 and oligomerization of BAX which form pores through which cytochrome *c* is released from the inner mitochondrial membrane into the cytosol. This activates a subsequent cascade leading to apoptosis of the damaged cells.

3.2   The adaptive immune system

The adaptive immune system, or "acquired immunity" includes humoral and cell-mediated immunity. More sophisticated mechanisms are involved in the adaptive immune response compared to the innate immune response. The adaptive immune system is characterized by its high specificity for particular pathogens and immunologic memory. While the innate immune response occurs within minutes to hours after contact with a pathogen, the adaptive immune response only becomes fully activated after a delay of 3-5 days following the initial encounter with the pathogen.[59]

The activation of the adaptive immune system after kidney transplantation is caused by human leucocyte antigens (HLA) which are unique to each person. These

cell surface antigens are responsible for the regulation of the immune system in humans. HLA class I is found on all nucleated cells, whereas HLA class II is present on antigen presenting cells (APCs) such as dendritic cells, macrophages and B cells.[60] After transplantation, HLA from the donor is recognized as foreign by the recipients immune system which initiates a cascade of immune events resulting in infiltration of the kidney transplant by inflammatory cells, culminating in acute rejection.[61]

The major components of the adaptive immune system are T cells and B cells and both are important in rejection. T cells and B cells are triggered by activated cells from the innate immune system (dendritic cells and macrophages) which present donor HLA molecules to naïve T cells. The T cells can recognize donor HLA by 3 distinct pathways; the direct pathway, the indirect pathway and the semi-direct pathway.[62] In the direct pathway, T cells from the recipient are activated directly by APCs from the donor, bearing intact HLA molecules on their surface. In the indirect pathway, T cells are stimulated by APCs from the recipient, which have taken up HLA fragments derived from the donor tissue, which are presented to the T cells. In the semi-direct pathway, T cells are activated by the fusion of an APC from the recipient with a donor-derived HLA molecule.[62] Activation of T cells leads to clonal expansion and migration of these cells from the secondary lymphoid tissue to the renal transplant where they cause an acute TCMR. Activated B cells produce donor-specific anti-HLA antibodies (DSAs) which bind to the endothelium of the microcirculation of the donor kidney and activate the complement system causing damage to the vascular endothelium resulting in an acute ABMR.[63]

4. Rejection of the kidney transplant

Rejection can be subdivided into different categories according to the timing of rejection (hyperacute, acute, chronic) or the pathophysiology (cellular or antibody-mediated).[64]

Hyperacute rejection occurs within minutes to hours after kidney transplantation and is mediated by preformed DSAs as a result of a previous transplant, blood transfusion or pregnancy.[65] It is characterized histologically by severe endothelial injury and vessel thrombosis.[65] When it occurs, the transplanted kidney usually cannot be salvaged and graft nephrectomy is indicated in most cases. Nowadays, hyperacute rejection can usually be prevented by testing for preformed DSAs before transplantation.[66]

Acute rejection is the most common form of rejection and occurs in 10-25% of patients within the first year after kidney transplantation.[67] Not all acute rejection episodes have the same risk for renal graft failure. Factors such as severity, number of acute rejections and degree of recovery of kidney function to baseline after treatment, all affect the long-term outcome.[68, 69] Acute rejection can be either TCMR or ABMR. Acute TCMR is caused by a cytotoxic T cell reaction directed against HLA of the transplanted kidney and is the most common type of acute rejection. The key pathological findings in acute TCMR are infiltration of the donor kidney by T cells which can affect different compartments of the donor kidney. Histopathology is characterized by interstitial infiltration of lymphocytes which invade renal tubules (tubulitis) and cause interstitial edema.[70, 71] In severe cases, arterial subendothelial mononuclear cell infiltration is seen (arteritis). Examples of the histopathological features of acute TCMR are shown in Figure 4.

Acute ABMR (or active ABMR) occurs most commonly within the first weeks after transplantation and is caused by preformed DSAs.[72] Acute ABMR occurs in approximately 1% to 10% of all kidney transplant recipients and up to a third of pre-sensitized recipients may develop acute ABMR after transplantation.[72, 73] The diagnosis of ABMR requires three components: (1) histologic evidence of acute tissue injury, (2) evidence of current / recent antibody interaction with vascular endothelium, *i.e.* C4d staining of endothelial cells of the peritubular capillaries (PTCs) and medullary vasa recta and/or peritubular capillaritis, and (3) detection of DSAs.[31] Histopathology is characterized by endothelial injury in the form of endothelial cell swelling, neutrophil infiltration in the glomeruli (glomerulitis) and PTCs, interstitial edema and fibrin thrombi.[70, 74] Examples of the histopathological features characteristic of acute ABMR are shown in Figure 5.

Detection of the complement split product C4d in renal allograft biopsies is an important marker of ABMR (Figure 5C). C4d staining in the microcirculation in kidney transplants with ABMR was first described by Feucht *et al*.[51, 75] C4d is a degradation product of the complement factor C4 which is a component of the classical and lectin pathways. The activation of C4 generates C4b which is then cleaved into C4c and smaller fragments such as C4d. Because C4d forms an internal thioester bond with the endothelial surface it can covalently bind to the endothelium, where it remains for several days to weeks. Therefore, it is a durable marker of local complement activation.[76-78] C4d positivity of the PTCs in cases of ABMR is found to be a specific marker of the interaction of DSAs with the endothelium of the renal microcirculation and is associated with poor kidney transplant survival.[79-82]

Nowadays, C4d staining of the PTCs is a well-established feature of ABMR. Most centers have incorporated routine C4d staining by either immunohistochemistry (IHC) or IF in the diagnostic pathologic evaluation of renal allograft biopsies.
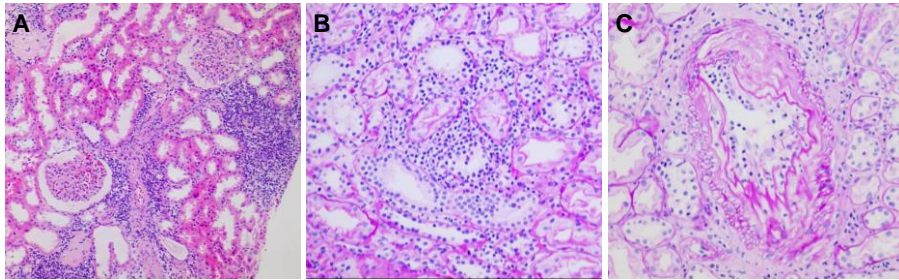
Figure 4. Representative micrographs illustrating the main histological features of acute T cell-mediated rejection; (A) infiltration of mononuclear cells in the interstitium (H&E, magnification 100x) and (B) tubules (tubulitis) (PAS+, magnification 200x). (C) In higher grade TCMR, inflammation in the arteriolar walls is observed (PAS+, magnification 200x).
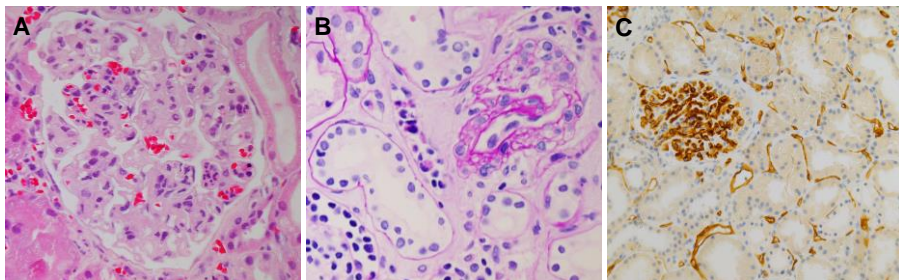
Figure 5. Representative micrographs illustrating the main histological features of antibody-mediated rejection; (A) infiltration of inflammatory cells in the glomeruli (glomerulitis) (H&E+, magnification 400x) and (B) peritubular capillaries (peritubular capillaritis) (PAS+, magnification 400x). (C) Immunohistochemistry showing linear staining of C4d in peritubular capillaries (magnification 200x).

Despite this, C4d staining in the PTCs in ABMR lacks sensitivity and specificity and there is strong evidence that DSAs can induce ABMR in the absence of C4d deposition.[83-85] This has led to the inclusion of C4d-negative ABMR in the 2013 Banff Classification.[86] The requirement of the detection of DSAs to diagnose ABMR is also subject of debate. ABMR is usually mediated by DSAs against HLA class I or class II proteins but evidence of ABMR in the absence of anti-HLA antibodies suggests the

existence of non-anti–HLA antibodies.[87] For example, antibodies against the angiotensin type 1 receptor have been associated with ABMR but the clinical implications of such antibodies remains unclear.[88, 89]

Chronic rejection can occur within months to years after transplantation. Up to 40% of transplanted kidneys are lost within 10 years as a result of chronic rejection.[71, 90] Chronic rejection can be subdivided in chronic-active TCMR (c-aTCMR) and chronic-active ABMR (c-aABMR). c-aTCMR may be manifest in the tubulointerstitial compartment as well as in the vascular compartment. Updated criteria for c-aTCMR were included in the 2017 Banff Classification.[31] Data showed that inflammation within areas of interstitial fibrosis and tubular atrophy (i-IFTA) is a consequence of chronic under-immunosuppression and previous acute TCMR.[91] Therefore, it was suggested that moderate i-IFTA plus moderate or severe tubulitis can represent c-aTCMR in the tubulointerstitial compartment.[31]

Chronic rejection is most often caused by c-aABMR resulting from the development of *the novo* DSAs. c-aABMR develops through a number of stages which cause chronic allograft injury. The diagnosis of c-aABMR requires histologic evidence of chronic tissue injury, C4d staining of PTCs and the presence of DSAs.[31] Chronic tissue injury is histologically characterized by chronic transplant vasculopathy, transplant glomerulopathy (TG) and peritubular capillary basement membrane multilayering.[92, 93] TG is characterized by pathological abnormalities of double contouring or multi-layering of the glomerular basement membrane and is often associated with a decline in renal function and poor outcome (Figure 6).[94]
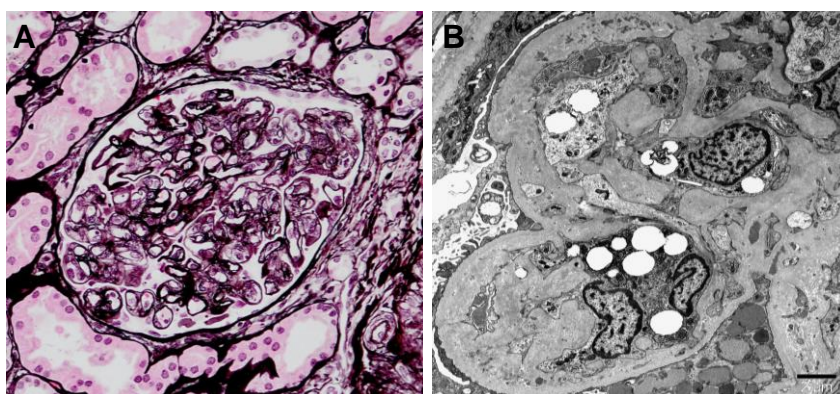

Figure 6. Representative micrographs illustrating transplant glomerulopathy; (A) histology showing patent capillary loops with thickened basement membrane with duplication (Jones, magnification 400x) and (B) electron microscopy showing reduplication of the basement membrane (magnification 4400x).

5.   Calcium oxalate depositions

Delayed graft function (DGF) is usually defined as impaired renal function with the need for dialysis in the first week after kidney transplantation.[95] It is a complication of primary concern in patients with a renal allograft from a deceased donor, occurring in approximately 20% to 50% of these cases.[96, 97] DGF is generally the consequence of acute tubular necrosis (ATN) caused by IRI.[98] It is strongly associated with a higher risk of acute rejection, which is presumably caused by IRI and the following inflammatory response with increased expression of cytokines and HLA molecules. Changes in maintenance immunosuppressive therapy, specifically calcineurin inhibitor (CNI) use, during a period of DGF can increase the chance of an acute rejection.[99-101]   Also, DGF is associated with inferior graft outcome.[100, 102] Different risk factors for DGF have been described including donor characteristics (donor age, donor type (deceased *versus* living) and the presence of hypertension and/or diabetes mellitus), recipient characteristics (immunological response, immunosuppressive medications) and conditions of organ retrieval (cold and warm ischemia time).[102, 103] The causative pathway resulting in DGF is often multifactorial and there are still many controversies about the most important factors associated with DGF.[104] Patients suspected of DGF are often biopsied after several days to exclude concomitant acute rejection in addition to ATN.[105]

Recently, the histological presence of calcium oxalate (CaOx) was suggested as a possible cause of impaired renal function in the early post-transplantation period.[106, 107] Oxalic acid is the end-product of different metabolic pathways and is predominantly excreted by the kidney.[108] When kidney function declines, oxalic acid elimination by the kidneys is impaired and the oxalic acid plasma concentration rises. High plasma oxalic acid concentrations are therefore observed in patients with ESRD.[109-111] Neither hemo- nor peritoneal dialysis can remove sufficient amounts of oxalic acid to normalize the oxalic acid plasma concentrations in patients with ESRD.[112, 113] After kidney transplantation, a large amount of oxalate is excreted by the newly-functioning kidney.[114] Urine may then become supersaturated with oxalate, resulting in the formation of CaOx crystals which can accumulate in the renal tubules.[115] These CaOx crystals attach to the renal tubular cells and can cause damage the tubular cells.[116, 117] Whether CaOx deposition may be a cause of impaired renal function in the early post-transplantation period will be examined in this thesis.

6.   **C3 glomerulopathy**

The complement system is not only important in the field of renal transplantation but also plays a role in various primary kidney diseases. C3 glomerulopathy is a rare form of glomerulonephritis and includes both C3 glomerulonephritis (C3GN) and dense deposit disease (DDD). It is caused by uncontrolled activation of the alternative complement pathway.[118] When the alternative complement pathway becomes activated, C3 is split into C3a and C3b by C3 convertase. C3b reacts with other components of the complement cascade leading to the formation of the MAC, which induces localized cell injury and inflammation. Degradation of C3b leads to the formation of C3c and the end product C3d.[71, 119, 120] These C3 fragments get trapped in the glomeruli causing damage to the kidney.[121, 122]

C3 glomerulopathy can display a range of features on LM and EM. The most significant feature is the finding of C3 deposits in the glomeruli by IF. In 2013, the definition of C3 glomerulopathy was defined by the presence of dominant C3 staining with a staining score being at least two orders of magnitude greater than the other stainings (IgA, IgM, IgG and C1q).[122, 123] In most laboratories, C3 is detected by IF using an antibody to C3c, one of the breakdown products of activated C3.[122, 124] Kidney transplantation is performed in more than 50% of patients with C3 glomerulopathy who have developed ESRD. Unfortunately, C3 glomerulopathy often recurs after kidney transplantation and the median time of transplant survival is around five years.[125-127]

7.   **Aims of this thesis**

The overall objective of the research described in this thesis was to evaluate potentially important diagnostic and prognostic pathological features of renal (transplant) biopsies. Histological features and immunohistochemical and molecular markers in renal biopsies were investigated.

- A kidney biopsy is considered the gold standard for transplant pathology evaluation and it is vital that renal tissue is stored in a fashion that maximizes tissue preservation. Optimal cutting temperature (OCT) compound is often used for embedding tissue for snap-freezing. However, analysis by mass

spectrometry is difficult due to polymers in the OCT. **Chapter 2** focusses on the use of Cryo-Gel as embedding compound for snap-freezing of renal biopsies in order to optimize protein extraction for mass spectrometry without impairing diagnostic analysis.

- In **Chapter 3** a retrospective analysis was performed in which the incidence of CaOx deposition in the renal transplant biopsy in the immediate post-operative phase was investigated. It was hypothesized that CaOx deposition in the renal allograft is recipient-derived and impairs renal transplant recovery.

- The innate immune system plays an important role in the immediate post-transplantation period. **Chapter 4** presents a study in which we investigated the expression of TLRs, complement- and apoptosis-related genes in pre-implantation biopsies and in biopsies from patients with acute rejection and whether these genes can predict long-term allograft survival.

- C4d staining in the PTCs is a well-established feature of c-aABMR. However, the relevance of C4d staining in other components of the renal allograft biopsy, in particular of the arterioles, is unclear. **Chapter 5** describes the significance of arteriolar C4d staining by IHC in patients with suspicious and diagnostic c-aABMR.

- C3-dominance by IF is a defining feature in the diagnosis of C3 glomerulopathy. However, clear-cut cases of C3 glomerulopathy not fulfilling the consensus criteria have been observed in both native renal biopsies and transplant renal biopsies. In **Chapter 6** it was hypothesized that C3d by IHC would be a more sensitive marker for the diagnosis of C3 glomerulopathy than C3c.

- **Chapter 7** is a general summary and discussion of the research performed in this thesis. **Chapter 8** describes the future perspectives.

References

1. Levey AS, Coresh J. Chronic kidney disease. *Lancet*. 2012;379(9811):165-80.

2. Agarwal R. Defining end-stage renal disease in clinical trials: a framework for adjudication. *Nephrol Dial Transplant*. 2016;31(6):864-7.

3. Fraser SD, Blakeman T. Chronic kidney disease: identification and management in primary care. *Pragmat Obs Res*. 2016;17;7:21-32.

4. Abecassis M, Bartlett ST, Collins AJ, et al. Kidney transplantation as primary therapy for end-stage renal disease: a National Kidney Foundation/Kidney Disease Outcomes Quality Initiative (NKF/KDOQITM) conference. *Clin J Am Soc Nephrol*. 2008;3(2):471-80.

5. Merrill JP, Murray JE, Harrison JH, Guild WR. Successful homotransplantation of the human kidney between identical twins. *J Am Med Assoc*. 1956;160(4):277-82.

6. Starzl TE. History of Clinical Transplantation. *World J Surg*. 2000;24(7):759–782.

7. Damodar Kumbala D, Rubin Zhang R. Essential concept of transplant immunology for clinical practice. *World J Transplant*. 2013;3(4):113–118.

8. Muntean A, Lucan M. Immunosuppression in kidney transplantation. *Clujul Med*. 2013;86(3):177-80.

9. Meier-Kriesche HU, Schold JD, Srinivas TR, Kaplan B. Lack of improvement in renal allograft survival despite a marked decrease in acute rejection rates over the most recent era. *Am J Transplant* 2004;4:378-383.

10. Lamb KE, Lodhi S, Meier-Kriesche HU. Long-term renal allograft survival in the United States: a critical reappraisal. *Am J Transplant*. 2011;11(3):450-62.

11. Brachemi S, Bollée G. Renal biopsy practice: What is the gold standard? *World J Nephrol*. 2014;3(4):287–294.

12. Salvadori M, Tsalouchos A. Biomarkers in renal transplantation: An updated review. *World J Transplant*. 2017;7(3):161–178.

13. https://www.transplantatiestichting.nl/cijfers-over-donatie-en-transplantatie.

14. Rangel EB, de Sá JR, Melaragno CS, et al. Kidney transplant in diabetic patients: modalities, indications and results. *Diabetol Metab Syndr*. 2009;1(1):2.

15. Allen PJ, Chadban SJ, Craig JC, et al. Recurrent glomerulonephritis after kidney transplantation: risk factors and allograft outcomes. *Kidney Int*. 2017;92(2):461-469.

16. Davis CL, Delmonico FL. Living-Donor Kidney Transplantation: A Review of the Current Practices for the Live Donor. *J Am Soc Nephrol*. 2005;16(7):2098-110.

17. Vinson AJ, Rose C, Kiberd BA, et al. Factors Associated With Prolonged Warm Ischemia Time Among Deceased Donor Kidney Transplant Recipients. *Transplant Direct*. 2018;4(5):e342.

18. Kayler L, Yu X, Cortes C, Lubetzky M, Friedmann P. Impact of Cold Ischemia time in Kidney Transplants From Donation After Circulatory Death Donors. *Transplant Direct*. 2017;3(7):e177.

19. Terasaki PI. Cold ischemia time-time to rethink the risk for kidneys? *Am J Transplant*. 2011;11(12):2551-2.

20. Humar A, Matas AJ. Surgical Complications After Kidney Transplantation. *Seminars in Dialysis* 2005;18(6):505–510.

21. Dhaun N, Bellamy CO, Cattran DC, Kluth DC. Utility of renal biopsy in the clinical management of renal disease. *Kidney Int.* 2014;85(5):1039-48.

22. Kitterer D, Gürzing K, Segerer S, et al. Diagnostic impact of percutaneous renal biopsy. *Clinical nephrol.* 2015;84(6):311-22.

23. Colvin R, Anthony Chang A. Diagnostic Pathology: Kidney Diseases. 2nd Edition.

24. Cohen AH, Nast CC, Adler SG, Kopple JD. Clinical utility of kidney biopsies in the diagnosis and management of renal disease. *Am J Nephrol.* 1989;9(4):309-15.

25. Glassock RJ. Con: Kidney biopsy: an irreplaceable tool for patient management in nephrology. Nephrol Dial Transplant 2015;30: 528–531.

26. Mengel M, Sisa B. An Appeal for Zero-Time Biopsies in Renal Transplantation. *Am J Transplant.* 2008;8(11),2181-2182.

27. Naesens M. Zero-Time Renal Transplant Biopsies: A Comprehensive Review. *Transplantation.* 2016;100(7):1425-39.

28. Kayler LK, Mohanka R, Basu A, Shapiro R, Randhawa PS. Correlation of histologic findings on preimplant biopsy with kidney graft survival. *Transpl Int.* 2008;21(9):892-8.

29. Ahmad I. Biopsy of the transplanted kidney. *Semin Intervent Radiol.* 2004;21(4):275-81.

30. Walker PD, Cavallo T, Bonsib SM; Ad Hoc Committee on Renal Biopsy Guidelines of the Renal Pathology Society. Practice guidelines for the renal biopsy. *Mod Pathol.* 2004;17(12):1555-63.

31. Haas M, Loupy A, Lefaucheur C, et al. The Banff 2017 Kidney Meeting Report: Revised diagnostic criteria for chronic active T cell-mediated rejection, antibody-mediated rejection, and prospects for integrative endpoints for next-generation clinical trials. *Am J Transplant.* 2018;18(2):293-307.

32. Solez K, Axelsen RA, et al. International standardization of criteria for the histologic diagnosis of renal allograft rejection: the Banff working classification of kidney transplant pathology. *Kidney Int.* 1993;44(2):411-22.

33. Marcussen N, Olsen TS, Benediktsson H, Racusen L, Solez K. Reproducibility of the Banff classification of renal allograft pathology. Inter- and intraobserver variation. *Transplant.* 1995; 60:1083–1089.

34. Furness PN, Taub N, Assmann KJ, et al. International variation in histologic grading is large, and persistent feedback does not improve reproducibility. *Am J Surg Pathol* 2003;27:805–810.

35. Furness PN, Taub N. International variation in the interpretation of renal transplant biopsies: Report of the CERTPAP Project. *Kidney Int.* 2001;60:1998–2012.

36. Reeve J, Sellarés J, Mengel M, et al. Molecular diagnosis of T cell-mediated rejection in human kidney transplant biopsies. *Am J Transplant.* 2013;13(3):645–655.

37. Halloran PF, Pereira AB, Chang J, et al. Potential impact of microarray diagnosis of T cell-mediated rejection in kidney transplants: The INTERCOM study. *Am J Transplant.* 2013;13(9):2352–2363.

38. Sellarés J, Reev J, Loupy A, et al. Molecular diagnosis of antibody-mediated rejection in human kidney transplants. *Am J Transplant.* 2013;13(4):971–983.

39. Halloran PF, Pereira AB, Chang J, et al. Microarray diagnosis of antibody-mediated rejection in kidney transplant biopsies: an international prospective study (INTERCOM). *Am J Transplant.* 2013;13(11):2865–2874.

40. Naesens M, Khatri P, Li L, et al. Progressive histological damage in renal allografts is associated with expression of innate and adaptive immunity genes. *Kidney Int.* 2011;80(12):1364-76.

41. Farrar CA, Kupiec-Weglinski JW, Sacks SH. The innate immune system and transplantation. *Cold Spring Harb Perspect Med*. 2013;3(10): a015479.

42. Ponticelli C. Ischaemia-reperfusion injury: a major protagonist in kidney transplantation. *Nephrol Dial Transplant.* 2014;29:1134–1140.

43. LaRosa DF, Rahman AH, Turka LA. The innate immune system in allograft rejection and tolerance. *J Immunol.* 2007;178(12):7503-9.

44. Alegre M-L, Goldstein DR, Chong AS. Toll-like receptor signaling in transplantation. Curr Opin Organ Transplant. 2008;13(4):358–365.

45. Arancibia SA, Beltrán CJ, Aguirre IM, et al. Toll-like receptors are key participants in innate immune responses. *Biol Res.* 2007;40(2):97-112.

46. Gluba A, Banach M, Hannam S, Mikhailidis DP, Sakowicz A, Rysz J. The role of Toll-like receptors in renal diseases. *Nat Rev Nephrol*. 2010;6(4):224-35.

47. Nilsen NJ, Vladimer GI, Stenvik J, et al. A role for the adaptor proteins TRAM and TRIF in toll-like receptor 2 signaling. *J Biol Chem.* 2015;290(6):3209-22.

48. Chong AS, Alegre ML. The impact of infection and tissue damage in solid-organ transplantation. *Nat Rev Immunol.* 2012;12(6):459-71.

49. Legendre C, Sberro-Soussan R, Zuber J, Frémeaux-Bacchi V. The role of complement inhibition in kidney transplantation. *Br Med Bull.* 2017;124(1):5-17.

50. Sarma JV, Ward PA. The complement system. *Cell Tissue Res.* 2011;343(1):227-35.

51. Noris M, Remuzzi G. Overview of Complement Activation and Regulation. *Semin Nephrol.* 2013;33(6):479–492.

52. Kale J, Osterlund EJ, Andrews DW. BCL-2 family proteins: changing partners in the dance towards death. *Cell Death Differ.* 2018;25(1):65-80.

53. Gillies LA, Kuwana T. Apoptosis regulation at the mitochondrial outer membrane. *J Cell Biochem*. 2014;115(4):632-40.

54. Dlugosz PJ, Billen LP, Annis MG, et al. Bcl-2 changes conformation to inhibit Bax oligomerization. *EMBO J.* 2006;25(11):2287-96.

55. Adams JM, Cory S. The Bcl-2 apoptotic switch in cancer development and therapy. *Oncogene.* 2007;26:1324–37.

56. Chipuk JE, Green DR. How do BCL-2 proteins induce mitochondrial outer membrane permeabilization? *Trends Cell Biol.* 2008;18(4):157-64.

57. Wolfs TG, de Vries B, Walter SJ, Peutz-Kootstra CJ, van Heurn LW, Oosterhof GO, Buurman WA. Apoptotic cell death is initiated during normothermic ischemia in human kidneys. *Am J Transplant.* 2005;5(1):68-75.

58. Saikumar P, Dong Z, Mikhailov V, Denton M, Weinberg JM, Venkatachalam MA. Apoptosis: definition, mechanisms, and relevance to disease. *Am J Med.* 1999;107(5):489-506.

59. Rabb H. The T cell as a bridge between innate and adaptive immune systems: Implications for the kidney. *Kidney Int.* 2002;61(6):1935-46.

60. Trivedi VB, Dave AP, Dave JM, Patel BC. Human leukocyte antigen and its role in transplantation biology. *Transplant Proc.* 2007;39(3):688-93.

61. Montgomery RA, Tatapudi VS, Leffell MS, Zachary AA. HLA in transplantation. *Nat Rev Nephrol.* 2018;14(9):558-570.

62. DeWolf S, Sykes M. Alloimmune T cells in transplantation. *J Clin Invest.* 2017;127(7):2473-2481.

63. Zhang R. Donor-Specific Antibodies in Kidney Transplant Recipients. *Clin J Am Soc Nephrol.* 2018;13(1):182-192.

64. Nankivell BJ, Alexander SI. Rejection of the kidney allograft. *N Engl J Med.* 20107;363(15):1451-62.

65. Moreau A, Varey E, Anegon I, Cuturi MC. Effector mechanisms of rejection. *Cold Spring Harb Perspect Med.* 2013;3(11).

66. Terasaki PI. Humoral theory of transplantation. *Am J Transplant.* 2003;3:665-673.

67. Clayton PA, McDonald SP, Russ GR, Chadban SJ. Long-Term Outcomes after Acute Rejection in Kidney Transplant Recipients: An ANZDATA Analysis. *J Am Soc Nephrol.* 2019;30(9):1697-1707.

68. Opelz G, Döhler B, Collaborative Transplant Study Report. Influence of time of rejection on long-term graft survival in renal transplantation. *Transplantation.* 2008; 85:661.

69. Madden RL, Mulhern JG, Benedetto BJ, et al. Completely reversed acute rejection is not a significant risk factor for the development of chronic rejection in renal allograft recipients. *Transpl Int.* 2000;13:344.

70. Katsuma A, Yamakawa T, Nakada Y, Yamamoto I, Yokoo T. Histopathological findings in transplanted kidneys. *Renal Replacement Therapy.* 2017;3:6.

71. Lusco MA, Fogo AB, Najafian B, Alpers CE. AJKD Atlas of Renal Pathology: Acute T-Cell-Mediated Rejection. *Am J Kidney Dis.* 2016;67(5):e29-30.

72. Mauiyyedi S, Colvin RB. Humoral rejection in kidney transplantation: new concepts in diagnosis and treatment. *Current Opinion in Nephrology and Hypertension.* 2002;11(6):609–618.

73. Puttarajappa C, Shapiro R, Tan HP. Antibody-Mediated Rejection in Kidney Transplantation: A Review. *J Transplant.* 2012;2012:193724.

74. Najafian B, Fogo AB, Lusco MA, Alpers CE. AJKD Atlas of Renal Pathology: acute antibody-mediated rejection. *Am J Kidney Dis.* 2015;66(5):e39-40.

75. Feucht HE. Complement C4d in graft capillaries—The missing link in the recognition of humoral alloreactivity. *AmJ Transplant.* 2003;3:646.

76. Murata K, Baldwin WM. Mechanisms of complement activation, C4d deposition, and their contribution to the pathogenesis of antibody-mediated rejection. *Transplant Rev (Orlando).* 2009;23(3):139-50.

77. Campbell RD, Gagnon J, Porter RR. Amino acidsequence around the thiol and reactive acyl groups of human complement component C4. *Biochem J.* 1981;199:359–370.

78. Regele H, Böhmig GA, Habicht A, et al. Capillary deposition of complement split product C4d in renal allografts is associated with basement membrane injury in peritubular and glomerular capillaries: a contribution of humoral immunity to chronic allograft rejection. *J Am Soc Nephrol.* 2002;13(9):2371-80.

79. Regele H, Exner M, Watschinger B, et al. Endothelial C4d deposition is associated with inferior kidney allograft outcome independently of cellular rejection. *Nephrol Dial Transplant.* 2001;16:2058–2066.

80. Herzenberg AM, Gill JS, Djurdjev O, Magil AB. C4d deposition in acute rejection: An independent long-term prognostic factor. *J Am Soc Nephrol.* 2002;13:234–241.

81. Mauiyyedi S, Pelle PD, Saidman S, et al. Chronic humoral rejection: Identification of antibody-mediated chronic renal allograft rejection by C4d deposits in peritubular capillaries. *J Am Soc Nephrol*. 2001;12:574–582.

82. Worthington JE, McEwen A, McWilliam LJ, Picton ML, Martin S. Association between C4d staining in renal transplant biopsies, production of donor-specific HLA antibodies, and graft outcome. *Transplantation.* 2007;83(4):398-403.

83. Takeda A, Otsuka Y, Horike K, et al. Significance of C4d deposition in antibody-mediated rejection. *Clin Transplant.* 2012;26 Suppl 24:43-8.

84. Corrêa RR, Machado JR, da Silva MV, et al. The importance of C4d in biopsies of kidney transplant recipients. *Clin Dev Immunol.* 2013;2013:678180.

85. Sis B, Halloran PF. Endothelial transcripts uncover a previously unknown phenotype: C4d-negative antibody-mediated rejection. *Curr Opin Organ Transplant. 2010*;15:42–8.

86. Haas M, Sis B, Racusen LC, et al. Banff 2013 meeting report: inclusion of c4d-negative antibody-mediated rejection and antibody-associated arterial lesions. *Am J Transplant.* 2014;14(2):272-83.

87. Dragun D, Catar R, Philippe A. Non-HLA antibodies in solid organ transplantation: recent concepts and clinical relevance. *Curr Opin Organ Transplant.* 2013;18(4):430-5.

88. Lefaucheur C, Viglietti D, Bouatou Y, et al. Non-HLA agonistic anti-angiotensin II type 1 receptor antibodies induce a distinctive phenotype of antibody-mediated rejection in kidney transplant recipients. *Kidney Int.* 2019;96(1):189-201.

89. Banasik M, Boratyńska M, Kościelska-Kasprzak K, et al. The influence of non-HLA antibodies directed against angiotensin II type 1 receptor (AT1R) on early renal transplant outcomes. *Transpl Int.* 2014;27(10):1029-38.

90. Ponticelli C. Progression of renal damage in chronic rejection. *Kidney Int.* Suppl. 2000;75:S62-70.

91. Lefaucheur C, Gosset C, Rabant M, et al. T cell-mediated rejection as a major determinant of inflammation in scarred areas in kidney transplant recipients. *Am J Transplant.* 2018;18(2):377-390.

92. Drachenberg CB, Papadimitriou JC. Endothelial injury in renal antibody-mediated allograft rejection: A schematic view based on pathogenesis. *Transplantation.* 2013;95:1073–1083.

93. Katsuma A, Yamakawa T, Nakada Y, Yamamoto I, Yokoo T. Histopathological findings in transplanted kidneys. *Renal Replacement Therapy.* 2017;3:6.

94. Lesage J, Noel R, Lapointe I, et al. Donor-specific antibodies, C4d and their relationship with the prognosis of transplant glomerulopathy. *Transplantation.* 2015;99(1):69–76.

95. Yarlagadda SG, Coca SG, Garg AX, et al. Marked variation in the definition and diagnosis of delayed graft function: a systematic review. *Nephrol Dial Transplant.* 2008;23(9):2995-3003.

96. Perico N, Cattaneo D, Sayegh MH, Remuzzi G. Delayed graft function in kidney transplantation. *Lancet.* 2004;364(9447):1814-27.

97. Ojo AO, Wolfe RA, Held PJ, Port FK, Schmouder RL. Delayed graft function: risk factors and implications for renal allograft survival. *Transplantation.* 1997;63(7):968-74.

98. Kosieradzki M, Rowiński W. Ischemia/reperfusion injury in kidney transplantation: mechanisms and prevention. *Transplant Proc.* 2008;40(10):3279-88.

99. Wu WK, Famure O, Li Y, Kim SJ. Delayed graft function and the risk of acute rejection in the modern era of kidney transplantation. *Kidney Int.* 2015;88(4):851-8.

100. Lim WH, Johnson DW, Teixeira-Pinto A, Wong G. Association Between Duration of Delayed Graft Function, Acute Rejection, and Allograft Outcome After Deceased Donor Kidney Transplantation. *Transplantation.* 2019;103(2):412-419.

101. Mannon RB. Delayed Graft Function: The AKI of Kidney Transplantation. *Nephron.* 2018;140(2):94-98.

102. Irish WD, Ilsley JN, Schnitzler MA, Feng S, Brennan DC. A risk prediction model for delayed graft function in the current era of deceased donor renal transplantation. *Am J Transplant.* 2010;10(10):2279-86.

103. Lebranchu Y, Halimi JM, Bock A, et al. Delayed graft function: risk factors, consequences and parameters affecting outcome-results from MOST, A Multinational Observational Study. *Transplant Proc.* 2005;37(1):345-7.

104. Malyszko J, Lukaszyk E, Glowinska I, Durlik M. Biomarkers of delayed graft function as a form of acute kidney injury in kidney transplantation. *Sci Rep.* 2015;5:11684.

105. Siedlecki A, Irish W, Brennan DC. Delayed graft function in the kidney transplant. *Am J Transplant.* 2011;11(11):2279-96.

106. Truong LD, Yakupoglu U, Feig D, et al. Calcium Oxalate Deposition in Renal Allografts: Morphologic Spectrum and Clinical Implications. *Am J Transplant.* 2004;4:1338–1344.

107. Pinheiro HS, Caˆmara NO, Osaki KS, De Moura LA, Pacheco-Silva A. Early presence of calcium oxalate deposition in kidney graft biopsies is associated with poor long-term graft survival. *Am J Transplant.* 2005;5:323–329.

108. Robertson WG. Kidney models of calcium oxalate stone formation. *Nephron Physiol.* 2004;98(2): p21-30.

109. Salyer WR, Keren D. Oxalosis as a complication of chronic renal failure. *Kidney Int.* 1973;4(1):61-6.

110. Worcester EM, Nakagawa Y, Bushinsky DA, Coe FL. Evidence that serum calcium oxalate supersaturation is a consequence of oxalate retention in patients with chronic renal failure. *J Clin Invest.* 1986;77(6):1888–1896.

111. Constable AR, Joekes AM, Kasidas GP, O'Regan P, Rose GA. Plasma level and renal clearance of oxalate in normal subjects and in patients with primary hyperoxaluria or chronic renal failure or both. *Clin Sci (Lond).* 1979;56(4):299-304.

112. Watts RW, Veall N, Purkiss P. Oxalate dynamics and removal rates during haemodialysis and peritoneal dialysis in patients with primary hyperoxaluria and severe renal failure. *Clin Sci (Lond).* 1984;66(5):591–7.

113. Hoppe B, Graf D, Offner G, et al. Oxalate elimination via hemodialysis or peritoneal dialysis in children with chronic renal failure. *Pediatr Nephrol.* 1996;10(4):488–92.

114. Elgstoen KB, Johnsen LF, Woldseth B, Morkrid L, Hartmann A. Plasma oxalate following kidney transplantation in patients without primary hyperoxaluria. *Nephrol Dial Transplant.* 2010;25:2341–2345.

115. Hoppe B, Beck BB, Milliner DS. The primary hyperoxalurias. *Kidney Int.* 2009;75:1264-1271.

116. Tsujihata M. Mechanism of calcium oxalate renal stone formation and renal tubular cell injury. *Int J Urol.* 2008;15(2):115–20.

117. Khan SR. Calcium oxalate crystal interaction with renal tubular epithelium, mechanism of crystal adhesion and its impact on stone development. *Urol Res.* 1995; 23(2):71–9.

118. Barbour TD, Pickering MC, Terence Cook H. Dense deposit disease and C3 glomerulopathy. *Semin Nephrol.* 2013;33(6):493-507.

119. Noris M, Remuzzi G. Glomerular Diseases Dependent on Complement Activation, Including Atypical Hemolytic Uremic Syndrome, Membranoproliferative Glomerulonephritis, and C3 Glomerulopathy: Core Curriculum 2015. *Am J Kidney Dis.* 2015;66(2):359-75.

120. Thurman JM, Holers VM. The central role of the alternative complement pathway in human disease. *J Immunol.* 2006;176(3):1305-10.

121. Fakhouri F, Frémeaux-Bacchi V, Noël LH, Cook HT, Pickering MC. C3 glomerulopathy: a new classification. *Nat Rev Nephrol.* 2010;6(8):494-9.

122. Pickering MC, D'Agati VD, Nester CM, et al. C3 glomerulopathy: consensus report. *Kidney Int.* 2013;84(6):1079-89.

123. Hou J, Markowitz GS, Bomback AS, et al. Toward a working definition of C3 glomerulopathy by immunofluorescence. *Kidney Int.* 2014;85(2):450-6.

124. West CD, Witte DP, McAdams AJ. Composition of nephritic factor-generated glomerular deposits in membranoproliferative glomerulonephritis type 2. *Am J Kidney Dis*. 2001;37(6):1120-30.
125. Regunathan-Shenk R, Avasare RS, et al. Kidney Transplantation in C3 Glomerulopathy: A Case Series. *Am J Kidney Dis*. 2019;73(3):316-323.
126. Zand L, Lorenz EC, Cosio FG, et al. Clinical findings, pathology, and outcomes of C3GN after kidney transplantation. *J Am Soc Nephrol.*2014;25(5):1110-7.
127. Koopman JJE, Teng YKO, Boon CJF, et al. Diagnosis and treatment of C3 glomerulopathy in a center of expertise. *Neth J Med*. 2019;77(1):10-18.

CHAPTER 2

Cryo-Gel embedding compound
for renal biopsy biobanking

Malou L. H. Snijders[1], Marina Zajec[2, 3], Laurens A. J. Walter[1],
Remco M. A. A. de Louw[1], Monique H. A. Oomen[1], Shazia Arshad[1],
Thierry P. P. van den Bosch[1], Lennard J. M. Dekker[2], Michail Doukas[1],
Theo M. Luider[2], Peter H. J. Riegman[1], Folkert J. van Kemenade[1]
& Marian C. Clahsen-van Groningen[1]

1. Department of Pathology, Erasmus MC, Rotterdam, The Netherlands.
2. Department of Neurology, Erasmus MC, Rotterdam, The Netherlands.
3. Department of Clinical Chemistry, Erasmus MC, Rotterdam, The Netherlands.

Abstract

Optimal preservation and biobanking of renal tissue is vital for good diagnostics and subsequent research. Optimal cutting temperature (OCT) compound is a commonly used embedding medium for freezing tissue samples. However, due to interfering polymers in OCT, analysis as mass spectrometry (MS) is difficult. We investigated if the replacement of OCT with Cryo-Gel as embedding compound for renal biopsies would enable proteomics and not disturb other common techniques used in tissue diagnostics and research. For the present study, fresh renal samples were snap-frozen using Cryo-Gel, OCT and without embedding compound and evaluated using different techniques. In addition, tissue samples from normal spleen, skin, liver and colon were analyzed. Cryo-Gel embedded tissues showed good morphological preservation and no interference in immunohistochemical or immunofluorescent investigations. The quality of extracted RNA and DNA was good. The number of proteins identified using MS was similar between Cryo-Gel embedded samples, samples without embedding compound and OCT embedded samples. However, polymers in the OCT disturbed the signal in the MS, while this was not observed in the Cryo-Gel embedded samples. We conclude that embedding of renal biopsies in Cryo-Gel is an excellent and preferable alternative for OCT compound for both diagnostic and research purposes, especially in those cases where proteomic analysis might be necessary.

1. Introduction

A renal biopsy is often necessary to make a diagnosis in various disease settings affecting both native and transplant kidneys. Biobanking of clinically indicated kidney biopsies is an optimal reservoir for research purposes which is of great importance in understanding the underlying pathophysiology in many kidney diseases.[1, 2] For future studies it is vital that renal tissue is stored in a fashion that maximizes tissue preservation which is crucial for the quality of RNA, DNA and protein retrieval, without interfering with diagnostic evaluation.

Proteomic analysis by mass spectrometry (MS) has been proven to be a powerful tool in the diagnosis and investigation of many kidney diseases.[3] MS is an analytical technique for protein assessment to identify and quantitate molecules based on their mass-to-charge of gas-phase ions. With the use of MS direct analysis of complete sets of proteins in a given tissue sample could be obtained.[4] This could help us in the identification of disease specific proteins in kidney tissue and to better understand the pathogenesis of kidney diseases. For example, MS is used as an ancillary tool for typing of amyloidosis and is used to confirm and identify immunoglobulins in immune-complex mediated proliferative glomerulonephritis and complement factors in complement mediated proliferative glomerulonephritis.[5, 6] Furthermore, the finding of disease specific proteins could lead to diagnostic and prognostic biomarkers for disease diagnosis and new therapeutic interventions.[7, 8]

Renal biopsies are often either fixed in formalin and then embedded in paraffin or fresh snap frozen. It is a challenge to perform proteomic analysis on formalin-fixed paraffin-embedded (FFPE) tissue due to the formation of both intra- and intercellular crosslinking between proteins.[9,-11] MS analyses perform best on proteins extracted from fresh snap frozen tissue. Since frozen tissue without embedding compound is difficult to cut an embedding medium is often used.

Currently the most common medium in which biopsy material is snap frozen is optimal cutting temperature (OCT) compound, a cryopreservative medium composed of polyethylene glycol (PEG), polyvinyl alcohol (PVA) and nonreactive ingredients.[12] OCT stabilizes tissue allowing easy positioning of tissue samples in the microtome. Since the consistency of frozen OCT is more or less the same as the frozen tissue sample and since OCT provides a smooth cutting surface, the quality of sectioning is good. Furthermore, OCT is effective in preserving morphologic and immunohistochemical characteristics.[4, 12] Unfortunately, OCT medium also has disadvantages. MS analyses of OCT embedded tissue is difficult due to the presence

of water soluble synthetic polymers. The interference of these polymers in the MS analysis causes suppression of ion formation.[9] In addition, the presence of high polymer peaks of OCT in the mass spectra may hide other smaller peaks.[13] It is therefore vital that OCT is removed from samples before MS analysis is performed which is a complex and time-consuming procedure resulting in a lower protein yield.[9, 12, 14, 15]

Cryo-Gel, a possible alternative embedding medium for OCT, is a highly viscous, biodegradable and completely water-soluble medium. Cryogels are polymeric gels formed after freezing of the solvent (most often water). They are known to be of significant interest in various areas and are often used in tissue engineering and biotechnology.[16, 17] In the current study we investigate the feasibility of Cryo-Gel for snap freezing of renal biopsies in routine diagnostics and subsequent research analysis. In addition, Cryo-Gel embedded tissue samples from normal spleen, skin, liver and colon were analyzed.

2.   Methods

Fresh samples of normal renal cortex were obtained within 2 hours after surgery from a 46-year-old male who had a total kidney resection due to a renal malignancy. Samples were snap frozen using either Cryo-Gel embedding medium (Leica, Surgipath, the Netherlands), Tissue-Tek OCT Compound (Sakura Finetek, the Netherlands) or no embedding compound. The quality of tissue histology, EM, DNA, RNA and proteins was evaluated (Figure 1). In addition, fresh samples from normal spleen, skin, liver and colon from surgical resections due to malignancies were collected. These tissues were snap frozen using Cryo-Gel, OCT and no compound. The quality of tissue histology, DNA, RNA and proteins was evaluated in these tissues. For each medium two samples were embedded. For renal tissues, the experiments were performed in duplicate. In addition, a section of a renal biopsy from a patient with known lupus nephritis was used to evaluate the quality of immunofluorescence (IF) on Cryo-Gel embedded tissue.
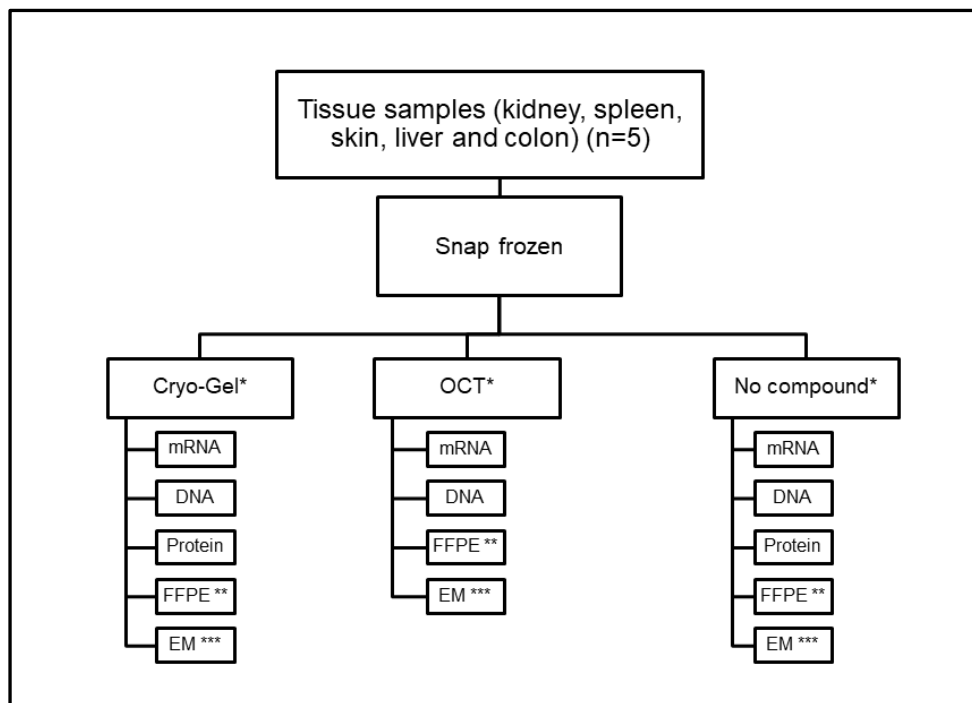
Figure 1. Flowchart showing the work-up protocol performed on normal tissue samples from kidney, spleen, skin, colon and liver. Samples were embedded in either Cryo-Gel, OCT or without compound.

*Two samples were embedded from the different tissues for each embedding medium. For the renal tissues, the additional performed techniques were all performed in duplicate.

**H&E was performed on all tissue samples. PAS, Jones, Trichrome and immunohistochemistry for AE1/AE3 and CD31 were performed on the renal samples. PAS, Trichrome, Sirius Red and Iron stain were performed on the liver samples.

***EM was only performed on the renal samples.

2.1 Cryosectioning

Tissue samples were placed in a cryomold and covered with either Cryo-Gel, OCT or no compound and immersed in cold isopentane with liquid nitrogen until snap-frozen. After solidification, the cryomolds were removed and tissues were stored at −80 °C until cryosectioning. Routine cryosectioning was performed using a cryostat (Leica CM 1950, Netherlands) at −20 °C. For the renal tissues, the experiments were performed after 9 months of storage. For all other tissue samples, the experiments were performed within a week after snap-freezing. For those tissues frozen without embedding compound, a small drop of NaCl was used to mount the

tissue sample on the cryostat microtome object holder to keep the tissue in place. Four micrometer cryostat sections were cut from the samples frozen with Cryo-Gel, OCT and without compound in a cryostat (Leica CM 1950, Netherlands) and subsequently stained with hematoxylin and eosin (H&E) and evaluated by light microscopy.

2.2   RNA

Five 10 µm cryostat sections from the tissue samples frozen with Cryo-Gel, OCT and without embedding compound were cut to analyze the quality and quantity of the RNA. The cryostat sections were placed in 700 µL Qiazol (Qiagen, Germany). The tissue sections were disrupted by shaking the tubes vigorously for about 5 sec. Total RNA was isolated according to the protocol of the miRNeasy mini kit (Qiagen, Germany). RNA samples were subsequently placed on ice for approximately 30 min prior to RIN measurement with the Bioanalyzer (Agilent RNA 6000 Nano kit, Agilent Technologies, Germany).[18] A RIN value of ≥6.5 was used as a cut-off for good RNA quality.[19, 20]

2.3   DNA

Five cryostat sections of 10 µm from the tissue samples frozen with Cryo-Gel, OCT and without embedding compound were cut and placed into individual eppendorf vials. Proteinase K (7.5 AU, Qiagen, Germany) was added to all the samples and left for protein digestion at 56 °C. Then, the samples were placed at 95 °C for 10 minutes for proteinase K deactivation and spun down at 14,000 RPM for 5 minutes.

For subsequent DNA quality assessment, we applied multiplex PCR on isolated DNA from the samples embedded in Cryo-Gel, OCT and without compound. PCR was performed using the following primers: TBXAS1//X9U, forward PCR, GCC CGA CAT TCT GCA AGT CC; reversed PCR, GGT GTT GCC GGG AAG GGT T (PCR product of 100 bp); RAG1/ X2U, forward PCR, TGT TGA CTC GAT CCA CCC CA; reversed PCR, TGA GCT GCA AGT TTG CT GAA (PCR product of 200 bp); PLZF/X1U, forward PCR, TCG GAT GTG GTC ATC ATG GTG; reversed PCR, CGT GTC ATT GTC GTC TGA GGC (PCR product of 300 bp) and AF4/X11U, forward PCR CCG CAG CAA GCA ACG AAC C and reversed PCR GCT TTC CTC TGG CGG CTC C (PCR product of 400 bp). PCR was performed in 15 µl reaction volumes containing 4.5 µl H2O, 7.5 µl KAPA2G HotstartReadymix, 1 µl each of forward and reverse primer with concentration of 100 ng/µl and 1 µl DNA. Cycling conditions were 3 min at 95 °C for initial denaturation, 35 cycles each with 15 sec at 95 °C, 15 sec at 60 °C and 15 sec at

72 °C for denaturation, annealing and extension, and a final elongation step of 7 min at 72 °C. This was followed by electrophoresis on agarose gel (1%) in Tris Broom EDTA (TBE) to analyze the bands of the corresponding PCR products.

2.4   **Proteomics**

In the renal samples, frozen tissue in Cryo-Gel and without compound was processed for proteomic analyses. In the other tissue samples (spleen, skin, liver and colon), proteomics was performed on the Cryo-Gel embedded samples, samples without compound and the OCT embedded tissue. Ten cryostat sections of 5 μm from the tissue samples were processed into 100 μl digestion buffer containing 0.1% Rapigest (Waters, United States) in 50 mM ammonium bicarbonate (Sigma Aldrich, Netherlands) and was lysed through sonication at 70% amplitude. Proteins were incubated at 60 °C for 30 minutes after reducing with a 100 mM dithiothreithol solution (Sigma Aldrich, Netherlands), and alkylated with a 300 mM iodoacetamide solution (Sigma Aldrich, Netherlands) at room temperature and in darkness for 30 min. Then trypsin (600 ng/sample, Promega) was added and samples were digested overnight at 37 °C. The digested samples were then acidified with trifluoroacetic acid (Sigma Aldrich, Netherlands) to a final concentration of 0.5%, and spun down at 14,000 RPM for 30 minutes. Supernatants were collected and transferred to a LC glass vial for further LC-MS measurement. Digested proteins were separated on a nano-LC (Ultimate 3000, Thermo Fisher Scientific, Germany) equipped with a reverse phase analytical column (PepMap C18, 75 μm ID 15 cm, 3 μm particle size and 100 Å pore size, Thermo Fisher Scientific, Netherlands) and peptides were eluted with the following gradient of solvent A and B: 4% to 38% of solvent B in 90 minutes. Solvent A consists of 0.1% aqueous formic acid in water and solvent B consists of 80% acetonitrile and 0.08% aqueous formic acid.

MS measurements were performed on a LTQ Orbitrap XL. For electro-spray ionization (ESI), nano ESI emitters (New Objective, United States) were used and a spray voltage of 1.5 kV was applied. For MS detection a data-dependent acquisition method was used: a high resolution MS scan from 400 to 1600 Th was performed in the Orbitrap, resolution 30.000, lock mass was set to 445.120025 Th (protonated $(Si(CH3)2 O)6$). Based on this MS scan, most intense ions were consecutively isolated and fragmented with a 'Top five' setting. After selection ions were placed on a dynamic exclusion list for 3 min. Settings for MS/MS fragmentation were: 30 ms maximal fill time; isolation width of 2.0 *m/z*; fragmentation by collision induced dissociation (CID) applying 35% normalized collision energy; detection of fragment

ions in the linear ion trap. After precursors were selected for MS/MS, they were excluded within a tolerance range of 10 ppm for further MS/MS analysis for 1 min.

To calculate the number of identified proteins and peptides we used Scaffold (version 4.8.4, Proteome Software Inc., United States). Filter criteria for protein identification were set to >99% protein probability and >99% peptide probability. Proteins that were associated with ≥1 peptides were included. The mean number of proteins identified in samples embedded in Cryo-Gel, OCT and without compound were calculated. Furthermore, the sum of all different proteins in each category was calculated in the renal samples.

2.5 Formalin-fixed paraffin embedded tissue

Half of each snap-frozen tissue sample embedded in Cryo-Gel, OCT and without embedding compound was subsequently processed for FFPE. Frozen tissue samples were thawed in formalin and after fixation, the tissue was dehydrated, cleared and infiltrated with melted paraffin wax. After solidification, 4 μm sections were cut and stained according to routine diagnostic practice for H&E. For the renal tissue, 2 μm sections were cut and subsequently stained by H&E, periodic acid–Schiff (PAS), Jones and Trichrome. In addition, immunohistochemical stainings for AE1/AE3 and CD31 were performed on the renal tissue to asses if snap freezing in different medium effects immunohistochemical staining. On the liver samples, PAS, Trichrome, Sirius Red staining and Iron staining were performed. The staining protocols are described in the Supplementary Methods. All slides were microscopically evaluated by three pathologists (MS, MD and MCvG). The quality of the different stainings was assessed by comparing the intensity of staining in both the cytoplasm and nuclei. Also, the degree of background staining was compared. The OCT embedded samples were used as golden standard.

2.6 Electron microscopy

The remaining tissue of snap-frozen kidney samples were processed for transmission EM. Semi-thin (1 μm) survey sections were stained with toluidine blue and investigated for the presence of glomeruli. Ultra-thin (40 nm–60 nm) sections were cut, mounted on copper grids and contrasted with uranyl acetate and lead citrate. The sections were examined using a Morgagni 268D EM microscope (Thermo Fisher Scientific, United States). EM quality was assessed by two pathologists (MS and MCvG) by evaluating different structures; glomerular basement membrane (*e.g.* thickness, double contours, splitting), podocytes (effacement of podocyte foot

processes), endothelium (swelling, loss of fenestration, tubuloreticular inclusions) and depositions (subepithelial, intramembranous, subendothelial, mesangial).

2.7   Immunofluorescence

To determine the effects of Cryo-Gel on IF, a biopsy sample of cortical renal tissue from a patient with known lupus nephritis was split. One half was embedded in OCT and the other half in Cryo-Gel. Three micrometer sections were cut and IF was performed for IgG, IgA, IgM, C3c, C1q, kappa and lambda according to standard diagnostic routine for both embedding compounds. The quality of the different stainings was assessed by two pathologists (MS and MCvG) by comparing the structures were deposition was observed, the pattern of staining (linear, granular) and the intensity of staining. The OCT embedded sample was used as golden standard.

2.8   Statistical analysis

SPSS Statistics version 24.0 was used (IBM SPSS Statistics for Windows. Armonk, NY:IBM Corp.). The One-way Anova was used to compare RIN values, RNA concentration and the number of proteins and peptides between the different embedding compounds. Differences with a (two sided) p-value $\leq$ 0.05 were considered statistically significant.

2.9   Medical ethics

The study protocol was consistent with international ethical and professional guidelines. The use of anonymized rest material is regulated under the code for proper secondary use of human tissue in the Netherlands. The local medical ethics committee of the Erasmus MC, University Medical Center Rotterdam, Rotterdam, The Netherlands, approved that our study is exempt from the requirement for approval (MEC-2016-350). Informed consent to the use of medical record data and rest material was waived in accordance with the Dutch regulations.

3.   Results

The work-up protocol was performed on normal tissue samples embedded in either Cryo-Gel, OCT or without compound (Figure 1). Sections of both Cryo-Gel

and OCT embedded samples were easily cut. However, samples snap-frozen without embedding compound were less stable and therefore less easily cut.

3.1   Histology, histochemistry and immunohistochemistry

Tissue morphology of H&E stained frozen sections and histochemistry and immunohistochemistry on sections of frozen samples converted to FFPE material showed good results in all methods of embedding (Figure 2 and Supplementary Figure 1). No differences in background staining were observed. However, OCT embedded tissue showed more eosinophilic cytoplasm in the liver and spleen tissue samples and the nuclei were darker in the renal tissue samples in the H&E staining.
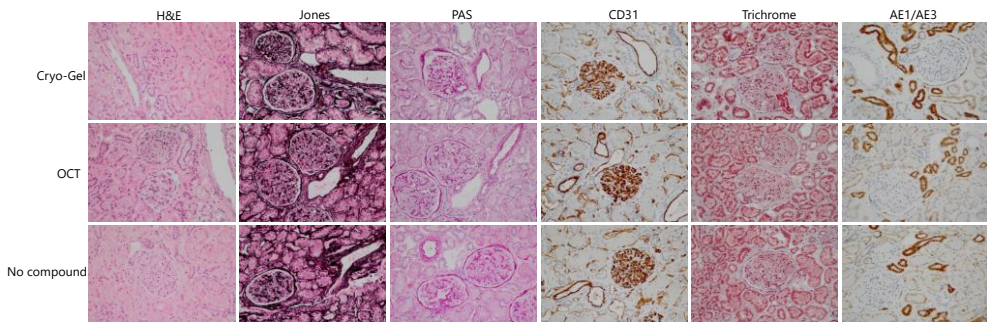
Figure 2. H&E, Jones, PAS, CD31, Trichrome and AE1/AE3 staining on frozen renal tissue samples embedded in Cryo-Gel, OCT and without compound converted to FFPE material (magnification 20x).

3.2   RNA

RNA analysis was performed in duplicate on both renal samples for each embedding method. In the renal tissues, the Cryo-Gel samples showed a mean RNA concentration of 289.8 ng/µl. In the OCT embedded samples and the samples without compound the mean RNA concentration was 210.0 ng/µl and 192.5 ng/µl respectively. No significant differences between RNA concentrations were measured between the different embedding methods ($p = 0.094$) in the renal samples. A mean RNA Integrity Number (RIN) of 9.43 ± 0.13, 9.08 ± 0.43 and 8.83 ± 0.22 was found for the renal samples embedded in Cryo-Gel, OCT and without compound, respectively (Figure 3). No significant difference was found between the RIN value in the Cryo-Gel and OCT embedded samples ($p = 0.167$). Interestingly, a significant higher RIN value was observed in the Cryo-Gel embedded samples compared to samples without compound ($p = 0.003$).

Skin, colon and liver tissues showed good RIN values in all different embedding compounds. Only the spleen tissue samples showed lower RIN values in all embedding compounds. In one of the skin samples without compound no RIN value could be detected while the other skin samples showed a good RIN value (Supplementary Table 1).
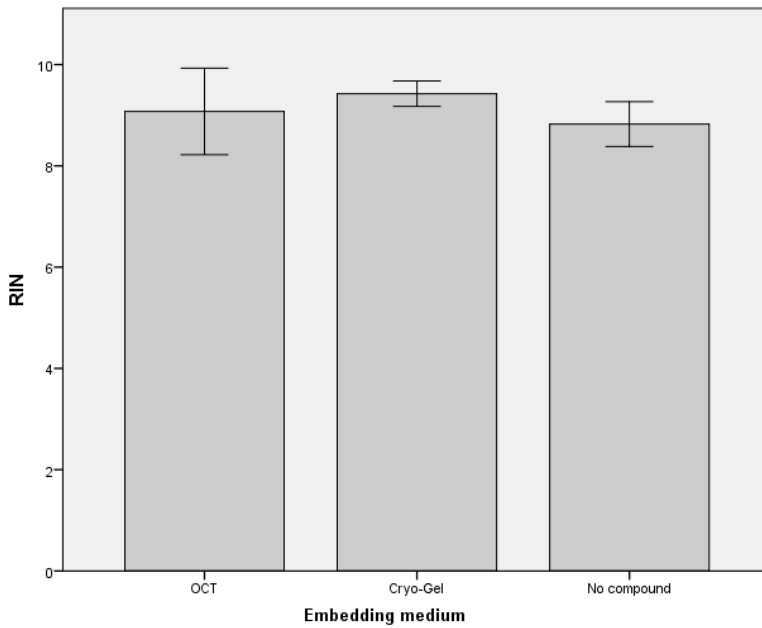
Figure 3. Mean RIN values for samples embedded in Cryo-Gel, OCT and without compound.

3.3   DNA

DNA analysis using PCR was performed in duplicate on the renal samples for each embedding method. All samples showed products at 400, 300, 200 and 100 bp representing a good quality of DNA in the kidney samples (Figure 4). Skin, colon and liver tissue samples all showed signals up to 400 bp. The spleen samples showed products up to 300 and 400 bp (Supplementary Table 2).
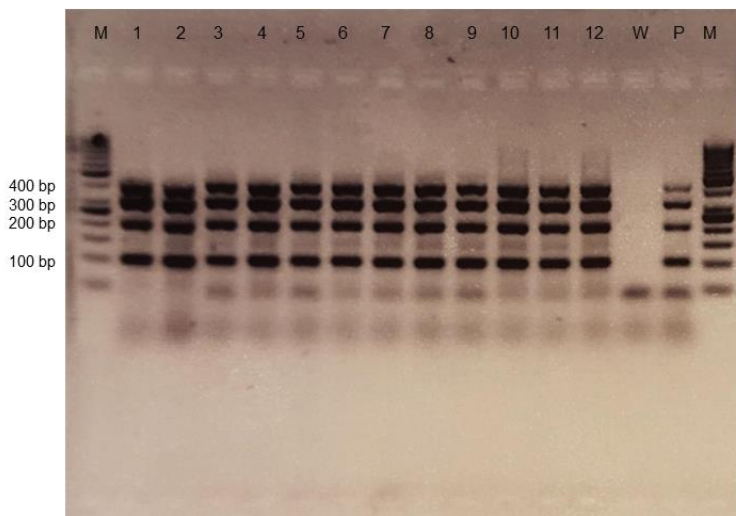
Figure 4. PCR results of Cryo-Gel samples (lane 1–4), OCT samples (lane 5–8) and samples without compound (lane 9–12) showing a product at 400, 300, 200 and 100 bp. All experiments included a positive control (P) and a negative water control (W).

3.4 Proteomics

Quantitative proteomic data from Cryo-Gel embedded renal tissues were compared to data from renal tissues without compound. The MS results showed no detectable polymers in both the Cryo-Gel samples and the samples without compound. A mean of 412 ± 64 proteins was identified in the Cryo-Gel samples and 451 ± 59 in the samples without compound (p = 0.398). In the Cryo-Gel samples 558 different proteins were identified versus 568 proteins in samples without compound. Four-hundred-seventy of the identified proteins were present in both groups (Figure 5). A mean of 2397 ± 97 peptides was identified in the Cryo-Gel samples and 3019 ± 59 in the samples without compound (p = 0.066). In Cryo-Gel samples 2903 different peptides were observed versus 3738 peptides in samples without compound (Figure 5).

The identified proteins were categorized by their cellular compartment and biological function using gene ontology (GO) software. Virtually identical percentages of proteins were identified in the different categories of Cryo-Gel samples and samples without compound (Supplementary Figure 2).

In tissue samples from spleen, liver, skin and colon, no differences between protein and peptide identification were observed between the different embedding methods (Supplementary Table 3). Polymers were found in the MS results from the

OCT embedded samples, but not in the Cryo-Gel embedded samples. These polymers can be observed as repeating peaks in the MS (Figure 6) and disturb the MS signal.
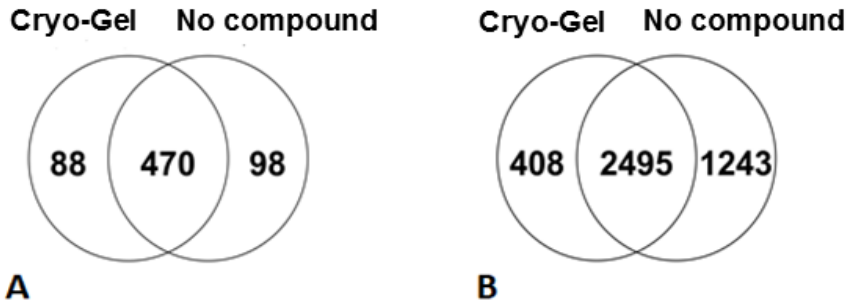
Figure 5. Venn diagram showing the number of different proteins (A) and peptides (B) identified by mass spectrometry and overlap between the samples embedded with Cryo-Gel and without compound.

3.5   Electron microscopy

Electron microscopy (EM) analysis on previously snap-frozen Cryo-Gel embedded renal samples showed well-preserved material. The results were similar to OCT embedded samples and samples without tissue compound (Figure 7). All samples showed well preserved podocytes and no depositions were observed. No differences in glomerular basement membrane thickness were found and no double contours were observed. The endothelium showed normal fenestration in all the three embedding methods.

3.6   Immunofluorescence

IF was performed on renal tissue from a patient with known lupus nephritis and showed similar results for Cryo-Gel and OCT embedded tissue. The intensity of the IF stainings was good in both the Cryo-Gel and OCT embedded renal tissue. No differences in staining pattern were observed between the renal samples embedded in Cryo-Gel and OCT. Intense granular membranous staining was seen for IgG. Moderate granular membranous staining was seen for IgA, IgM, C3c, C1q, kappa, and lambda (Figure 8).
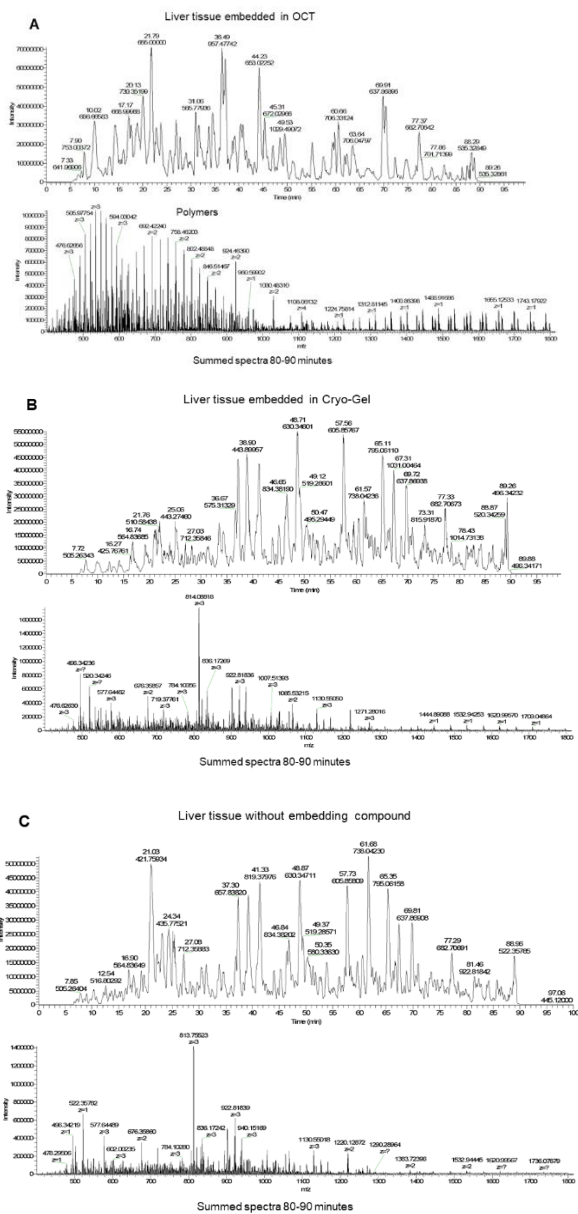
Figure 6. Mass spectra from liver samples embedded in OCT, Cryo-Gel and without compound. The summed spectra at 80–90 minutes show repeating polymer peaks in the OCT embedded samples disturbing the signal, but not in the samples embedded in Cryo-Gel and without compound.
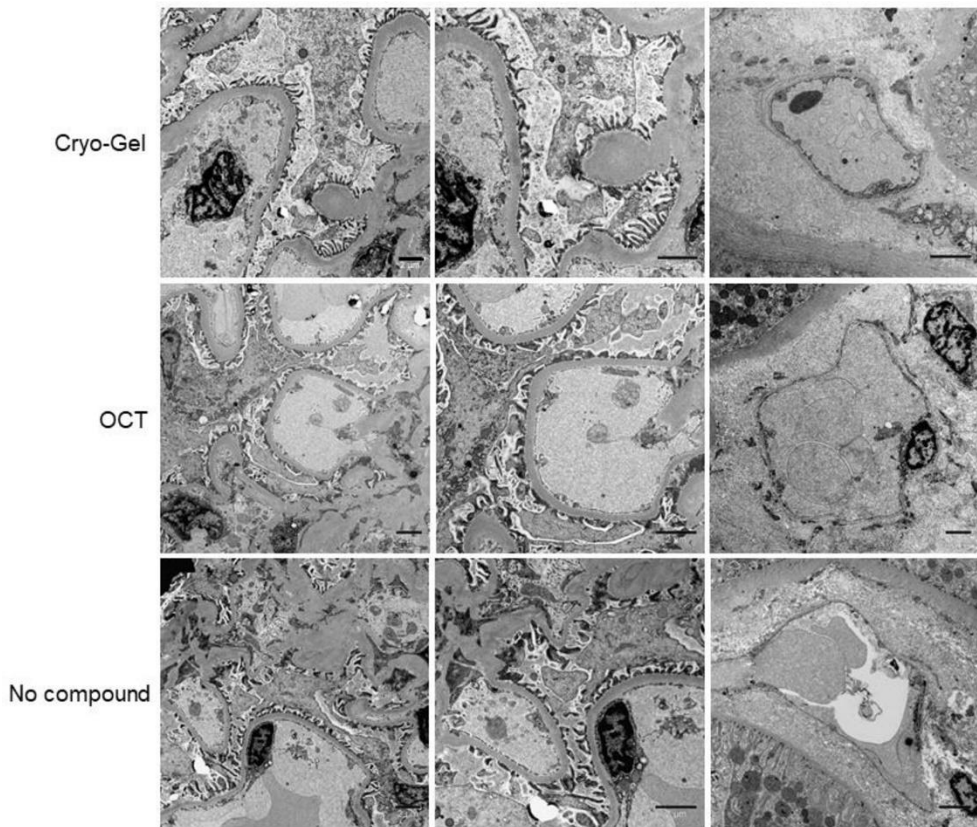
Figure 7. Electron microscopy for samples embedded with Cryo-Gel, OCT and without compound. Left: glomerular filtration membrane (magnification 4400x); middle: higher magnification of glomerular filtration membrane (magnification 7100x); right: peritubular capillary (magnification 7100x, 4400x and 5600x, respectively). Scale bar = 2 µm.
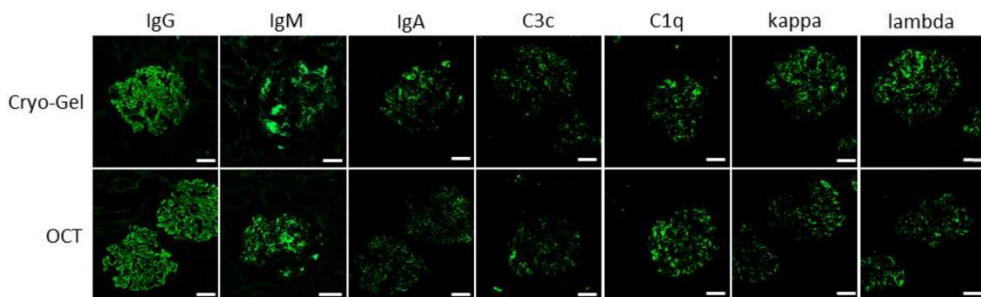
Figure 8. Immunofluorescence staining for IgG, IgM, IgA, C3c, C1q, kappa and lambda from renal cortex form a patient with lupus nephritis embedded in Cryo-Gel and OCT compound (magnification 20x; scale bar = 50 µm).

4.   Discussion

Adequate biobanking of renal biopsies is necessary for diagnostics and subsequent research.[1] The issues that have to be considered regarding proteomics are the quality and quantity of the proteins that can be extracted. OCT is widely used for embedding tissue for snap-freezing, however it is not ideal for MS due to interfering polymers (*e.g.* PVA and PEG) in the OCT.[9, 13] Therefore, we investigated the use of Cryo-Gel as embedding compound. This study shows that Cryo-Gel can be used without any technical problems in MS, which is a big advantage when compared to OCT compound.

Research in kidney proteomics is a fast moving area and has mainly been focused on urine due to non-invasiveness.[21-23] However, using urine as sample source it is not possible to link the expressed proteins in kidney disease to their specific site of production and they might even originate from outside the kidney. The performance of proteomics on renal tissue itself allows for investigation of proteins within the affected kidney compartments.[3] This can be optimized using laser capture microdissection (LCM) in combination with MS. With LCM, areas of interest, such as glomeruli, interstitium or tubuli can be isolated by cutting away the surrounding tissue, making it easier to evaluate protein profiles in specific structures.[6, 24]

Protein extraction of samples embedded in Cryo-Gel was feasible and Cryo-Gel showed no interference in MS analysis. In renal samples, the number of proteins identified in Cryo-Gel embedded tissue was comparable to tissue without compound with a high overlap of identified proteins, although there were slightly fewer peptides identified (NS).

MS on OCT embedded tissue was performed on spleen, skin, colon and liver samples. In these tissue samples, the number of proteins detected was not significant different between the Cryo-Gel and OCT embedded tissues and the tissues without compound. Although, polymers were detected in the MS data from the OCT embedded samples and not in the Cryo-Gel embedded samples. The polymers in the OCT embedded tissue suppress other signals in the MS.[9, 13]

In the present study, the MS data is obtained on an older type of mass spectrometer which is slower compared to the newest generation of MS equipment. The polymers mainly suppress lower abundant signals in the samples which are, because of the speed of the used instrument, probably not sequenced. This could be a potential explanation for the fact that no difference in the amount of protein

identifications is observed even while the polymer signal is clearly present in the acquired spectra.

The polymers in OCT are very hydrophobic and have a strong interaction with the C18 stationary phase of the MS columns. Stringent washing steps of the columns are required to remove these polymers from the columns. A portion of the polymers may even bind irreversibly and effect the lifetime and the separation performance of the columns considerably. The performance of MS analysis on OCT embedded tissue samples is therefore discouraged. We recommend the use of Cryo-Gel embedding compound to not exclude the possibility of MS analysis.

Methods to remove OCT from the tissue samples before protein extraction and MS have been described.[10, 25] Recently, Vrana *et al.* described an optimized method to extract proteins from OCT embedded tissue samples.[12] They removed the excess of frozen OCT compound around the kidney tissue samples before thawing the tissue. Then diethyl ether/methanol extraction was performed to remove the remaining of OCT. To decrease the risk of ion suppression by OCT in the MS analysis, a second cleaning step with methanol/chloroform/water extraction was added to the procedure. This shows that the removal of OCT from the tissue samples for MS analysis is a time-consuming procedure which takes multiple steps.

Unfortunately, the chemical compounds of Cryo-Gel are confidential. Since Cryo-Gel did not cause interference in MS analysis, we assume that Cryo-Gel does not contain polymers like those in OCT compound. It is also possible that Cryo-Gel only contains polymers that can be broken down in the preparation steps for proteomic analysis (trypsinization and digestion) and that therefore no problems in MS analysis are observed.

Tissue morphology and different stainings on the Cryo-Gel embedded samples showed similar results to tissue embedded in OCT and those without compound. Also, the quality of DNA was good in the different tissues and no major differences were observed between the different embedding compounds. RNA showed comparable yield in Cryo-Gel and OCT embedded tissues and tissues without embedding compound. No significant difference was observed between the RIN value in Cryo-Gel and OCT embedded renal tissues. Interestingly, renal tissue without embedding compound had a significantly lower RIN value, although the RNA was still of good quality. Spleen samples showed a lower RIN value in all different embedding methods compared to the other tissue types. This is probably caused by external conditions, such as changes in tissue temperature, causing RNA

degradation, for which spleen tissue is more sensitive than the other tissues that were used.

A limitation of the present study is the small number of tissue samples used for evaluation. However, different types of tissue were analyzed and different experiments to test the use of Cryo-Gel were performed. Furthermore, two samples of all different tissue types were obtained for each embedding compound and the experiments on the renal tissue samples were performed in duplicate. A vital issue for tissue biobanking for future research is the maintaining of protein stability over time. We show that Cryo-Gel compound has good protein preservation in renal tissue after 9 months of storage at −80 °C. Further research is necessary to analyze the protein stability of Cryo-Gel embedded tissue after a longer storage time.

We conclude that Cryo-Gel is an excellent compound for snap-freezing renal biopsies for both diagnostic and research purposes involving not only histomorphology and immunofluorescence, but also RNA, DNA and protein analysis.

References

1. Riegman PH, van Veen EB. Biobanking residual tissues. *Hum Genet*. 2011;130(3):357–68.

2. Zatloukal K, Hainaut P. Human tissue biobanks as instruments for drug discovery and development: impact on personalized medicine. *Biomark Med*. 2010;4(6):895–903.

3. Charonis A, Luider T, Baumann M, Schanstra JP. Is the time ripe for kidney tissue proteomics? *Proteomics Clin Appl*. 2011;5(5-6):215–21.

4. Schwartz SA, Reyzer ML, Caprioli RM. Direct tissue analysis using matrix-assisted laser desorption/ionization mass spectrometry: practical aspects of sample preparation. *J Mass Spectrom*. 2003;38(7):699–708.

5. Sethi S. Mass spectrometry-based proteomic diagnosis of renal immunoglobulin heavy chain amyloidosis. *Clin J Am Soc Nephrol*. 2010;5(12):2180–7.

6. Sethi S, Vrana JA, Theis JD, Dogan A. Mass spectrometry based proteomics in the diagnosis of kidney disease. *Curr Opin Nephrol Hypertens*. 2013;22(3):273–80.

7. Haas M. Glomerular Disease Pathology in the Era of Proteomics: From Pattern to Pathogenesis. *J Am Soc Nephrol*. 2018;29(1):2–4.

8. Thongboonkerd V. Current status of renal and urinary proteomics: ready for routine clinical application? *Nephrol Dial Transplant*. 2010;25(1):11–16.

9. Shah P, Zhang B, Choi C, et al. Tissue Proteomics Using Chemical Immobilization and Mass Spectrometry. *Anal Biochem*. 2015;469:27–33.

10. Zhang W, Sakashita S, Taylor P, Tsao MS, Moran MF. Comprehensive proteome analysis of fresh frozen and optimal cutting temperature (OCT) embedded primary non-small cell lung carcinoma by LC-MS/MS. *Methods*. 2015;81:50–5.

11. Magdeldin S, Yamamoto T. Toward deciphering proteomes of formalin-fixed paraffin-embedded (FFPE) tissues. *Proteomics*. 2012;12(7):1045–58.

12. Vrana M, Goodling A, Afkarian M, Prasad B. An Optimized Method for Protein extraction from OCT-embedded human kidney tissue for protein quantification by LC-MS/MS proteomics. *Drug Metab Dispos*. 2016;44(10):1692–6.

13. Setou M. Imaging mass spectrometry: protocols for mass microscopy. Vol. 2010. (Springer, 2010).

14. Weston LA, Hummon AB. Comparative LC-MS/MS analysis of optimal cutting temperature (OCT) compound removal for the study of mammalian proteomes. *Analyst*. 2013;138(21):6380–4.

15. Palmer-Toy DE, Krastins B, Sarracino DA, Nadol JB Jr, Merchant S. N. Efficient method for the proteomic analysis of fixed and embedded tissues. *J Proteome Res*. 2005;4(6):2404–11.

16. Henderson TMA, Ladewig K, Haylock DN, McLean KM, O'Connor AJ. Cryogels for biomedical applications. *J Mater Chem B*. 2013;1:2682–2695.

17. Lozinsky VI. Cryostructuring of Polymeric Systems. 50. Cryogels and Cryotropic Gel-Formation: Terms and Definitions. *Gels*. 2018;4(3):77.

18. Schroeder A, Mueller O, Stocker S, et al. The RIN: an RNA integrity number for assigning integrity values to RNA measurements. *BMC Mol Biol.* 2006;7:3.

19. Fasold M, Binder H. Estimating RNA-quality using GeneChip microarrays. *BMC Genomics.* 2012;13;186.

20. Strand C, Enell J, Hedenfalk I, Fernö M. RNA quality in frozen breast cancer samples and the influence on gene expression analysis – a comparison of three evaluation methods using microcapillary electrophoresis traces. *BMC Mol Biol.* 2007;8:38.

21. Sedor JR. Tissue proteomics: a new investigative tool for renal biopsy analysis. *Kidney Int.* 2009;75(9):876–9.

22. Beasley-Green A. Urine Proteomics in the Era of Mass Spectrometry. *Int Neurourol J.* 2016;20(Suppl2):S70–75.

23. Thomas S, Hao L, Ricke WA, Li L. Biomarker discovery in mass spectrometry-based urinary Proteomics. *Proteomics Clin. Appl.* 2016;10(4):358–70.

24. Fend F, Raffeld M. Laser capture microdissection in pathology. *J Clin Pathol.* 2000;53(9):666–72.

25. Johnson H, White FM. Quantitative analysis of signaling networks across differentially embedded tumors highlights interpatient heterogeneity in human glioblastoma. *J Proteome Res.* 2014;13(11);4581–93.

Author contributions

Conceptualization: M.S., P.R., F.v.K. and M.C.v.G.; analysis: M.S., M.Z., L.d.W., R.d.L., M.O., S.A., T.v.d.B., L.D. and T.L.; data interpretation: S.A., M.S., M.Z., L.D., M.D., T.L. and M.C.v.G.; writing—original draft: M.S., M.Z. and M.C.v.G.; writing—review and editing: M.S., M.Z., L.W., R.d.L., M.O., S.A., T.v.d.B., T.L., F.v.K., P.R. and M.C.v.G.

Competing interests

Supplementary Files

Table S1. RNA analysis in spleen, skin, liver and colon tissue.

	Embedding compound		RIN value	RNA concentration (ng/µl)
Spleen	OCT	1	5,4	90
		2	5,5	119
	Cryo-Gel	1	5,1	297
		2	5,1	357
	No compound	1	5,4	163
		2	5,3	259
Skin	OCT	1	8,5	11
		2	9,9	51
	Cryo-Gel	1	9,6	90
		2	9,2	17
	No compound	1	8	22
		2	NA	3
Liver	OCT	1	8,9	47
		2	8,6	24
	Cryo-Gel	1	9	200
		2	8,9	91
	No compound	1	8,8	262
		2	8,9	111
Colon	OCT	1	8,5	14
		2	8,7	21
	Cryo-Gel	1	7,1	10
		2	10	26
	No compound	1	8	17
		2	9,7	10

The RIN (RNA Integrity Number) and RNA concentration were measured in the spleen, skin, liver and colon tissue samples embedded in OCT, Cryo-Gel and without compound.

NA = not available

Table S2. DNA analysis in spleen, skin, liver and colon tissue.

		OCT		Cryo-Gel		No compound	
		DNA concentration (ng/ul)	PCR	DNA concentration (ng/ul)	PCR	DNA concentration (ng/ul)	PCR
Spleen	1	33,1	signal up to 400bp	26,0	signal up to 300bp	42,3	signal up to 400bp
	2	35,7	signal up to 400bp	54,0	signal up to 300bp	36,2	signal up to 300bp
Skin	1	2,52	signal up to 400bp	2,97	signal up to 400bp	3,58	signal up to 400bp
	2	0,99	signal up to 400bp	1,50	signal up to 400bp	1,12	signal up to 400bp
Liver	1	10,5	signal up to 400bp	16,5	signal up to 400bp	17,1	signal up to 400bp
	2	9,4	signal up to 400bp	15,7	signal up to 400bp	14,0	signal up to 400bp
Colon	1	3,91	signal up to 400bp	3,23	signal up to 400bp	3,93	signal up to 400bp
	2	4,69	signal up to 400bp	3,12	signal up to 400bp	3,16	signal up to 400bp

PCR was performed on the spleen, skin, liver and colon tissue samples embedded in OCT, Cryo-Gel and without compound. DNA concentration and PCR signals were measured.

Table S3. Proteomic analysis in spleen, skin, liver and colon tissue.

	Embedding compound		Protein identification	P	Peptide identification	P
Spleen	OCT	1	367	0.064	2214	0.187
		2	370		2389	
	Cryo-Gel	1	388		2484	
		2	409		2655	
	No compound	1	370		2279	
		2	366		2419	
Skin	OCT	1	73	0.866	678	0.683
		2	64		562	
	Cryo-Gel	1	63		555	
		2	69		595	
	No compound	1	52		467	
		2	74		623	
Liver	OCT	1	463	0.145	3251	0.455
		2	473		3285	
	Cryo-Gel	1	474		3304	
		2	473		3285	
	No compound	1	463		3259	
		2	460		3287	
Colon	OCT	1	291	0.518	2422	0.343
		2	144		1321	
	Cryo-Gel	1	246		1460	
		2	124		553	
	No compound	1	252		1779	
		2	329		2197	

Proteomic analysis was performed on the spleen, skin, liver and colon tissue samples embedded in OCT, Cryo-Gel and without compound. The number of proteins and peptides identified in samples embedded in OCT, Cryo-Gel and without compound showed no significant differences.

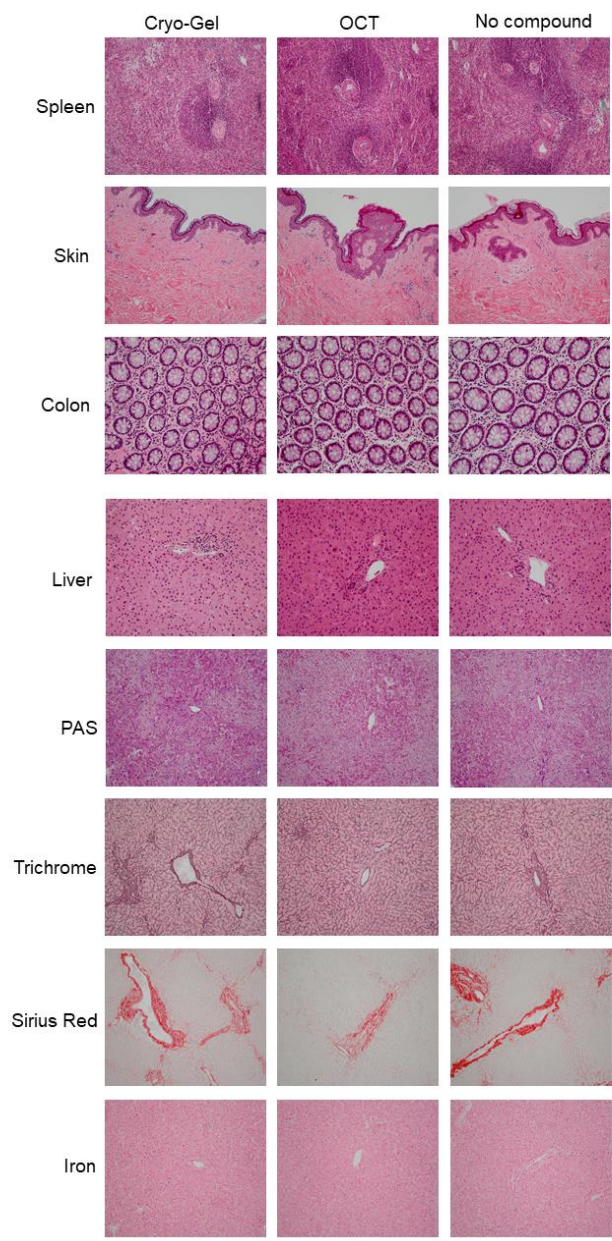Figure S1. H&E staining on spleen, skin and colon samples and H&E, PAS, Trichrome, Sirius Red and Iron staining on liver samples embedded in Cryo-Gel, OCT and without compound converted to FFPE material (magnification 20x).
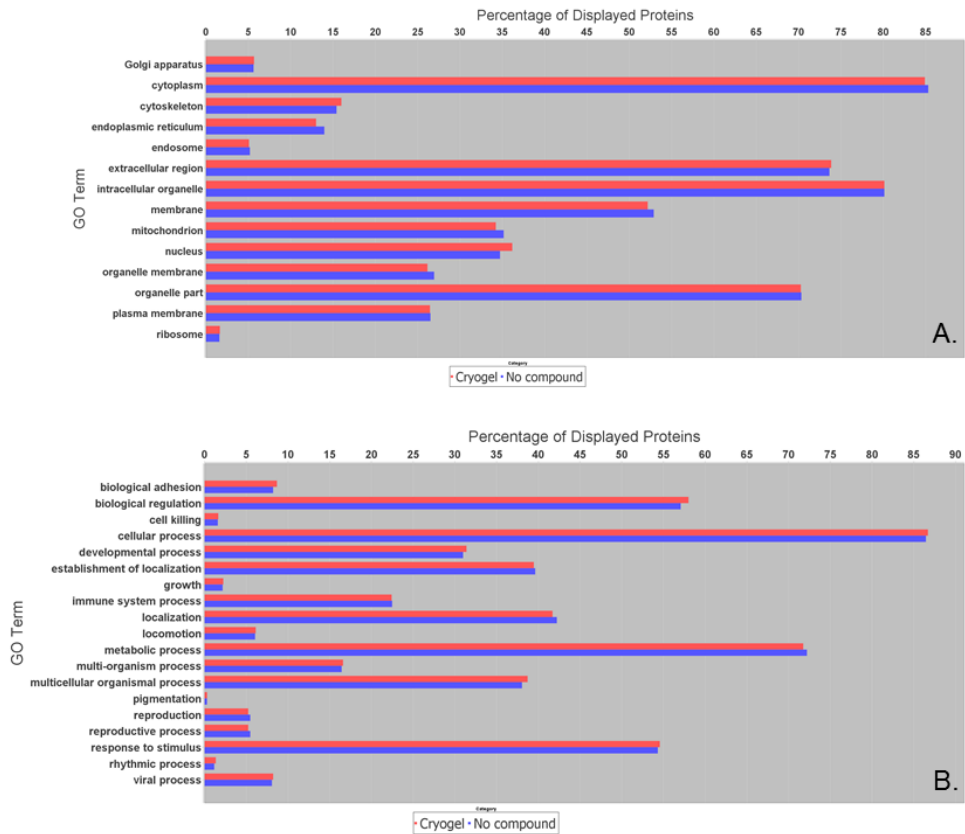
Figure S2. Gene ontology analysis of proteins identified by mass spectrometry for renal samples embedded in Cryo-Gel and without compound categorized by cellular localization (A) and biological process (B).

Supplementary Methods

Protocols of different stainings on FFPE sections:

FFPE sections were stained with H&E using the Automated Ventana Symphony stainer according to manufactures instructions. Histochemical staining for PAS, Trichrome, Jones, Sirius Red and Iron was performed were performed on automated Ventana special stains after deparaffination.

In brief for PAS, slides were heated till 75°C and diastase was added for 12 minutes. Next, Schiffs reagents was added for 20 minutes and lastly a counterstain with hematoxylin was performed.

For Jones, slides were heated till 75°C and then cooled till 60 °C. Jones Silver B reagents was added for 16 minutes and lastly eosin was added as counterstain.

For Trichrome, Trich bouins A was added for 32 minutes and after additional washing steps, hematoxylin A+B was added for 12 minutes. After further washing steps, Trich Red was added for 8 minutes, Trich Mordant was added for 12 minutes and Trich Blue was added for 16 minutes.

For Sirius Red, Fosformolybdeen acid 0,2% was added for 2 minutes and after a washing step, Picro-Sirius Red was added for 60 minutes.

For the Iron staining, slides were heated till 75°C and Iron reagent A was added for 4 minutes. After a washing step, Iron reagent B was added for 4 minutes. After a washing step, Iron NFR was added for 8 minutes.

Immunohistochemical staining for AE1/AE3 and CD31 was performed. For CD31, following deparaffinization and heat-induced antigen retrieval with CC1 (#950-124, Ventana) for 16 minutes, the tissue samples were incubated with CD31 (JC70, #760-4378, Cell Marque) for 20 minutes at 36°C.

For AE1/AE3, following deparaffinization, protease for 3-4 minutes (protease3: 7601-2020, Ventana) and heat-induced antigen retrieval with CC1 (#950-124, Ventana) for 20 minutes, the tissue samples were incubated with AE1/AE3 (E08171, #760-2135, Ventana) for 4 minutes at 37°C.

All stainings were done with appropriate controls.

CHAPTER 3

Oxalate deposition in renal allograft biopsies within 3 months after transplantation is associated with allograft dysfunction

Malou L. H. Snijders[1, 2], Dennis A. Hesselink[2, 3],
Marian C. Clahsen-van Groningen[1, 2]* & Joke I. Roodnat[2, 3]*

1. Department of Pathology, Erasmus MC, University Medical Center Rotterdam, Rotterdam, The Netherlands.
2. Rotterdam Transplant Group, Erasmus MC, University Medical Center Rotterdam, Rotterdam, The Netherlands.
3. Department of Internal Medicine, Division of Nephrology and Transplantation, University Medical Center Rotterdam, Rotterdam, The Netherlands.
* These authors contributed equally to this work.

Abstract

Background: Calcium oxalate (CaOx) deposition in the kidney may lead to loss of native renal function but little is known about the prevalence and role of CaOx deposition in transplanted kidneys.

Methods: In patients transplanted in 2014 and 2015, all for-cause renal allograft biopsies obtained within 3 months post-transplantation were retrospectively investigated for CaOx deposition. Additionally, all pre-implantation renal biopsies obtained in 2000 and 2001 were studied.

Results: In 2014 and 2015, 388 patients were transplanted, of whom 149 had at least one for-cause renal biopsy. Twenty-six (17%) patients had CaOx deposition. In the population with CaOx deposition: Patients had significantly more often been treated with dialysis before transplantation (89 vs. 64%; p = 0.011); delayed graft function occurred more frequently (42 vs. 23%;p = 0.038); and the eGFR at the time of first biopsy was significantly worse (21 vs. 29 ml/min/1.73m2; p = 0.037). In a multivariate logistic regression analysis, eGFR at the time of first biopsy (OR 0.958, 95%-Cl: 0.924–0.993, p = 0.019), dialysis before transplantation (OR 4.868, 95%-Cl: 1.128–21.003, p = 0.034) and the time of first biopsy after transplantation (OR 1.037, 95%-Cl: 1.013–1.062, p = 0.002) were independently associated with CaOx deposition. Graft survival censored for death was significantly worse in patients with CaOx deposition (p = 0.018). In only 1 of 106 pre-implantation biopsies CaOx deposition was found (0.94%).

Conclusion: CaOx deposition appears to be primarily recipient-derived and is frequently observed in for cause renal allograft biopsies obtained within 3 months post-transplantation. It is associated with inferior renal function at the time of biopsy and worse graft survival.

1.   Introduction

Oxalic acid is a small decarboxylate ion (C_2O_4) and is the end-product of many metabolic pathways. Oxalic acid is eliminated through free glomerular filtration and secretion by the proximal tubule.[1] The plasma concentration of oxalic acid is determined by the balance between dietary intake, intestinal absorption, endogenous production and renal excretion.[2] Normal plasma concentrations are below 5 µmol/l.[3, 4]

Hyperoxaluria, defined as an excessive urinary excretion of oxalic acid, can be classified as primary or secondary hyperoxaluria. Primary hyperoxaluria is caused by rare autosomal recessive disorders which cause an excessive production of oxalic acid.[5-7] In primary hyperoxaluria, persistently elevated plasma oxalic acid concentrations cause CaOx deposition in the kidney which leads to permanent loss of renal function. Combined liver-kidney transplantation is recommended in these cases.[5, 6, 8] Secondary hyperoxaluria is a more common disorder which can be caused by enteric conditions and increased dietary intake of oxalate. In enteric hyperoxaluria, increased absorption of oxalic acid occurs. These are mostly patients with malabsorption as a result of *e.g.* small bowel resections, pancreatic insufficiency or gastric bypass. A high intake of oxalic acid-containing food puts these patients at risk of renal stones or CaOx deposition in their kidneys.[9-11] In addition, studies suggest a contribution of dietary oxalate in renal CaOx deposition in patients without enteric conditions as well.[12-15]

When the GFR drops below 30–40 ml/min/1.73 m^2 oxalic acid elimination by the kidneys is impaired and the plasma concentration rises.[5] In patients with end-stage renal disease (ESRD), high plasma oxalic acid concentrations, that may be up to 10 times above normal levels, may occur.[16-18] Neither hemo- nor peritoneal dialysis can remove sufficient amounts of oxalic acid to normalize the oxalic acid plasma concentrations in patients with ESRD, although it is suggested that the clearance of oxalic acid by hemodialysis exceeds that of peritoneal dialysis.[19, 20] The plasma oxalic acid concentration can be reduced by at least 60% following a single hemodialysis session. However, it returns to pre-dialysis levels within 48 hours.[21, 22]

Plasma oxalic acid concentrations generally normalize within days to weeks after a successful kidney transplantation.[23-25] However, in the first few days after transplantation, a large amount of oxalate is excreted.[25] The urine becomes supersaturated with oxalate when concentrations >30 µmol/L are reached, and this may result in the formation of CaOx crystals, which can deposit in the renal tubules.[5]

Therefore, it can be expected that CaOx deposition is mainly formed in the early post transplantation period, while it probably is less prevalent in the late post transplantation period. However, it is unknown whether this phenomenon affects renal transplant outcome.

The purpose of the present study was to examine if 1) CaOx deposition is associated with kidney allograft dysfunction in the immediate post-operative phase; 2) CaOx deposition is associated with inferior graft survival; and 3) CaOx deposition in the transplanted kidney is recipient- rather than donor-derived. To investigate this, the incidence of CaOx deposition was studied in for-cause kidney allograft biopsies obtained within the first 3 months after transplantation, as well as in a series of preimplantation renal biopsies.

2.   **Patients and methods**

All patients transplanted between January 2014 and December 2015 in the Erasmus MC, University Medical Center Rotterdam, Rotterdam, The Netherlands, were included. The databases of the Departments of Renal Transplantation and Pathology were searched to identify all for-cause renal allograft biopsies performed in these patients within the first 3 months after transplantation. No biopsies were performed for the sake of the present study. Clinical and demographic data of these patients were collected. These included: age at transplantation, type of dialysis (hemodialysis or peritoneal dialysis) and time on dialysis, donor age and type (living or deceased), cold ischemia time (CIT), first warm ischemia time (1_{st} WIT), second warm ischemia time (2_{nd} WIT) and delayed graft function (DGF). For those patients with a for-cause renal biopsy we collected: time to first biopsy, histologic diagnosis (acute rejection/acute tubular necrosis (ATN)/ other), best estimated GFR (eGFR) before biopsy and eGFR at time of the for-cause biopsy. DGF was defined as the need for dialysis during the first week after transplantation.[26, 27]

In addition, all pre-implantation renal transplant biopsies (time zero, t0) obtained in 2000 and 2001 were retrospectively searched (in the database of the Department of Pathology) and re-analyzed for the presence of CaOx, as described below. Both living and deceased donor t0 biopsies were included.

2.1   Histological evaluation

All for-cause and t0 biopsies were processed according to standardized routine diagnostic practice. Light microscopy was performed on 3 µm sections of formalin-fixed paraffin embedded tissue that was stained by hematoxylin and eosin (H&E). CaOx deposition was analyzed on these sections using polarized light by two pathologists (MS and MCvG) who were blinded to patient information. In case of disagreement, consensus regarding the presence of CaOx deposition was reached. CaOx deposition was scored by counting the total number of oxalate depositions in each biopsy. Biopsies were defined as positive for CaOx when ≥1 CaOx deposits were found within the tubular lumen, tubular epithelial cells and/or interstitial space. The surface area of the biopsies with CaOx deposition was measured using the software program ImageJ and expressed as mm^2.[28, 29] The amount of CaOx depositions per mm^2 was calculated as described in the study by Bagnasco *et al*.[30]

2.2   Statistical analysis

SPSS Statistics version 23.0 was used for all statistical analyses (IBM SPSS Statistics for Windows. Armonk, NY: IBM Corp.). For comparison of continuous variables, the one-way ANOVA-test was used. Categorical variables were compared using the Chi-square test. Data were presented as mean ± standard deviation (SD) for continuous variables and as percentages for categorical variables. Differences with a (two sided) p-value of less than or equal to 0.05 were considered statistically significant. Univariate and multivariate logistic regression analysis was used to evaluate which variables are independently associated with CaOx deposition. Graft survival censored for death was compared using Kaplan Meier analysis and log rank test.

2.3   Medical ethics

The study protocol was consistent with professional guidelines; non WMO compliant research is research not residing under the Dutch law on medical research with patients and is regulated by the Dutch Code of Conduct (Federa). The local medical ethics committee of the Erasmus MC, University Medical Center Rotterdam, Rotterdam, The Netherlands, approved that our study is exempt from the requirement for approval (MEC-2018-1580). Informed consent to the use of medical record data and rest material was waived in accordance with the Dutch regulations. All data were anonymized prior to analysis.

3. Results

3.1 Patient characteristics

A total of 388 patients were transplanted in the period studied (2014 and 2015). Of these 388 patients, 77 (19.8%) had DGF. At least one for-cause renal transplant biopsy was performed in 149 patients (38%) and these patients were included in the present study. The characteristics of these patients are depicted in Table 1. In the period studied, 1 patient with primary hyperoxaluria underwent a combined kidney and liver transplantation. Interestingly, a renal allograft biopsy of this patient 9 months after transplantation did not show CaOx deposition. Renal function of this patient remains good 3 years after transplantation. Three patients with enteric hyperoxaluria as the primary kidney disease were transplanted in the period studied. Of these, one was not biopsied during the first year after transplantation. The other two were biopsied in the first 3 months after transplantation. In one patient, the renal biopsy showed CaOx deposition, whereas in the other patient no CaOx deposition was seen. Transplant function remains good in all patients 3.5 years after transplantation. All 4 patients described above had received oxalate lowering treatment pre- and post-transplantation.[31]

A total of 196 biopsies from 149 patients was analyzed, with a median of 1 biopsy per patient (range 1–3). Patients' age ranged from 19 to 79 years (mean 54 ± 14 years). Ninety-seven patients (65%) received a graft from a living donor and 52 patients (35%) from a deceased donor. The histological diagnosis was rejection in 69 patients (46%), ATN in 36 patients (24%), and ''other'' in the remaining 44 (30%) patients (Table 1).

3.2 CaOx deposition in the renal allograft biopsy

Twenty-six patients (17%) showed CaOx deposition in their for-cause biopsy obtained within 3 months after transplantation. In 111 patients only 1 biopsy was performed and CaOx deposition was observed in 14 of them. Thirty-eight patients had more than 1 biopsy within 3 months after renal transplantation and CaOx deposition was observed in 12 of them; in 3 patients CaOx deposition was found in all the biopsies, in 3 patients CaOx deposition was observed in the first biopsy but not in the second (or third) biopsy. Six patients showed CaOx deposition in their repeat biopsy only.

Table 1. Characteristics of patients with and without CaOx depositions.

Parameters	All	No oxalate	Oxalate	P
N (%)	149	123 (83)	26 (17)	
Recipient age (years)	54±14	55±14	52±15	0.409
Time on dialysis (months)	19±25	18±26	23±21	0.833
RRT before transplantation				0.011
HD/PD	102 (68.5)	79 (64)	23 (89)	
None	47 (31.5)	44 (36)	3 (11)	
Donor age (years)	55±14	55±14	55±13	0.934
Living donor (%)	97 (65)	84 (68)	13 (50)	0.062
CIT (min)	362±321	346±316	436±344	0.201
1st WIT (min)	4.8±5.7	4.8±5.4	5.1±7.2	0.777
2nd WIT (min)	21.1±6	20.9±6	21.8±6	0.493
Time of first biopsy (days after Tx)	20±24	19±23	26±29	0.123
Diagnosis (%)				0.411
ATN	36 (24)	29 (23)	7 (27)	
Rejection	69 (46)	55 (45)	14 (54)	
Other/none	44 (30)	39 (32)	5 (19)	
DGF	39 (26)	28 (23)	11 (42)	0.038
Best eGFR before biopsy (ml/min/1.73m^2)	36±24	37±23	33±26	0.398
eGFR at first biopsy (ml/min/1.73m^2)	27±17	29±17	21±17	0.037

RRT, renal replacement therapy; HD, hemodialysis; PD, peritoneal dialysis; CIT, cold ischemia time; WIT, warm ischemia time; ATN, acute tubular necrosis; DGF, delayed graft function; eGFR, estimated glomerular filtration rate.

The CaOx crystals were translucent in H&E sections and birefringent structures were seen using polarized light (Figure 1). CaOx deposits were mostly observed in the lumen and within the epithelial cells of the tubules in the cortex. Occasionally, CaOx deposits were observed in the medulla. The mean surface of the biopsies containing CaOx deposition was 7.9 ± 2.3 mm^2 (range 4.1–12.6 mm^2) and the total amount of CaOx deposition varied between 1 and 33 deposits per biopsy (mean 6 ± 7 CaOx deposits per biopsy). The density of CaOx deposition varied between 0.1 and 0.4 deposits/ mm^2 (mean density 0.8 ± 1.0 deposits/ mm^2).

Table 1 shows the patient characteristics of patients with and without CaOx depositions. Significantly more patients with CaOx deposition had renal replacement therapy (RRT) (hemodialysis or peritoneal dialysis) before transplantation ($p = 0.011$). CaOx depositions were more frequently observed in the population with RRT compared to those who were transplanted pre-emptively but the difference was not significant for peritoneal dialysis and hemodialysis separately ($p = 0.051$). Time on dialysis was not significantly different between those patients with and those without CaOx depositions ($p = 0.88$). The best eGFR before biopsy was not significantly different between patients with and those without CaOx deposition. However, eGFR at time of the first biopsy was significantly lower in patients with CaOx deposition ($p = 0.037$). DGF occurred more frequently in patients with CaOx deposition ($p = 0.038$). No histological diagnosis (rejection, ATN or other) prevailed in the CaOx group. All other variables were not significantly different between the groups. In addition, no significant association was observed between CaOx density ($\geq$ 0,8 deposits/ mm^2 *vs.* < 0,8 deposits/ mm^2) and eGFR at time of first biopsy ($p = 0.297$) and between CaOx density and DGF ($p = 0.190$).

As there were 26 patients with CaOx deposition in their allograft biopsy, the number of variables that could be analyzed at the same time in the regression analysis was limited. Three variables showed a significant influence on CaOx deposition in the univariate analysis: eGFR at the time of first biopsy (odds ratio (OR) 0.971, 95%-CI: 0.945–0.999, $p = 0.040$), DGF (OR 2.488, 95%-CI: 1.027–6.028, $p = 0.043$) and RRT before transplantation (OR 4.270, 95%-CI: 1.213–15.029, $p = 0.024$). A stepwise multivariate analysis with backward elimination was performed, adding all variables with $p < 0.2$ in the univariate analysis. Eventually, three variables were independently associated with CaOx deposition in the multivariate analysis: eGFR at the time of first biopsy (OR 0.958, 95%-CI: 0.924–0.993, $p = 0.019$), RRT before transplantation (OR 4.868, 95%-CI: 1.128–21.003, $p = 0.034$) and time of first biopsy after transplantation (OR 1.037, 95%-CI: 1.013–1.062, $p = 0.002$).
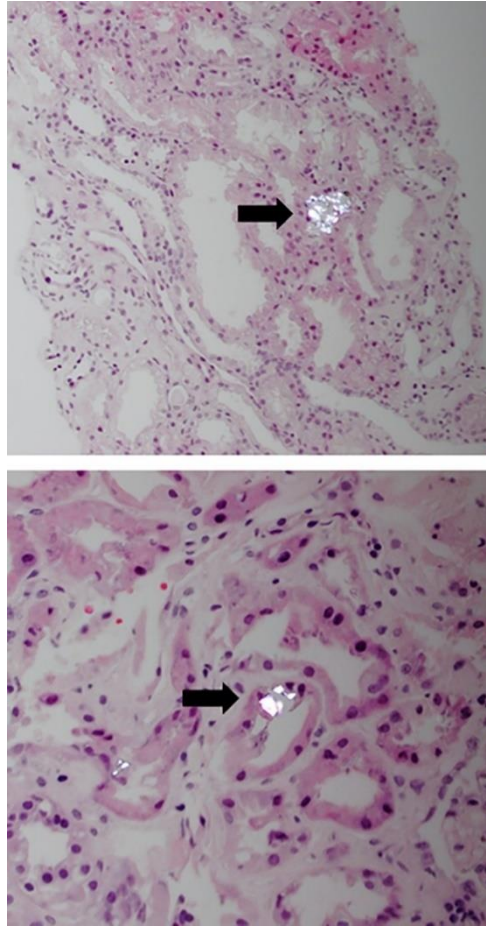
Figure 1. Examples of an H&E staining of a renal allograft biopsy examined by polarized light showing CaOx deposition (arrow) (magnification 10x and 20x respectively).

3.3 CaOx in renal transplantectomies

Of all patients transplanted between January 2014 and December 2015, a total of 8 transplantectomies were performed within 3 months after transplantation. In 3 of them CaOx deposition was found. Of these 3 patients 1 had a prior allograft biopsy that showed CaOx deposition, 1 had an allograft biopsy without CaOx deposition and 1 did not have an allograft biopsy prior to explantation. These 3 transplantectomies were performed on day 8, 11 and 12 after transplantation. The diagnosis was acute T cell-mediated rejection in all 3 patients and all had urine production after transplantation. The remaining 5 transplantectomies did not show

CaOx deposition, and all were explanted within 4 days after transplantation. No prior allograft biopsy was performed in these patients. The diagnosis was thrombosis in 4 of the cases and hyperacute rejection in 1 case. Two of these patients did not have urine production after transplantation and in the other 3 urine volume had been low. The transplantectomies were not included in any of the statistical analysis performed in this manuscript.

3.4 Graft failure

Graft failure censored for death was worse in the group of patients with CaOx deposition in their renal allograft biopsy within the first 3 months after transplantation compared to those patients without CaOx deposition in their allograft biopsy (p = 0.018; Figure 2). In the CaOx group, 5 grafts failed (19%) vs. 7 (6%) in the group without CaOx deposition. Both DGF and eGFR ≤ 27 ml/min/1,73m2 at time of first biopsy were not associated with graft loss (p = 0.238 and p = 0.519 respectively; Figure 3A and 3B). No significant association was observed between CaOx density ≥ 0.8 deposits/ mm2 and graft loss (p = 0.133).

3.5 CaOx in pre-implantation renal transplant biopsies (t0)

A total of 106 t0 kidney biopsies were available for analysis. Fifty-six (53%) biopsies were from living donors and 50 (47%) from deceased donors. CaOx deposition was found in 1 t0 biopsy (0.94%) which was from a living unrelated donor. This otherwise completely healthy donor was diagnosed with his first renal stone (type unknown) 7 years after donation.
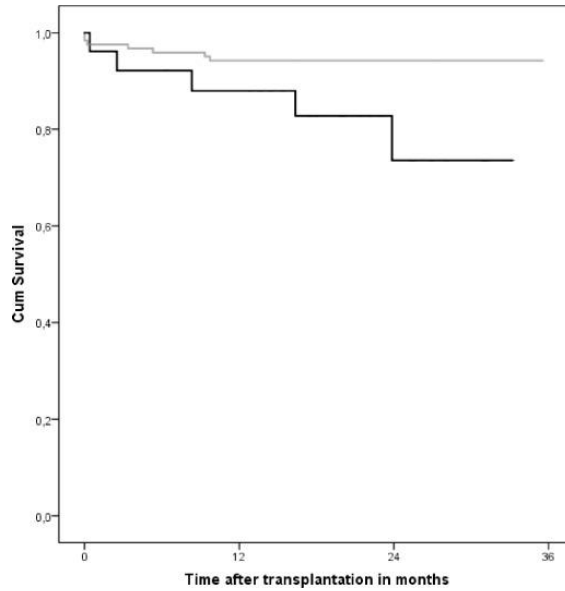
Figure 2. Graft survival censored for death in the group with CaOx deposition (N = 26) and the group without CaOx deposition (N = 123) within the first 3 months after transplantation (p = 0.018).
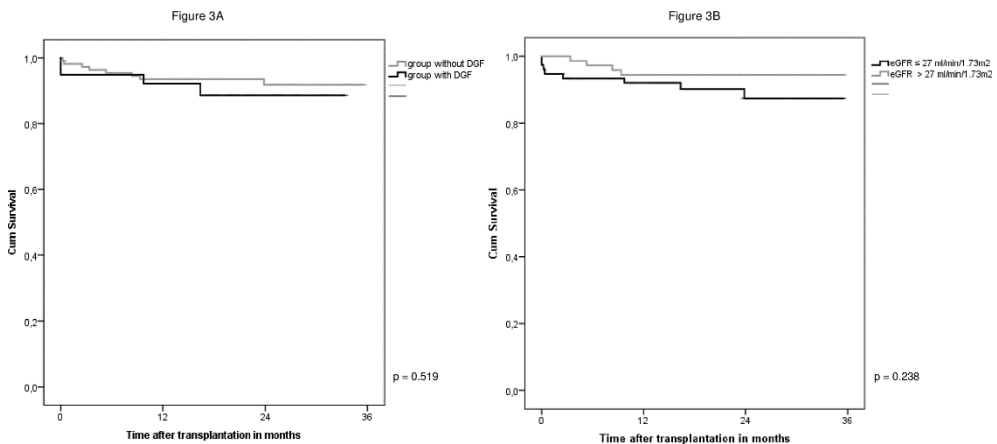

Figure 3. (A) Graft survival censored for death in the group with DGF (N = 39) and the group without DGF (N = 110) (p = 0.519). (B) Graft survival censored for death in the group with eGFR ≤27 ml/min/1,73m^2 at time of first biopsy (N = 76) and the group with eGFR >27 ml/min/1,73m^2 at time of first biopsy (N = 73) (p = 0.238).

4.   Discussion

This study demonstrates that CaOx deposition is present in as many as 17% of the patients with a for-cause renal allograft biopsy within the first 3 months after transplantation and that these deposits are primarily recipient-derived. DGF was more common in patients with CaOx in their biopsies. In addition, the presence of CaOx was associated with a significantly lower eGFR at the time of biopsy in both univariate and multivariate analysis.

As there was no significant difference in best eGFR before biopsy, this indicates that patients with CaOx deposition had a greater loss of renal function prior to biopsy. The presence of CaOx deposits may have contributed to the impairment of renal allograft function. Risk factors for CaOx deposition are a high concentration of oxalic acid in the urine, damage to renal tubular cells, volume depletion and oliguria that leads to low tubular flow.[32, 33] The CaOx crystals attach to the renal tubular cells and can cause (further) damage to the tubular cells.[34, 35] This all can lead to a vicious circle of damage to the allograft due to CaOx deposition and renal function impairment.

Only a handful of other studies have examined CaOx deposition in renal allograft biopsies. Truong *et al.* reported CaOx deposition in about 4% of unselected renal allograft biopsies (13/315). These CaOx positive biopsies were performed between 4 days and 10 months after transplantation.[36] Bagnasco *et al.* observed CaOx deposition in 9% of renal allograft recipients with at least one for-cause biopsy in the first year after transplantation.[30] The study by Pinheiro *et al.* found CaOx deposition in 52.8% of renal allograft biopsies within 3 months after transplantation.[37] The percentage reported in the latter study is remarkably high in comparison to the present and previous studies. There are several possible explanations for this difference. The use of naftidrofuryl oxalate, a peripheral vasodilator that was used in that time period for the management of vascular disease, may have been responsible for the high incidence of CaOx observed by Pinheiro *et al.* Naftidrofuryl oxalate is now known to cause high serum oxalic acid concentrations.[38, 39] The study by Pinheiro *et al.* was performed in Sao Paulo, Brazil. Different dietary habits between populations may play a role, while the oxalic acid content in food may also differ considerably dependent on the oxalate content of the soil where it was grown. In a very recent study, Palsson *et al.* showed comparable

results to our study as they observed CaOx deposition in 19.4% (67/346) of the patients with a renal allograft biopsy within 3 months after transplantation.[40]

In our study, patients with CaOx deposition significantly more often received RRT before transplantation. Both univariate and multivariate analysis confirmed an association between RRT and CaOx deposition, although the duration of RRT did not influence results. Most probably the newly transplanted kidney is exposed to higher pre-transplant oxalic acid levels in patients dependent on RRT compared to those with impaired but functioning kidneys. Previous studies showed that hemodialysis is more efficient in removing oxalic acid than peritoneal dialysis.[19, 20] However, no difference in CaOx deposition between these treatment modalities was found in the present study. Possibly patients with peritoneal dialysis were treated more recently than patients treated with hemodialysis as the first mentioned is done on a daily basis. However, the number of patients included in our study might be too small to make this distinction.

Multivariate analysis showed that the time after transplantation until performance of the first allograft biopsy significantly influenced the prevalence of CaOx deposition: a longer period was associated with a higher risk of CaOx deposition. Surprisingly, donor type (living or deceased) did not influence the prevalence of CaOx deposition in the population with a biopsy obtained within 3 months after transplantation.

DGF was significantly more common among patients with CaOx deposition compared to those without (43% vs. 24%). This is consistent with the findings of Pinheiro *et al.* who found a significantly higher incidence of DGF among patients with CaOx in their renal allograft biopsy compared to those without CaOx deposition.[37] The sequence in the relationship between CaOx deposition and DGF in the renal allograft is challenging. CaOx can cause direct injury to the tubular cells which may promote the pathogenesis of DGF in the post-transplantation period.[41, 42] However, it is also possible that injury to the tubular epithelial cells and low tubular flow as a result of DGF facilitate CaOx deposition. In our study, acute tubular injury was consistently observed in the majority of biopsies with CaOx deposits.

It is remarkable that our early transplantectomies did not show CaOx deposition, while transplantectomies from day 8 onwards did. An explanation may be that in cases with early transplantectomy there was no renal function and no urine production at all after transplantation, for example due to thrombosis or hyperacute rejection.

We found that graft survival censored for death was significantly worse in patients with CaOx deposition within 3 months after transplantation compared to those without, while DGF and eGFR at time of first biopsy were not associated with graft loss. Due to the limited number of patients with graft loss during follow up, a multivariable analysis to investigate the independent causal association of CaOx deposition on graft survival could not be performed. Our graft survival results are in line with those reported by Pinheiro *et al.* who showed a 1-year renal allograft survival of 72.5% in the group with CaOx deposition and 89.1% in the group without CaOx (p = 0.013).[37]

Histological evaluation of pre-implantation biopsies provides information on organ quality and can help predict short and long-term outcomes of the renal allografts.[43-45] Bagnasco *et al.* were the first to study the prevalence of CaOx deposition in t0 biopsies (n = 26) and found no CaOx deposition in any of the donor kidney biopsies.[30] Our results are in line with these findings as we only observed CaOx deposition in 0.94% of t0 kidney biopsies. These findings suggest that CaOx deposition in the renal transplant is recipient rather than donor derived.

The 106 t0 biopsies were studied in the population that donated in 2000 and 2001. No t0 biopsies were performed in the population that donated to our patient cohort transplanted in 2014 and 2015. However, it is unlikely that the results will be different in this specific donor population. Unfortunately, plasma oxalic acid levels pre-transplantation were not available in the present study. Additional studies are needed on the relationship between plasma oxalic acid levels pre-transplantation and the risk for CaOx deposition and inferior graft survival post-transplantation. This could aid in differentiating those patients that might benefit from preventive treatment to reduce plasma oxalic acid levels pre- and post-kidney transplantation. Avoidance of food products with high oxalic acid content and/or adequate hemodialysis treatment in the direct pre-transplant phase might prevent unnecessary CaOx deposition in the new renal allograft. In this study, we showed that CaOx deposition coincides with other causes of renal function impairment in the setting of decreased urinary flow such as DGF.

We showed that CaOx deposition in the renal allograft biopsy shortly after transplantation is common and associated with inferior long-term graft outcome. Therefore, we strongly advise the systematic examination of all for-cause renal allograft biopsies by polarized light for CaOx deposition.

References

1. Robertson WG. Kidney models of calcium oxalate stone formation. *Nephron Physiol*. 2004;98(2):p21–30.

2. Verkoelen CF, Romijn JC. Oxalate transport and calcium oxalate renal stone disease. *Urol Res*. 1996;24(4):183–91.

3. Zarembski PM, Hodgkinson A. The fluorimetric determination of oxalic acid in blood and other biological materials. *Biochem J*. 1965;96(3):717–721.

4. Wolthers BG, Hayer M. The determination of oxalic acid in plasma and urine by means of capillary gas chromatography. *Clin Chim Acta*. 1982;120(1):87–102.

5. Hoppe B, Beck BB, Milliner DS. The primary hyperoxalurias. *Kidney Int*. 2009;75:1264–1271.

6. Hoppe B. An update on primary hyperoxaluria. *Nat Rev Nephrol*. 2012;8(8):467–75.

7. Strauss SB, Waltuch T, Bivin W, Kaskel F, Levin TL. Primary hyperoxaluria: spectrum of clinical and imaging findings. *Pediatr Radiol*. 2017;47(1):96–103.

8. Herden U, Kemper M, Ganschow R, et al. Surgical aspects and outcome of combined liver and kidney transplantation in children. *Transpl Int*. 2011;24(8):805–11.

9. Nazzal L, Puri S, Goldfarb DS. Enteric hyperoxaluria: an important cause of end-stage kidney disease. *Nephrol Dial Transplant*. 2016;31(3):375–82.

10. Lorenz EC, Michet CJ, Milliner DS, Lieske JC. Update on Oxalate Crystal Disease. *Curr Rheumatol Rep*. 2013;15(7):340.

11. Duffey BG, Alanee S, Pedro RN, et al. Hyperoxaluria is a longterm consequence of Roux-en-Y Gastric bypass: a 2-year prospective longitudinal study. *J Am Coll Surg*. 2010;211(1):8–15.

12. Holmes RP, Goodman HO, Assimos DG. Contribution of dietary oxalate to urinary oxalate excretion. *Kidney Int*. 2001;59:270–276.

13. Getting JE, Gregoire JR, Phul A, Kasten MJ. Oxalate nephropathy due to 'juicing': case report and review. *Am J Med*. 2013;126(9):768–72.

14. Makkapati S, D'Agati VD, Balsam L. "Green Smoothie Cleanse" Causing Acute Oxalate Nephropathy. *Am J Kidney Dis*. 2018;71(2):281–286.

15. Syed F, Mena-Gutierrez A, Ghaffar U. A case of iced-tea nephropathy. *N Engl J Med*. 2015;372(14):1377–8.

16. Salyer WR, Keren D. Oxalosis as a complication of chronic renal failure. *Kidney Int*. 1973;4(1):61–6.

17. Worcester EM, Nakagawa Y, Bushinsky DA, Coe FL. Evidence that serum calcium oxalate supersaturation is a consequence of oxalate retention in patients with chronic renal failure. *J Clin Invest*. 1986;77(6):1888–1896.

18. Constable AR, Joekes AM, Kasidas GP, O'Regan P, Rose GA. Plasma level and renal clearance of oxalate in normal subjects and in patients with primary hyperoxaluria or chronic renal failure or both. *Clin Sci (Lond)*. 1979;56(4):299–304.

19. Watts RW, Veall N, Purkiss P. Oxalate dynamics and removal rates during haemodialysis and peritoneal dialysis in patients with primary hyperoxaluria and severe renal failure. *Clin Sci (Lond)*. 1984;66(5):591–7.

20. Hoppe B, Graf D, Offner G, et al. Oxalate elimination via hemodialysis or peritoneal dialysis in children with chronic renal failure. *Pediatr Nephrol*. 1996;10(4):488–92.

21. Illies F, Bonzel KE, Wingen AM, Latta K, Hoyer PF. Clearance and removal of oxalate in children on intensified dialysis for primary hyperoxaluria type 1. *Kidney Int*. 2006;70(9):1642–8.

22. McConnell KN, Rolton HA, Modi KS, Macdougall AI. Plasma oxalate in patients with chronic renal failure receiving continuous ambulatory peritoneal dialysis or hemodialysis. *Am J Kidney Dis*. 1991;18(4):441–5.

23. Worcester EM, Fellner SK, Nakagawa Y, Coe FL. Effect of renal transplantation on serum oxalate and urinary oxalate excretion. *Nephron*. 1994;67:414–418.

24. Hoppe B, Kemper MJ, Bo¨kenkamp A, Portale AA, Cohn RA, Langman CB. Plasma calcium oxalate supersaturation in children with primary hyperoxaluria and end-stage renal failure. Kidney International, Vol. 56 (1999), pp. 268–274.

25. Elgstoen KB, Johnsen LF, Woldseth B, Morkrid L, Hartmann A. Plasma oxalate following kidney transplantation in patients without primary hyperoxaluria. *Nephrol Dial Transplant*. 2010;25:2341–2345.

26. Yarlagadda SG, Coca SG, Garg AX, et al. Marked variation in the definition and diagnosis of delayed graft function: a systematic review. *Nephrol Dial Transplant*. 2008;23(9):2995–3003.

27. Malyszko J, Lukaszyk E, Glowinska I, Durlik M. Biomarkers of delayed graft function as a form of acute kidney injury in kidney transplantation. *Sci Rep*. 2015;5:11684.

28. Collins TJ. ImageJ for microscopy. *Biotechniques*. 2007;43(1 Suppl):25–30.

29. Hartig SM. Basic image analysis and manipulation in ImageJ. *Curr Protoc Mol Biol*. 2013;Chapter 14:Unit14.15.

30. Bagnasco SM, Mohammed BS, Mani H, et al. Oxalate deposits in biopsies from native and transplanted kidneys, and impact on graft function. *Nephrol Dial Transplant*. 2009;24(4):1319–25.

31. Roodnat JI, De Mik—van Egmond AME, Visser WJ, et al. A successful approach to kidney transplantation in patients with enteric (secondary) hyperoxaluria. *Transplantation Direct*. 2017;3:e331.

32. Coe FL, Parks JH, Asplin JR. The Pathogenesis and Treatment of Kidney Stone. *N Engl J Med*. 1992;327:1141–1152.

33. Khan SR. Renal tubular damage/dysfunction: key to the formation of kidney stones. *Urol Res*. 2006;34(2):86–91.

34 .Tsujihata M. Mechanism of calcium oxalate renal stone formation and renal tubular cell injury. *Int J Urol*. 2008;15(2):115–20.

35. Khan SR. Calcium oxalate crystal interaction with renal tubular epithelium, mechanism of crystal adhesion and its impact on stone development. *Urol Res*. 1995;23(2):71–9.

36. Truong LD, Yakupoglu U, Feig D, et al. Calcium Oxalate Deposition in Renal Allografts: Morphologic Spectrum and Clinical Implications. *Am J Transplant*. 2004;4(8):1338–1344.

37. Pinheiro HS, Caˆmara NO, Osaki KS, De Moura LA, Pacheco-Silva A. Early presence of calcium oxalate deposition in kidney graft biopsies is associated with poor long-term graft survival. *Am J Transplant*. 2005;5:323–329.

38. Moesch C, Charmes JP, Bouthier F, Leroux-Robert C. Calcium oxalate crystalluria in elderly patients and treatment with naftidrofuryl oxalate. *Age Ageing*. 1995;24(6):464–7.

39. Le Meur Y, Moesch C, Rince´ M, Aldigier JC, Leroux-Robert C. Potential nephrotoxicity of intravenous infusions of naftidrofuryl oxalate. *Nephrol Dial Transplant*. 1995;10(9):1751–5.

40. Palsson R, Chandraker AK, Curhan GC, Rennke HG, McMahon GM, Waikar SS. The association of calcium oxalate deposition in kidney allografts with graft and patient survival. *Nephrol Dial Transplant*. 2018 Aug. doi: 10.1093/ndt/gfy271.

41. Schepers MS, van Ballegooijen ES, Bangma CH, Verkoelen CF. Crystals cause acute necrotic cell death in renal proximal tubulecells, but not in collecting tubule cells. *Kidney Int*. 2005;68:1543–1553.

42. Schepers MS, van Ballegooijen ES, Bangma CH, Verkoelen CF. Oxalate is toxic to renal tubular cells only at supraphysiologic concentrations. *Kidney Int*. 2005;68(4):1660–9.

43. Mengel M, Sisa B. An Appeal for Zero-Time Biopsies in Renal Transplantation. *Am J Transplant*. 2008;8(11):2181–2182.

44. Naesens M. Zero-Time Renal Transplant Biopsies: A Comprehensive Review. *Transplantation*. 2016;100(7):1425–39.

45. Kayler LK, Mohanka R, Basu A, Shapiro R, Randhawa PS. Correlation of histologic findings on preimplant biopsy with kidney graft survival. *Transpl Int*. 2008;21(9):892–8.

Supporting information

S1 File. The database used in this study. (XLSX). This file 1 is available on request by the first author.

Author contributions

Conceptualization: Malou L. H. Snijders, Marian C. Clahsen-van Groningen, Joke I. Roodnat. Data curation: Malou L. H. Snijders. Formal analysis: Malou L. H. Snijders, Joke I. Roodnat. Methodology: Malou L. H. Snijders, Marian C. Clahsen-van Groningen, Joke I. Roodnat. Project administration: Malou L. H. Snijders. Supervision: Marian C. Clahsen-van Groningen, Joke I. Roodnat. Writing – original draft: Malou L. H. Snijders, Dennis A. Hesselink, Marian C. Clahsen-van Groningen, Joke I. Roodnat.

CHAPTER 4

**Elevated intragraft expression
of innate immunity and cell death-
related markers is a risk factor for
adverse graft outcome**

Jianxin Yang[1], Malou L. H. Snijders[2], Geert W. Haasnoot[1], Cees van Kooten[3], Marko Mallat[3], Johan W. de Fijter[3], Marian C. Clahsen-van Groningen[2], Frans H. J. Claas[1] & Michael Eikmans[1]

1. Department of Immunohematology and Blood Transfusion, Leiden University Medical Center, Leiden, The Netherlands
2. Department of Pathology, Erasmus Medical Center, Rotterdam, The Netherlands
3. Department of Nephrology, Leiden University Medical Center, Leiden, The Netherlands

Abstract

Background: Molecules of the innate immune response are increasingly recognized as important mediators in allograft injury during and after kidney transplantation. We therefore aimed to establish the relationship between the expression of these genes at implantation, during an acute rejection (AR) and on graft outcome.

Methods: A total of 19 genes, including Toll like receptors (TLRs), complement components and regulators, and apoptosis-related genes were analyzed at the mRNA level by qPCR in 123 biopsies with acute rejection and 75 paired pre-transplantation biopsies.

Results: Before transplantation, the BAX:BCL2 ratio (apoptosis marker) and relative mRNA expression of several complement genes was significantly higher in tissue samples from deceased donors compared to living donors. During AR, TLRs and complement genes showed an increased expression compared to pre-transplantation conditions, whereas complement regulators were decreased. A relatively high TLR4 expression level and BAX:BCL2 ratio during AR in the deceased donor group was associated with adverse graft outcome, independently of clinical risk factors.

Conclusions: Complement- and apoptosis-related gene expression is elevated in deceased donor transplants before transplantation. High BAX:BCL2 ratio and TLR4 expression during AR may reflect enhanced intragraft cell death and immunogenic danger signals, and pose a risk factor for adverse graft outcome.

1.   Introduction

The occurrence of an acute kidney allograft rejection, associated with infiltration of recipient immune cells to the kidney, is a risk factor for adverse graft outcome.[1] The role of innate immunity, including pattern recognition receptors and the complement system in rejection, has been appreciated.[2, 3] Toll like receptors (TLRs) are a family of transmembrane proteins that are capable of recognizing pathogen-associated molecular patterns (PAMPs) and damage-associated molecular patterns (DAMPs).[4] TLR stimulation leads to dendritic cell maturation, characterized by upregulation of pro-inflammatory cytokines, chemokines, and co-stimulatory molecules, which initiate an immune response.[5] Endogenous ligands including heat-shock proteins (HSP), uric acid, high-mobility group box 1 protein (HMGB1), and genomic double-stranded DNA may stimulate TLRs.[6-10] The interaction between HMGB1 and TLR4 leads to proinflammatory responses in the graft: after kidney transplantation, recipients with a donor graft containing a genotype variant in the coding sequence of TLR4 had lower expression of proinflammatory genes MCP-1 and TNFα and higher expression of anti-inflammatory heme oxygenase 1, and they showed an increased rate of immediate graft function.[11] Association of TLR2 and TLR4 expression was found with renal ischemia reperfusion injury (IRI) and early kidney allograft outcomes.[12, 13] Other TLRs have not been investigated in the context of delayed graft function (DGF) and acute rejection (AR).

The complement system plays a pivotal role in IRI and allograft rejection after transplantation.[3] The expression of complement components is significantly increased in deceased donor kidneys after cold ischemia.[14, 15] Activation of the complement cascade leads to the release of anaphylatoxins (C3a and C5a) and the formation of the membrane attack complex (MAC) C5b–C9, which mediates the injury following transplantation.[16, 17] C2 and C4 are essential components in the classical and lectin pathway, and C3 plays a central role in all pathways of the complement system. Complement regulators act as inhibitors of the complement cascade through various mechanisms.[18, 19] For example, the decay acceleration factor (CD55) prevents the formation of C3 convertase. CD46 acts as cofactor for inactivating C3b and C4b by serum factor I. Complement receptor 1 both has decay-accelerating activity and cofactor activity. CD59 prevents the formation of MAC. Deficiency of CD55 and CD59 in experimental settings leads to increased renal ischemia reperfusion injury.[20, 21] In C4d-negative biopsy specimens during allograft dysfunction local CD55 expression was related to favorable transplant outcome.[22]

The role of apoptosis in IRI after kidney transplantation is increasingly being recognized.[23, 24] The anti-apoptotic protein B-cell lymphoma 2 (BCL2) was significantly decreased and pro-apoptotic protein BCL2-associated X protein (BAX) was increased during normothermic ischemia.[25] The augmentation of BCL2 protects renal tubular cells from IRI through reducing renal tubular epithelial cell apoptosis.[26] High ratios of BAX:BCL2 in pre-transplantation biopsies are associated with an increased risk of DGF.[27]

In the present study, we examined innate-immune-related and apoptosis-related markers in kidney biopsies of patients before transplantation and during an acute rejection episode, and investigated their relation to clinical outcome.

2.   Methods

2.1   Patient characteristics

Patients who had received a kidney allograft at the Leiden University Medical Center (LUMC) during 1995–2005 were included. A total of 123 for-cause biopsy samples in case of clinical suspicion of AR were obtained within 6 months after transplantation. Patient characteristics are shown in Table 1. Also, 77 pre-transplantation biopsies (75 biopsies paired to the subsequent AR biopsy) were taken at time of transplantation before reperfusion. DGF was defined as dialysis-dependency in the first week after transplantation.

2.2   Ethics

Written informed consent was obtained from donors for use of part of the human material for scientific purposes. The study was performed in accordance with the Declaration of Helsinki Good Clinical Guidelines and approved by the local medical ethics committee.

2.3   Gene selection

The innate immune related genes (TLR1-TLR10), potentially acting as initiators of inflammation, were studied. The key complement component (C2, C3, C4) and complement regulators (CR1, CD46, CD55, CD59), which inhibit complement activation, were included. The apoptosis related genes BAX and BCL2, which may be associated with IRI and DGF, were also tested.

Table 1. Demographics of patient cohort.

Variable	Number (%)
Recipient age (≥50 years)	53 (43.1%)
Recipient gender (Female)	40 (32.5%)
Donor age (≥50 years)	52 (42.6%)
Donor gender (Female)	74 (60.7%)
Donor type (Living)	24 (19.5%)
Time from transplant to rejection (days, IQR)	14 (9–37)
First transplantation (Yes)	103 (84.4%)
HLA–A/B matching (Yes)	20 (16.4%)
HLA-DR matching (Yes)	43 (35.2%)
Virtual PRA (0–5%)	81 (66.4%)
DGF (Yes)	33 (28.7%)
Steroid responsiveness	68 (56.2%)
Cold ischemia time (≤ 18 h)	31 (29.8%)
Banff score	
Glomerulitis (g=0/1/2/3)	74/25/7/3
Interstitial inflammation (i=0/1/2/3)	5/44/36/24
Tubulitis (t=0/1/2/3)	11/39/38/21
Intimal arteritis (v=0/1/2/3)	62/24/7/7
Interstitial fibrosis (ci=0/1/2)	61/41/7
Tubular atrophy (ct=0/1/2)	60/44/5
C4d diffuse positive	14 (11.4%)
Rejection characteristics	
No rejection	7 (5.7%)
Borderline rejection	33 (27.0%)
Interstitial rejection	42 (34.4%)
Vascular rejection	40 (32.8%)
Graft survival (Death censored)	
> 1 year	106 (92.2%)
> 6 year	101 (87.8%)

HLA, human leukocyte antigen; PRA, panel reactive antibodies; DGF, delayed graft function.

2.4   RNA extraction and cDNA synthesis

RNA isolation and quality check, and cDNA synthesis were performed as described previously.[28]

2.5   Real time quantitative PCR analysis

Optimal primer pairs were selected using Primer 3 version 4.0.0. To prevent amplification of genomic DNA reverse and forward primers were designed to target separate exons, spanning at least one intron with a size of 800 bp or more. All primer sets were tested on control cDNA, and PCR efficiencies were between 90% and 110%. The 15-µL qPCR reaction contained 3 µL of 25-times-diluted cDNA, 15 pmol forward and reverse primers, 7.5 µL of PCR Mix (Applied Biosystems by Life Technologies, Austin, Texas, USA), and nuclease-free water.[29] Relative gene expression levels were normalized to the geometric mean of the reference genes β-actin and glyceraldehyde 3-phosphate dehydrogenase (GAPDH).

2.6   Immunohistochemistry

Immunohistochemical stainings were performed on an independent set of 34 formalin-fixed and paraffin-embedded (FFPE) kidney biopsy samples: 25 from patients with AR and 9 protocol biopsies from patients with stable graft function. Patients included in this group were transplanted between 2006 and 2015. Monoclonal anti-human antibodies against BAX (ab32503, Abcam, 1:1400 dilution), BCL2 (Sp66, Ventana), TLR4 (ab22048, Abcam, 1:800 dilution), and TLR9 (clone 26C593.2, Novus, 1:800 dilution) were used for immunohistochemistry on sequential 4-µm sections. Staining procedures have been described in a previous publication.[30] Semi quantitative scoring of the number of BCL2, TLR4, and TLR9 positive tubular epithelial cells was performed blindly by two observers (MS and MCvG) using a scale from 0 to 5 (0=0%, 1≤10%, 2=10–25%, 3=26–50%, 4=51–75%, 5=76–100%).

2.7   Statistical analyses

Gene expression differences in the paired tissue samples were analyzed using Wilcoxon signed ranks test. Differences in gene expression between deceased and living donors and the occurrence of DGF were assessed by Mann-Whitney U tests (two-sided). Correlations between innate immunity mRNA expression levels and mRNA expression of general inflammation markers were analyzed by Spearman's rank correlation coefficients (two-sided). The Bonferroni method was used to correct for multiple comparisons. Death-censored graft survival curves were created using

the Kaplan-Meier method, and differences between curves were calculated using log rank tests.

A high expression level of inflammatory markers (CD163, CD68, CD20, CD3e) was defined as recipients with deceased donor graft with the highest one-third of gene expression. Risk factors affecting graft survival in the deceased donor group were analyzed by multivariate Cox-regression model including the variables that showed a borderline significance (P < 0.1) in univariate test. Statistical analyses were performed using SPSS statistics, version 23. Due to the limited number of graft loss events, penalized survival analysis by lasso method, including clinical and molecular risk factors, were performed using the "penalized" R (3.4.0 version) package.[31]

3.   Results

3.1   Relation of pre-transplantation gene expression with donor type

No significant difference was observed between deceased (n=66) and living (n=11) donors regarding the donor age and donor gender. A short cold ischemia time (< 18 h) was more frequently seen in the living donation group. Sixteen genes, including the TLRs and membrane-bound complement regulators C4 and BAX, were not significantly different in their expression between living and deceased donors (Table 2). The expression of the complement genes C2 and C3 was >4-fold higher in the deceased donors compared to the living donors (Table 2). A significantly higher BAX:BCL2 ratio was observed in biopsies of deceased donor kidneys compared to living donor kidneys (Figure 1). Within the deceased donation group, recipients with relatively high expression of C2, C3 and BAX:BCL2 did not differ from recipients with relatively low expression in the incidence of DGF, steroid resistant rejection, and graft survival (data not shown).

3.2   No association of pre-transplantation gene expression with DGF

All recipients with DGF (28.7%) had received a deceased donor renal allograft. Donor age of >50 years was a risk factor for DGF. In the pre-transplantation biopsies of deceased donors, none of the genes investigated showed difference in expression between patients with DGF and those with no DGF (Table 2).

Table 2. Association between donor type, DGF, and gene expression in the pre-transplantation biopsies.[a]

	Living (N=11)	**Deceased** (N=66)	**P**	**DGF** (N=22)	**No DGF** (N=44)	**P**[f]
TLR1	1.0 (0.86-1.95)	1.45 (0.90-2.06)	0.25	1.05 (0.61–1.56)	1.0 (0.65–1.42)	0.72
TLR2	1.0 (0.38-1.65)	1.42 (0.76-2.38)[b]	0.05	1.10 (0.69–1.87)	1.0 (0.56–1.80)[b]	0.73
TLR3	1.0 (0.79-1.55)	1.28 (0.95-1.66)[b]	0.30	0.99 (0.68–1.55)	1.0 (0.75–1.28)[b]	0.90
TLR4	1.0 (0.69-1.19)	0.96 (0.64-1.34)	0.69	1.25 (0.83–1.65)	1.0 (0.70–1.44)	0.17
TLR5	1.0 (0.82-2.29)	1.20 (0.67-1.89)[b]	0.58	1.45 (0.56–2.05)	1.0 (0.70–1.88)[b]	0.43
TLR6	1.0 (0.48-2.17)	1.26 (0.70-2.49)[b]	0.50	1.14 (0.63–2.29)	1.0 (0.54–2.08)[b]	0.69
TLR7	1.0 (0.64-2.03)	1.68 (1.05-3.07)[c]	0.03	0.86 (0.46–2.05)	1.0 (0.67–1.51)[c]	0.73
TLR8	1.0 (0.62-2.47)	1.49 (0.81-2.45)	0.63	1.53 (1.01–2.76)[b]	1.0 (0.59–2.02)[d]	0.10
TLR9	1.0 (0.82-2.70)	1.00 (0.38-3.13)	0.80	1.19 (0.38–3.68)[b]	1.0 (0.54–3.15)	0.90
TLR10	1.0 (0.44-4.29)	2.14 (0.72-6.42)	0.29	0.90 (0.29–2.54)[b]	1.0 (0.31–3.87)[b]	0.74
CD46	1.0 (0.94-1.15)	0.86 (0.67-1.06)	0.02	0.90 (0.72–1.18)	1.0 (0.77–1.21)	0.45
CD55	1.0 (0.92-1.50)	0.90 (0.63-1.32)	0.09	1.06 (0.84–1.55)	1.0 (0.72–1.53)	0.36
CD59	1.0 (0.83-1.16)	0.97 (0.85-1.26)	0.61	0.99 (0.89–1.25)	1.0 (0.87–1.29)	0.74
C2	1.0 (0.38-1.28)	4.28 (1.81-6.81)	5.20E-6*	1.01 (0.40–1.72)	1.0 (0.48–1.58)	0.95
C3	1.0 (0.83-1.52)	5.81 (2.88-14.43)	5.98E-6*	1.21 (0.74–2.09)	1.0 (0.47–2.97)	0.59
C4	1.0 (0.89-1.65)	2.17 (1.38-3.03)	0.01	0.97 (0.53–1.39)	1.0 (0.70–1.38)	0.53
CR1	1.0 (0.75-2.07)	0.99 (0.67-1.54)[b]	0.60	1.26 (0.89–1.82)	1.0 (0.68–1.81)[b]	0.41
BCL2	1.0 (0.87-1.49)	0.71 (0.48-1.01)	2.35E-3*	1.11 (0.66–1.66)	1.0 (0.74–1.37)	0.61
Bax	1.0 (0.83-1.24)	1.18 (0.99-1.53)	0.12	1.13 (1.00–1.58)	1.0 (0.85–1.38)	0.13
Bax:BCL2	1.0 (0.80-1.18)	1.78 (1.50-2.34)	8.41E-6*	1.09 (0.89–1.42)	1.0 (0.87–1.30)	0.34

a Gene expression data shown as medians with interquartile range.

b, c, d, e Data missing for one[b], two[c], four[d] and five[e] patients.

f The expression level of patients with and without DGF was analyzed in the deceased donor group.

∗ Statistically significant p-values after Bonferroni correction ($P < 0.0025$). P values were calculated by Mann-Whitney U tests (two-sided).
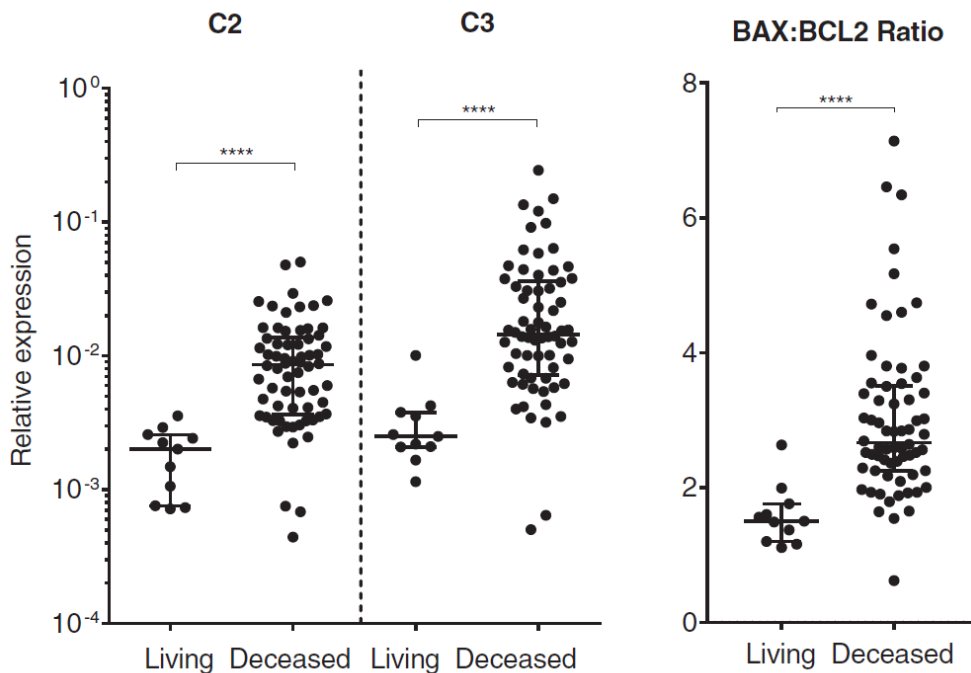
Figure 1. Gene expression in pre-transplantation biopsies of living and deceased donors. The relative expression of C2 and C3 was significantly lower in living donors than in deceased donors in the pre-transplantation biopsies. The BAX:BCL2 ratio was significantly lower in living donors in the pre-transplantation biopsies.

Flags show median with interquartile range. P values were calculated by Mann-Whitney U tests (two-sided), ****P < 0.0001 (corrected for Bonferroni).

3.3 Comparison of pre-transplantation and acute rejection biopsies

Paired pre-transplantation and acute rejection biopsies of 75 patients were available for analysis of gene expression dynamics (Table 3). The expression levels of TLR6, TLR7, TLR8, TLR9, and TLR10 were elevated >5.5 fold at the moment of AR, and the expression levels of TLR1, TLR2, TLR3, and C2 were increased 1.2–4.4 fold compared to the expression levels before implantation. The expression levels of TLR4, TLR5, C3 and CR1 were similar between both biopsies, and levels of C4, BCL2 and the complement regulators (CD46, CD55, and CD59) were slightly decreased during AR (Figure 2). Patients whose C3 expression increased between pre-transplantation and AR did not differ from patients whose C3 expression decreased with respect to incidence of steroid resistant rejection and death censored graft survival (data not shown).
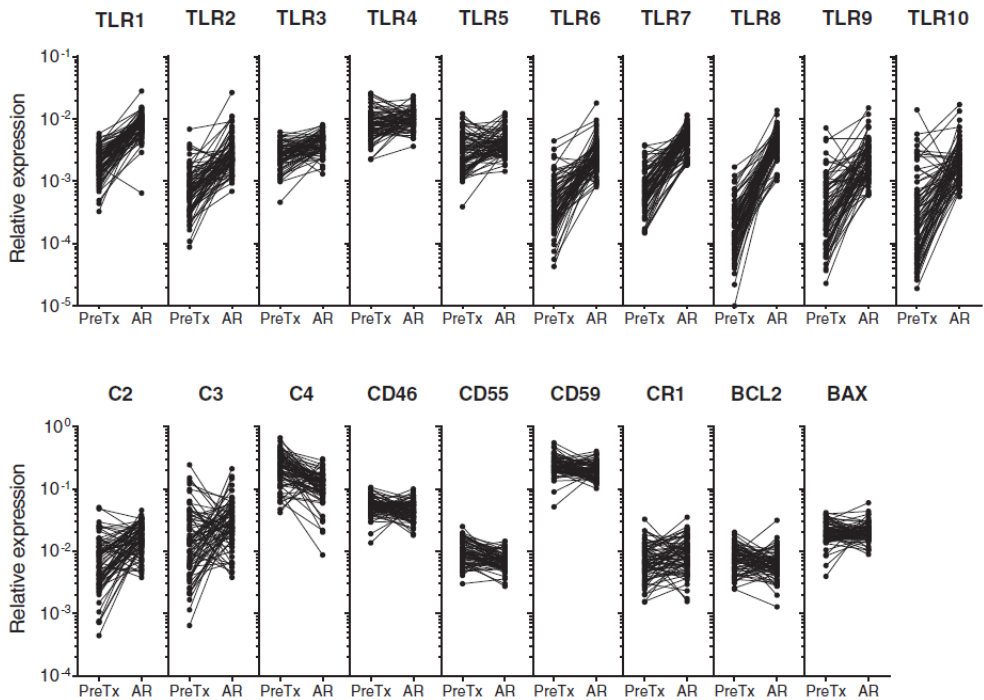
Figure 2. Gene expression dynamics in kidney biopsies. The paired pre-transplantation biopsies (PreTx) and acute rejection biopsies (AR) of 75 patients were used for comparison. The mRNA levels were quantified by qPCR and normalized to reference genes.

3.4 Gene expression correlated with inflammation and Banff score

Since all TLRs showed elevated levels during AR, we investigated whether this upregulation could be ascribed to infiltration of inflammatory cells. Correlations of innate immunity expression levels with expression of key inflammatory markers (CD163, CD68, CD20, CD3e) and Banff classification are summarized in Table S2. Except for TLR2, TLR3 and TLR5, all TLRs correlated with one or more inflammatory cell marker. C2 and C3 were significantly correlated with macrophage markers, whereas CD46 and CD59 showed a negative association with these molecules. In addition, CR1 demonstrated association with T cell, B cell, macrophage markers, and interstitial inflammation score. Apoptosis-related genes did not correlate with any of the inflammatory molecules. In summary, the altered gene expression may in part be the result of infiltrating inflammatory cells.

Table 3. Pairwise comparison of gene expression between pre-transplantation biopsies and biopsies with acute rejection.

	Pre-transplantation	Acute rejection	P
TLR1	1.0 (0.65 - 1.46)	4.36 (3.24 - 5.34)	5.50E-14*
TLR2	1.0 (0.52 - 1.63)	3.42 (2.63 - 5.21)	4.60E-12*
TLR3	1.0 (0.74 - 1.29)[a]	1.42 (1.20 - 1.86)[a]	5.38E-08*
TLR4	1.0 (0.70 - 1.37)	1.21 (0.95 - 1.56)	0.019
TLR5	1.0 (0.56 - 1.59)	1.40 (1.01 - 1.70)	0.0028
TLR6	1.0 (0.56 - 1.97)	5.59 (4.18 - 8.47)	2.22E-13*
TLR7	1.0 (0.61 - 1.55)[a]	7.40 (4.60 - 9.79)[a]	1.48E-13*
TLR8	1.0 (0.57 - 1.73)[b]	27.04 (18.94 - 34.87)[b]	3.56E-13*
TLR9	1.0 (0.39 - 3.07)[a]	7.66 (4.99 - 13.14)[a]	1.62E-11*
TLR10	1.0 (0.31 - 2.83)[c]	8.96 (4.55 - 14.31)[c]	2.25E-09*
CD46	1.0 (0.78 - 1.22)	0.80 (0.62 - 1.07)	2.19E-03*
CD55	1.0 (0.71 - 1.48)	0.72 (0.58 - 0.84)	4.34E-07*
CD59	1.0 (0.86 - 1.25)	0.84 (0.63 - 1.04)	4.92E-04*
C2	1.0 (0.47 - 1.76)	2.49 (1.71 - 3.56)	4.34E-07*
C3	1.0 (0.43 - 2.35)	2.04 (1.32 - 3.65)	8.41E-03
C4	1.0 (0.65 - 1.44)	0.49 (0.36 - 0.61)	2.19E-10*
CR1	1.0 (0.70 - 1.54)	1.26 (0.87 - 1.97)	0.0087
BCL2	1.0 (0.67 - 1.35)[c]	0.76 (0.60 – 1.06)[c]	3.14E-4*
Bax	1.0 (0.84 - 1.31)[c]	0.98 (0.85 - 1.27)[c]	0.44
Bax:BCL2	1.0 (0.76 - 1.30)[c]	1.24 (0.95 - 1.49)[c]	6.20E-5*

a, b, c Data missing for one[a], five[b] and two[c] patients.

∗ Statistically significant p-values based on Bonferroni correction (P < 0.0025), P values were calculated by Wilcoxon signed ranks test.

3.5 TLR4 expression and BAX:BCL2 ratio predicts graft outcome

The relative expression of TLR4 at the moment of AR in living and deceased patients was comparable. The patients with a deceased donor graft were divided into two groups based on their gene expression levels. One-third of patients who showed the highest TLR4 expression were defined as high expression group (open circles); and the rest of patients as low expression group (black dots) (Figure 3A). At 12.5 years post-transplantation, patients with high TLR4 expression showed significant inferior graft survival (59.2%) compared to patients who had relative low TLR4 expression (79.6%, P = 0.04, Figure 3A). >10% of the patients with high TLR4 expression lost their graft within the first 3 months. As for the BAX:BCL2 ratio: patients in the deceased donor group with a BAX:BCL2 ratio higher than in the living donation group were defined as the high ratio group (open circles) (Figure 3B). The group of patients with relatively high BAX:BCL2 ratio at time of AR had an inferior graft survival (57.9%) compared to patients with a low BAX:BCL2 ratio (79.8%) and those with a living donor allograft (88.3%, P = 0.03, Figure 3B). In univariate analysis, Banff classification score did not predict long term graft survival.

In multivariate cox regression analysis within deceased donor group (Table 4), only high TLR4 expression (HR = 3.46; CI= 1.17–10.23; P = 0.025) and a high BAX:BCL2 ratio (HR = 4.6; CI = 1.44–14.73; P = 0.01) were a significant independent risk factor for graft loss. The penalized cox regression model using the lasso showed that high TLR4 expression, higher donor age (>50 year) and high BAX:BCL2 ratio were the most significant (Figure S1). Expression levels in the pre-transplantation biopsies were not associated with graft survival.

3.6 Localization of TLR4, TLR9, and BCL2 expression

To verify clinically relevant mRNA markers at the protein level and localize their expression in the tissue, immunohistochemical staining for TLR4, BAX and BCL2 were performed on kidney biopsies (Figure 4). In addition, we investigated TLR9 which was increased during AR, and which has been shown to be an inducer of proinflammatory signals.[32] Quantification of BAX expression could not be performed since almost no staining was observed in the biopsies (positive area <10%). TLR4 protein expression was detected in tubular epithelial cells and in inflammatory cells (Figure 4A and 4B). Semi-quantitative scoring showed a significantly higher expression in biopsies with AR than in those with stable graft function. Protein expression of TLR9 was predominantly seen in tubular epithelial cells and varied considerably within the AR group (Figure 4C and 4D). BCL2 expression was observed

in the cytoplasm of tubular epithelial cells and in infiltrating inflammatory cells, and showed a wide range of expression among AR biopsies (Figure 4E and 4F). The extent of protein expression of BCL2 and TLR9 during AR was increased in comparison to the stable graft group, however this difference was not significant after correction for multiple comparisons (Table 5).
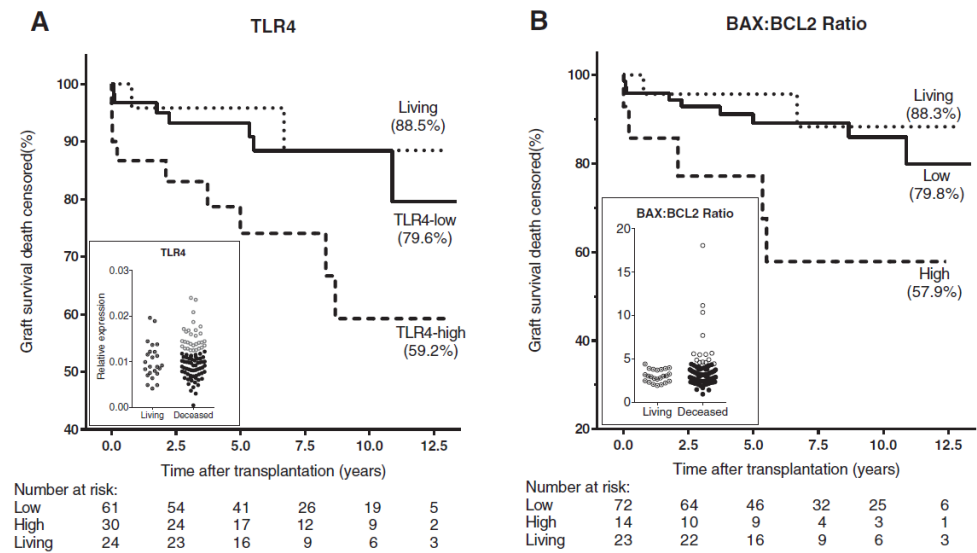
Figure 3. Association between gene expression at time of acute rejection and kidney graft survival. (A) The TLR4-high expression patient group (n=30; dash line) had significantly inferior graft survival compared to the TLR4-low expression patient group (n=61; solid line) and living donor group (n=24; dots line). (B) The high BAX:BCL2 ratio patient group (n=14; dash line) had significantly inferior graft survival rate compared to the low BAX:BCL2 ratio patient group (n=72; solid line) and the living donor group (n=23; dots line).

Table 4. Cox regression analysis of transplant-related risk factors and post-transplantation gene expression levels at time of acute rejection with death censored graft survival.

	Univariate		Multivariate	
	HR (Lower-Upper)	P	HR (Lower-Upper)	P
Recipient age (> 50 year)	1.19 (0.47 - 3.01)	0.72		
Transplantation date (<1999)	0.93 (0.25–3.42)	0.91		
Donor age (> 50 year)	2.10 (0.78–5.68)	0.14		
ABDR mismatching	0.95 (0.27–3.34)	0.94		
Cold ischemia time(<18h)	0.88 (0.25–3.14)	0.85		
Delayed Graft function	1.61 (0.60–4.33)	0.35		
Vascular rejection	1.28 (0.46–3.54)	0.63		
Steroid resistant	1.94 (0.72–5.21)	0.19		
Number of transplants (>1)	2.88 (1.00–8.32)	0.05		
CD163 (high expression level)	1.52 (0.55–4.20)	0.42		
CD68 (high expression level)	1.78 (0.62–5.07)	0.28		
CD20 (high expression level)	0.42 (0.12–1.47)	0.17		
CD3e (high expression level)	1.14 (0.41–3.16)	0.80		
TLR4 (high expression level)	2.89 (1.08–7.78)	0.04*	3.46 (1.17–10.23)	0.025*
Ratio BAX:BCL2 (higher than living)	3.22 (1.09–9.51)	0.03*	4.60 (1.44–14.73)	0.01*

*Statistically significant difference ($P < 0.05$).

4.   Discussion

In the present study, mRNA expression levels of TLRs, key complement components and regulators, and apoptosis-related genes were investigated in biopsies obtained before graft implantation and at time of AR. We found that in deceased donors, C2 and C3 expression and BAX:BCL2 ratio were already elevated before transplantation but were not indicative of DGF. High TLR4 levels and a high BAX:BCL2 ratio at the time of an AR were both independent risk factors of graft loss. Results from this exploratory study suggest that innate immune activation occurs both at time of graft implantation and during episodes of acute rejection. Although the TLR/MyD88 pathway was found to be redundant for host defense against most natural infections, depletion of a functional TLR pathway in mice, by knocking out

either TLR2, TLR4 or MyD88, protects against IRI and kidney dysfunction, and limits an increase in expression of cytokines, chemokines and infiltration of inflammatory cells.[33-35] In human kidney transplants, the expression of TLR4 and HMGB1 (an endogenous ligand of TLR4) was significantly elevated in pre-transplantation biopsies from deceased donors but not in those from living donors.[11] However, in our study we could not confirm these findings (Table 2), and none of the markers investigated was associated with DGF.
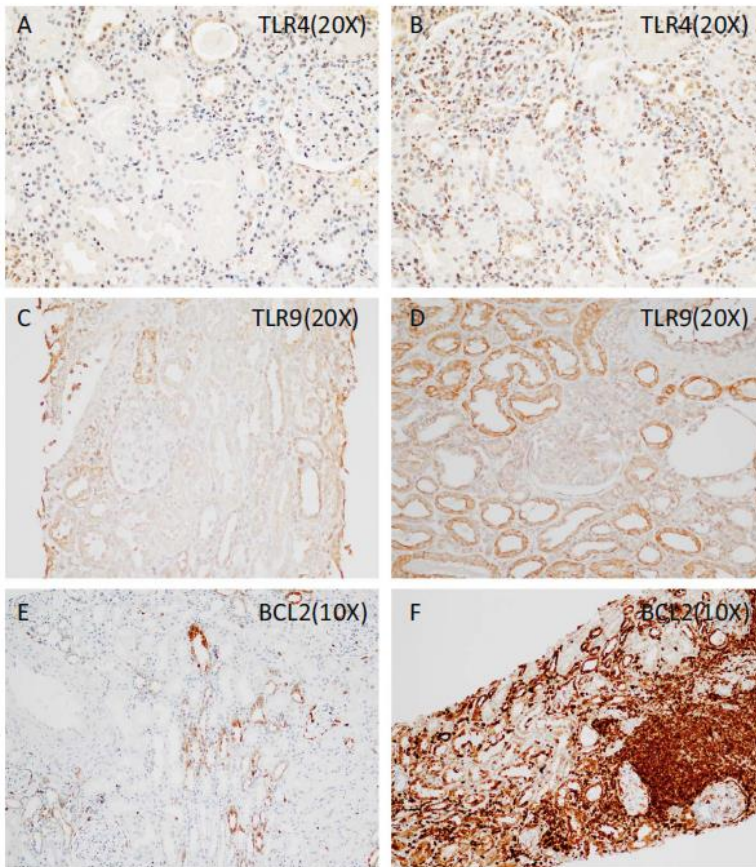
Figure 4. Immunohistochemical staining pattern of TLR4, TLR9, and BCL2 in kidney transplant biopsies. TLR4 protein expression was detected in tubular epithelial cells and in inflammatory cells (A–B). TLR9 was observed in the tubular epithelial cells (C–D). BCL2 was detected in tubular epithelial cells and infiltrated lymphocytes (E–F). Both BCL2 and TLR9 expression varied extensively between acute rejection biopsies. Two representative samples from the acute rejection group are shown.

Table 5. Immunohistochemical scoring of TLR4, TLR9, and BCL2 in biopsies with stable graft function and acute rejection biopsies.

IHC score	1	2	3	4	5	P
TLR9						0.069
SGF	1	5	1	0	0	
AR	4	4	7	4	4	
TRL4						0.008*
SGF	4	2	1	0	0	
AR	2	7	5	5	3	
BCL2						0.024
SGF	1	3	2	1	0	
AR	0	3	8	8	3	

IHC, Immunohistochemistry; SGF, stable graft function; AR, acute rejection.
* Statistically significant p-values based on Bonferroni correction (P < 0.016), P values were calculated by Mann-Whitney Test.

Earlier studies showed that the expression of TLRs is significantly upregulated during allograft rejection, mainly because of infiltration of leukocytes.[13, 36] However, none of the previous studies has documented gene expression dynamics in a large patient cohort. We showed that the expression of all TLRs, except TLR4 and TLR5, was significantly increased in AR biopsies when compared to pre-transplantation biopsies (Table 3). Moreover, expression of the majority of the TLRs was positively correlated with one or more inflammatory cell markers at the moment of AR (Table S1), suggesting that the elevated expression of TLRs is a result of inflammatory cell presence. Both TLR2 and TLR3, which showed only minor increase during an AR, were not correlated with any inflammatory markers, and their expression may be dominant in renal parenchymal tissue. Similar expression patterns of TLR3 were reported by Dessing *et al*.[36] The expression of TLR4 correlated with CD163 and CD68 but was not increased during AR, and may be expressed by both parenchymal and myeloid cells. In addition, patients with relatively high levels of TLR4 during AR exhibited inferior graft survival 12.5 years after transplantation, which may mean that intracellular ligands released after cell damage bind to TLR4 and thereby provide additional inflammatory signals leading to long term graft loss. Expression of TLR4 in the renal allograft biopsy has been described previously.[11, 13] TLR4 by immunohistochemical staining was expressed in tubular cells and infiltrated lymphocytes, with significantly higher expression during AR compared to stable graft conditions. The possible explanation, that on one hand no increase in TLR4 mRNA

was seen between AR and pre-transplantation and on the other hand immunohistochemistry showed significantly higher expression during AR compared to stable graft conditions, may be that the epithelium expresses low levels of mRNA but relatively high levels of protein. The endogenous pattern recognition receptor TLR9 is involved in immune complex kidney disease.[37] Immunohistochemical staining showed that TLR9 was increased during AR compared to the stable graft group with borderline significance.

The complement system acts as a bridge to the adaptive system and facilitates clearance of immune complexes and cellular debris. It has been shown that the MAC plays a central role in renal IRI and that locally synthesized C3 is important in kidney graft survival.[17, 38] In line with a previous study, the mRNA levels of C2 and C3 in the living donor group were significantly lower than those in the deceased donor group at time of implantation, which supports the notion that the local C3 expression is induced by donor brain death.[14, 15] The observation of a slight increase in C4 expression in deceased donors is also in line with this previous study.[14] However, inconsistent with that study, the expression level of CR1 was comparable between deceased and living donor biopsies in our relatively large cohort. The increased C2 during AR may represent a higher activity of the classical and lectin pathway, whereas the decreased C4 expression during AR may be a result of injury of renal parenchymal cells.

The complement regulators CD46, CD55, and CD59 act as inhibitors of activation of the complement pathway. Hypersensitized rats treated with sCR1 displayed significantly prolonged cardiac graft survival.[39] Similarly, kidneys of animals treated with CR1 derivatives (APT070) showed less acute tubular injury, and the animals had a significantly higher graft survival rate.[40] CD55 had a protective effect on renal function in C4d-negative grafts and antibody-mediated cardiac allograft rejection.[22, 41] We found that expression of CD46, CD55 and CD59 was significantly reduced during an AR compared to that in the pre-transplantation biopsies. However, none of the complement regulators were predictive for the development of DGF, steroid resistant rejection and graft survival in the present study. Interestingly, Budding *et al.* showed that serum sCD59 is elevated at the time of bronchiolitis obliterans syndrome (BOS) after lung transplantation, and the patients with higher serum sCD59 titers (>400 pg/mL) had a significantly lower chance of BOS free survival. We observed that the expression of complement regulators at time of AR was slightly decreased compared to pre-transplantation conditions, and that it negatively correlated with expression of macrophage markers.

It has been shown that kidney cell apoptosis is involved in IRI and that apoptotic cells are frequently present in AR biopsies.[23, 24] In the present study, the mRNA of BCL2, an anti-apoptotic molecule, was lower in deceased donor biopsies than in living donor biopsies. The higher BAX:BCL2 ratio suggests that the extent of apoptosis is already increased in deceased donors. The BAX:BCL2 ratio tended to be higher in the DGF group in the deceased donor cohort but this was only marginal (Table 2), which is inconsistent with findings from a previous study.[27] During an AR, the BAX:BCL2 ratio was marginally increased and it significantly correlated with expression of macrophage markers. Protein investigations by immunohistochemical staining showed that BAX was rarely detected in the biopsy samples. The BCL2 expression was mainly observed in tubular epithelial cell and inflammatory cells, with a wide range of staining within the AR group. Patients who received a living donor graft had superior graft survival compared to those with a graft from a deceased donor, and thus this group acted as a reference. Moreover, patients with relatively high BAX:BCL2 ratio during AR in their deceased donor graft demonstrated significantly inferior graft survival rates (57.9%) 12.5 years after transplantation compared to those with a low ratio or to patients who had received a living donor graft (Figure 3). High BAX:BCL2 ratio during AR possibly reflects an increased number of apoptotic cells, which leads to attraction of phagocytic cells to the graft.[42, 43] The accumulated phagocytes may be triggered by immunogenic danger signals and mediate subsequent chronic allograft loss.[44, 45]

In conclusion, complement and apoptosis pathways are elevated before kidney transplantation. Increased expression of the majority of genes partly reflect the infiltration of inflammatory cells during an AR. Relatively high TLR4 expression and high BAX:BCL2 ratio during AR, possibly reflecting enhanced immunogenic danger signals, were both independent risk factors for adverse outcome after transplantation of a deceased donor kidney. The results of this study suggest that the different impact of AR on outcome between living and deceased donor transplants may partly be ascribed to differences in TLR4 regulation and cell death related mechanisms. They form a basis to further validate and explore the functional relevance of these pathways in relation to transplant outcome.

References

1. Suthanthiran M, Strom TB. Renal transplantation. *N Engl J Med*. 1994;331(6):365–376.

2. Wood KJ, Goto R. Mechanisms of rejection: current perspectives. *Transplantation*. 2012;93(1):1–10.

3. Sacks SH, Zhou W. The role of complement in the early immune response to transplantation. *Nat Rev Immunol*. 2012;12(6):431–42.

4. Janeway CA Jr, Medzhitov R. Innate immune recognition. *Annu Rev Immunol*. 2002;20:197–216.

5. Matzinger P. The danger model: a renewed sense of self. *Science*. 2002;12;296(5566):301-5.

6. Ohashi K, Burkart V, Flohe S, Kolb H. Cutting edge: heat shock protein 60 is a putative endogenous ligand of the toll-like receptor-4 complex. *J Immunol*. 2000;164(2):558–61.

7. Shi Y, Evans JE, Rock KL. Molecular identification of a danger signal that alerts the immune system to dying cells. *Nature*. 2003;425(6957):516–21.

8. Scaffidi P, Misteli T, Bianchi ME. Release of chromatin protein HMGB1 by necrotic cells triggers inflammation. *Nature*. 2002;418(6894):191–5.

9. Park JS, Svetkauskaite D, He Q, et al. Involvement of toll-like receptors 2 and 4 in cellular activation by high mobility group box 1 protein. *J Biol Chem*. 2004;279(9):7370–7.

10. Ishii KJ, Suzuki K, Coban C, et al. Genomic DNA released by dying cells induces the maturation of APCs. *J Immunol*. 2001;167(5):2602–2607.

11. Kruger B, Krick S, Dhillon N, et al. Donor Toll-like receptor 4 contributes to ischemia and reperfusion injury following human kidney transplantation. *Proc Natl Acad Sci*. 2009;106(9):3390–5.

12. Andrade-Oliveira V, Campos EF, Goncalves-Primo A, et al., TLR4 mRNA levels as tools to estimate risk for early Posttransplantation kidney graft dysfunction. *Transplantation*. 2012;94 (6):589–95.

13. Stribos EG, van Werkhoven MB, Poppelaars F, et al. Renal expression of Tolllike receptor 2 and 4: dynamics in human allograft injury and comparison to rodents. *Mol Immunol*. 2015;64 (1):82–9.

14. Naesens M, Li L, Ying L, et al. Expression of complement components differs between kidney allografts from living and deceased donors. *J Am Soc Nephrol*. 2009:20(8):1839–51.

15. Damman J, Nijboer WN, Schuurs TA, et al. Local renal complement C3 induction by donor brain death is associated with reduced renal allograft function after transplantation. *Nephrol Dial Transplant*. 2010;26(7):2345–54.

16. Damman J, Schuurs TA, Ploeg RJ, Seelen MA. Complement and renal transplantation: from donor to recipient. *Transplantation*. 2008;85(7):923–7.

17. Zhou W, Farrar CA, Abe K, et al. Predominant role for C5b-9 in renal ischemia/reperfusion injury. *J Clin Investig*. 2000;105(10):1363-71.

18. Roumenina LT, Zuber J, Fremeaux-Bacchi V. Physiological and therapeutic complement regulators in kidney transplantation. *Curr Opin Organ Transplant.* 2013;18(4):421–9.

19. Zipfel PF, Skerka C. Complement regulators and inhibitory proteins. *Nat Rev Immunol.* 2009;9(10):729–40.

20. Yamada K, Miwa T, Liu J, Nangaku M, Song WC. Critical protection from renal ischemia reperfusion injury by CD55 and CD59. *J Immunol.* 2004;172(6):3869–75.

21. Turnberg D, Botto M, Lewis M, et al. CD59a deficiency exacerbates ischemia reperfusion injury in mice. *Am J Pathol.* 2004;165(3):825–32.

22. Brodsky SV, Nadasdy GM, Pelletier R, et al. Expression of the decay-accelerating factor (CD55) in renal transplants - a possible prediction marker of allograft survival. *Transplantation.* 2009;88(4):457–64.

23. Havasi A, Borkan SC. Apoptosis and acute kidney injury. *Kidney Int.* 2011;80(1):29–40.

24. Kosieradzki M, Rowinski W. Ischemia/reperfusion injury in kidney transplantation: mechanisms and prevention. *Transplant Proc.* 2008;40(10):3279-88.

25. Wolfs TGAM, de Vries B, Walter SJ, et al. Apoptotic cell death is initiated during normothermic ischemia in human kidneys. *Am J Transplant.* 2005;5(1):68–75.

26. Suzuki C, Isaka Y, Shimizu S, et al. Bcl-2 protects tubular epithelial cells from ischemia reperfusion injury by inhibiting apoptosis. *Cell Transplant.* 2008;17(1–2):223–9.

27. Goncalves-Primo A, Mourao TB, Andrade-Oliveira V, et al. Investigation of apoptosis-related gene expression levels in preimplantation biopsies as predictors of delayed kidney graft function. *Transplantation.* 2014;97(12):1260–5.

28. Rekers NV, Bajema IM, Mallat MJ, et al. Quantitative polymerase chain reaction profiling of immunomarkers in rejecting kidney allografts for predicting response to steroid treatment. *Transplantation.* 2012;94(6):596–602.

29. Yang J, Kemps-Mols B, Spruyt-Gerritse M, Anholts J, Claas F, Eikmans M. The source of SYBR green master mix determines outcome of nucleic acid amplification reactions. *BMC Res Notes.* 2016;9:292.

30. Schonkeren D, van der Hoorn ML, Khedoe P, et al. Differential distribution and phenotype of decidual macrophages in preeclamptic versus control pregnancies. *Am J Pathol.* 2011;178 (2):709–17.

31. Goeman JJ. L1 penalized estimation in the cox proportional hazards model. *Biom J.* 2010;52 (1):70–84.

32. Chen L, Ahmed E, Wang T, et al. TLR signals promote IL-6/IL-17-dependent transplant rejection. *J Immunol.* 2009;182(10):6217–25.

33. von Bernuth H, Picard C, Jin Z, et al. Pyogenic bacterial infections in humans with MyD88 deficiency. *Science.* 2008;321(5889):691–6.

34. Leemans JC, Stokman G, Claessen N, et al. Renal-associated TLR2 mediates ischemia/reperfusion injury in the kidney. *J Clin Invest.* 2005;115(10):2894–2903.

35. Wu H, Chen G, Wyburn KR, et al. TLR4 activation mediates kidney ischemia/reperfusion injury. *J Clin Invest.* 2007;117(10):2847–59.

36. Dessing MC, Bemelman FJ, Claessen N, ten Berge IJ, Florquin S, Leemans JC. Intragraft toll-like receptor profiling in acute renal allograft rejection. *Nephrol Dial Transplant*. 2010;25(12):4087–4092.

37. Anders HJ, Banas B, Schlöndorff D. Signaling danger: toll-like receptors and their potential roles in kidney disease. *J Am Soc Nephrol*. 2004;15(4):854–67.

38. Pratt JR, Basheer SA, Sacks SH. Local synthesis of complement component C3 regulates acute renal transplant rejection. *Nat Med*. 2002;8(6):582–7.

39. Pruitt SK, Bollinger RR. The effect of soluble complement receptor type 1 on hyperacute allograft rejection. *J Surg Res*. 1991;50(4):350–5.

40. Patel H, Smith RA, Sacks SH, Zhou W. Therapeutic strategy with a membranelocalizing complement regulator to increase the number of usable donor organs after prolonged cold storage. *J Am Soc Nephrol*. 2006;17(4):1102–11.

41. Gonzalez-Stawinski GV, Tan CD, Smedira NG, Starling RC, Rodriguez ER. Decay-accelerating factor expression may provide immunoprotection against antibody-mediated cardiac allograft rejection. *J Heart Lung Transplant*. 2008;27(4):357–61.

42. Lauber K, Bohn E, Kröber SM, et al. Apoptotic cells induce migration of phagocytes via caspase-3-mediated release of a lipid attraction signal. *Cell*. 2003;113(6):717–30.

43. Gregory CD, Devitt A. The macrophage and the apoptotic cell: an innate immune interaction viewed simplistically? *Immunology*. 2004;113(1):1–14.

44. Ricardo SD, van Goor H, Eddy AA. Macrophage diversity in renal injury and repair. *J Clin Invest*. 2008;118(11):3522–30.

45. Rekers NV, Bajema IM, Mallat MJ, et al. Beneficial immune effects of myeloid related proteins in kidney transplant rejection. *Am J Transplant*. 2016;16(5):1441–55.

Author contributions

Jianxin Yang and Malou L.H. Snijders performed experiments and analyzed data. Jianxin Yang and Michael Eikmans interpreted the results and composed the initial draft of the manuscript. Malou L.H. Snijders, Geert W. Haasnoot, Cees van Kooten, Marko Mallat, Johan W. de Fijter, Marian C. Clahsen-van Groningen, Frans H.J. Claas, and Michael Eikmans edited and revised the manuscript. Frans H.J. Claas and Michael Eikmans provided intellectual content of critical importance to the work described and approved the version to be published.

Supplementary files

Table S1. Primer sequence and amplification efficiency.

Genes	Forward primer (5'-3')	Reverse primer (5'-3')	Product size (bp)	Efficiency (%)
TLR1	ACACCAAGTTGTCAGCGATG	GGGCTAATTTTGGATGGGCA	135	94.5
TLR2	GTGATAGGTGTGAGGCAGGT	GTGGCCGCCTTGATTCATAG	136	100.8
TLR3	GAACCTCCAGCACAATGAGC	TGACAAGCCATTATGAGACAGA	169	99.6
TLR4	ACCTCCCCTTCTCAACCAAG	GGCTCTGATATGCCCCATCT	150	106.9
TLR5	TGAAGTCTTTAAACAACCAGGGA	TCCAAACACAGGACCGGC	142	108.1
TLR6	CTCTCCACTCTGCTTTCCCA	CTCCGAGGACTGGTGCATAT	109	107.1
TLR7	TGCTCTCTTCAACCAGACCT	CACGATCACATGGTTCTTTGGA	196	103.5
TLR8	TACCACCTTGAAGAGAGCCG	TGCTTTGGTTGATGCTCTGC	112	99.5
TLR9	AGATGGAGGGGAGAAGGTCT	CAAGGTGAAGTTGAGGGTGC	112	98.6
TLR10	TCCAGAGCTGCCAGAAGAAA	AAATCCAGTGTCGTTGTGGC	102	97.5
CD46	ATTCAGTGTGGAGTCGTGCT	AATTGTGTCGCTGCCATCG	167	95.8
CD55	TCCTGGCGAGAAGGACTCAGTGA	AGCCTTGTTGGCACCTCGCA	96	98.0
CD59	GCGTGTCTCATTACCAAAGCT	CCTTCTTGCAGCAGTAGTACG	127	95.9
C2	TCTGAACCTCTACCTGCTCC	ACATGAGGACTTTGGGCTCT	164	92.8
C3	AGCAGTCAAGGTCTACGCC	TTGTCCAGCCGTTCTTCCA	180	95.3
C4	CTGAACAACCGCCAGATTCG	TGGCAGGTCGTGTTCTTCAT	149	98.9
CR1	TGTTTGCGATGAAGGGTTCC	GAGTTCCTGTGTGTCTCCCA	155	101.4
BCL2	GCCCTGTGGATGACTGAGTA	CTTCAGAGACAGCCAGGAGA	135	100.4
BAX	CGCCCTTTTCTACTTTGCCA	CCAATGTCCAGCCCATGATG	92	102.1
B-actin	ACCACACCTTCTACAATGAG	TAGCACAGCCTGGATAGC	161	94.0
GAPDH	ACCCACTCCTCCACCTTTGAC	TCCACCACCCTGTTGCTGTAG	110	98.0
CD3e	CCGCCATCTTAGTAAAGTAACAG	AATACCACCCATTTCTTCATTACC	131	90
CD163	TGGAGTGACCTGCTCAGATG	CACCGTCCTTGGAATTTGAT	99	103.8
CD68	TTCCCCTATGGACACCTCAG	TTGTACTCCACCGCCATGTA	86	103.9
CD20	GGGGCTGTCCAGATTATGAA	CCAGGAGTGATCCGGAAATA	148	97.2

Table S2. Correlations of innate immunity markers with inflammatory markers and Banff lesions.

		CD163	CD68	CD20	CD3e	g	i	t	v	ci	ct
TLR1	R	0.46	0.44	0.35	0.35	0.01	0.30	0.25	-0.02	0.13	0.16
	P	7.16^{E}-8*	2.93^{E}-7*	7.20^{E}-5*	7.57^{E}-5*	0.92	1.71^{E}-3	0.01	0.86	0.18	0.09
TLR2	R	0.02	0.09	0.16	0.06	0.04	0.08	0.01	0.01	0.21	0.19
	P	0.84	0.34	0.07	0.53	0.67	0.40	0.91	0.90	0.03	0.05
TLR3	R	-0.19	-0.22	-0.11	0.05	-0.13	-0.21	-0.02	-0.11	-0.08	-0.04
	P	0.04	0.02	0.24	0.61	0.16	0.03	0.87	0.28	0.43	0.65
TLR4	R	0.48	0.52	0.16	0.23	0.10	0.11	0.19	0.12	0.13	0.20
	P	1.73^{E}-8*	8.8^{E}-10*	0.08	0.01	0.29	0.25	0.04	0.22	0.17	0.04
TLR5	R	0.21	0.09	0.24	0.15	-0.08	0.11	0.08	0.02	0.16	0.19
	P	0.02	0.35	0.01	0.1	0.43	0.23	0.39	0.83	0.10	0.05
TLR6	R	0.08	0.1	0.32	0.11	-0.02	0.13	0.09	-0.05	0.24	0.20
	P	0.38	0.25	3.97^{E}-4*	0.22	0.88	0.16	0.38	0.65	0.01	0.04
TLR7	R	0.44	0.52	0.45	0.44	0.03	0.23	0.33	-0.18	0.12	0.07
	P	2.62^{E}-7*	1.12^{E}-9*	1.80^{E}-7*	2.77^{E}-7*	0.77	0.02	4.66^{E}-4	0.08	0.22	0.45
TLR8	R	0.42	0.51	0.17	0.18	0.22	0.27	0.24	0.05	0.17	0.13
	P	1.01^{E}-6*	1.33^{E}-9*	0.06	0.05	0.02	0.00	0.01	0.59	0.08	0.17
TLR9	R	-0.10	-0.05	0.37	0.1	-0.12	0.11	0.10	-0.18	0.25	0.13
	P	0.25	0.58	2.70^{E}-5*	0.26	0.20	0.24	0.31	0.08	0.01	0.18
TLR10	R	-0.1	-0.05	0.5	0.17	-0.11	0.18	0.14	-0.13	0.20	0.09
	P	0.27	0.56	6.87^{E}-9*	0.05	0.27	0.07	0.16	0.21	0.04	0.37

Table S2. Continued.

CD46	R	-0.48	-0.47	-0.11	-0.07	-0.11	-0.19	-0.11	-0.23	-0.19	-0.04
	P	$1.92^{E}{-}8$*	$3.61^{E}{-}8$*	0.25	0.46	0.26	0.04	0.27	0.02	0.05	0.69
CD55	R	0.2	0.1	0.11	0.03	0.03	0.03	$1.85^{E}{-}4$	0.07	0.04	0.28
	P	0.03	0.26	0.23	0.73	0.74	0.72	1.00	0.50	0.65	$3.07^{E}{-}3$
CD59	R	-0.37	-0.36	-0.30	-0.18	0.15	-0.17	-0.15	0.02	-0.14	$-4.32^{E}{-}3$
	P	$3.03^{E}{-}5$*	$4.66^{E}{-}5$*	$7.91^{E}{-}4$*	0.05	0.11	0.07	0.13	0.84	0.15	0.96
C2	R	0.64	0.68	0.21	0.42	0.07	0.32	0.32	0.13	0.29	0.20
	P	$3.1^{E}{-}15$*	$9.0^{E}{-}18$*	0.02	$1.74^{E}{-}6$*	0.50	$7.82^{E}{-}4$	$7.76^{E}{-}4$	0.19	$2.79^{E}{-}3$	0.04
C3	R	0.4	0.4	0.26	0.22	0.09	0.33	0.10	0.08	0.31	0.17
	P	$5.41^{E}{-}6$*	$6.71^{E}{-}6$*	0.01	0.02	0.34	$5.85^{E}{-}4$	0.30	0.45	$1.08^{E}{-}3$	0.09
C4	R	-0.23	-0.18	0.05	0.08	-0.14	0.06	0.09	-0.15	-0.07	0.04
	P	0.01	0.05	0.59	0.38	0.14	0.51	0.36	0.14	0.45	0.70
CR1	R	0.7	0.52	0.43	0.33	0.00	0.44	0.27	0.12	0.25	0.26
	P	$6.5^{E}{-}19$*	$1.16^{E}{-}9$*	$8.98^{E}{-}7$*	$1.96^{E}{-}4$*	0.96	$1.59^{E}{-}6$*	$4.18^{E}{-}3$	0.22	0.01	0.01
BCL2	R	-0.28	-0.27	0.22	0.15	-0.26	-0.08	0.06	-0.05	-0.07	-0.08
	P	$2.20^{E}{-}3$*	$2.30^{E}{-}3$*	0.02	0.09	0.01	0.42	0.53	0.66	0.47	0.40
BAX	R	0.16	0.04	0.11	0.10	-0.05	0.03	0.03	0.12	0.16	0.13
	P	0.07	0.70	0.24	0.29	0.59	0.79	0.74	0.24	0.10	0.19
BAX:BCL	R	0.45	0.33	-0.18	-0.18	0.24	0.07	-0.05	0.15	0.24	0.17
	P	$2.13^{E}{-}7$*	$2.42^{E}{-}4$*	0.06	0.05	0.01	0.47	0.64	0.14	0.01	0.09

g, glomerulitis; i, interstitial inflammation; t, tubulitis; v, intimal arteritis; ci, interstitial fibrosis; ct, tubular atrophy; R, Spearman Correlation Coefficient; P, P value.

* Statistically significant p-values after Bonferroni correction ($P < 0.00025$).
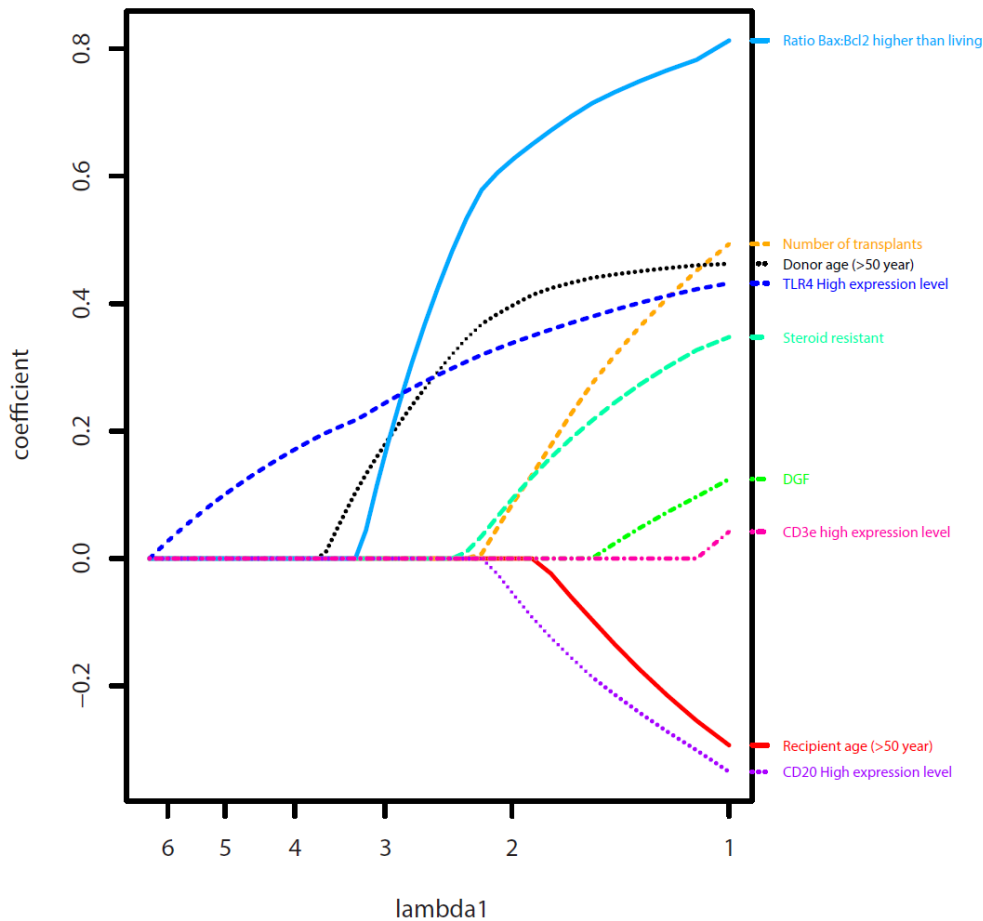
Figure S1. Penalized survival analysis of clinical risk factors. The plot shows the effect of lambda on the fitted regression coefficients. High TLR4 expression, donor age >50, and high Bax:Bcl2 ratio were the top three parameters in the penalized lasso model.

CHAPTER 5

Clinical relevance of arteriolar C4d staining in patients with chronic-active antibody-mediated rejection:
A pilot study

Malou L. H. Snijders[1], Kasia A. Sablik[2], Thierry P. P. van den Bosch[1], Dennis A. Hesselink[2], Michiel G. H. Betjes[2], Ibrahim Batal[3] & Marian C. Clahsen-van Groningen[1]

1. Rotterdam Transplant Group, Department of Pathology, Erasmus MC, University Medical Center Rotterdam, The Netherlands
2. Rotterdam Transplant Group, Department of Internal Medicine, Division of Nephrology and Renal Transplantation, Erasmus MC, University Medical Center Rotterdam, The Netherlands
3. Department of Pathology and Cell Biology, Columbia University, New York, USA

Abstract

Introduction: C4d staining in peritubular capillaries (PTCs) is a well-established feature of antibody-mediated rejection (ABMR). The relevance of C4d staining outside PTCs is not well understood. We investigated the significance of arteriolar C4d staining in c-aABMR.

Methods: All for-cause renal allograft biopsies performed in 2007-2014 at the Erasmus MC and meeting the criteria for suspicious/diagnostic c-aABMR using the Banff Classification 2015, were included. For comparison, renal allograft biopsies from a matched control group and native renal biopsies were analyzed. Arteriolar C4d staining was semi-quantitatively scored as negative (0), small deposits in 1 arteriole (1+), small/large deposits in >1 arterioles (2+) or at least extensive deposits in most arterioles (3+).

Results: Thirty-four of 40 (85%) patients with c-aABMR showed arteriolar C4d staining. A significant difference in arteriolar C4d score was observed between cases and matched controls (p = 0.01) and a trend toward significance difference between cases and native renal biopsies (p = 0.05). In the cases, arteriolar C4d staining was significantly associated with severity of arteriolar hyalinosis (ah) (p = 0.004) and ≥2 arteriolar C4d staining was independently associated with better graft outcome in a multivariate Cox regression analysis (hazard ratio 0.260, 95%-CI: 0.104-0.650, p = 0.004).

Conclusion: This pilot study shows that arteriolar C4d staining is more common in biopsies with c-aABMR compared to those without and that it is associated with ah. ≥2 arteriolar C4d staining is associated with superior graft outcome. However, larger studies are needed to examine these findings in more detail to asses if arteriolar C4d staining is truly related to antibody-mediated injury.

1.   Introduction

Late kidney allograft failure remains an important clinical problem and is mainly caused by chronic-active antibody-mediated rejection (c-aABMR).[1-3] The diagnosis of c-aABMR according to the Banff Classification 2015 requires both pathological and clinical laboratory criteria, namely: (1) histologic evidence of chronic tissue injury, (2) evidence of current / recent antibody interaction with vascular endothelium, *i.e.* C4d staining on endothelial cells of the peritubular capillaries (PTCs) and medullary vasa recta and/or peritubular capillaritis (ptc) + glomerulitis (g) ≥2, and (3) detection of donor-specific anti-HLA antibodies (DSAs).[4] Cases with histologic features of c-aABMR with either evidence of current / recent antibody interaction with vascular endothelium or the presence of DSAs but not both, may be diagnosed as "suspicious for c-aABMR".

C4d staining was first described in renal allograft biopsies by Feucht *et al*. and has broadened our understanding of the pathogenesis and clinical consequences of ABMR.[5, 6] C4d is a degradation product of the complement factor C4 which participates in the classical and lectin pathways of complement activation. The activation of C4 generates C4b which is then cleaved into C4d and larger fragments such as C4c. Because C4d forms an internal thioester bond with the endothelial surface it can covalently bind to the endothelium, where it remains for several days or weeks. Therefore, it is a durable marker of local complement activation.[7-9]

C4d positivity in the PTCs in cases of ABMR was found to be a specific marker for interaction of DSAs with the endothelium of the renal microcirculation and is associated with poor kidney transplant survival.[10-14] C4d staining by immunohistochemistry or immunofluorescence is also advised by the Banff Classification to be offered in the routine diagnostic pathologic evaluation of all renal allograft biopsies.[15]

Peer reviewed literature on C4d immunohistochemistry has mainly focused on staining in the PTCs. The significance of C4d staining outside the PTCs and in particular the renal arterioles of patients with c-aABMR is unclear. This pilot study was designed to investigate the prevalence of C4d staining in the arterioles in cases with suspicious and diagnostic c-aABMR. In addition, the relationship with other histological and clinical features was analyzed.

2. Methods

In this retrospective pilot study, the database of the Department of Pathology of the Erasmus MC, University Medical Center Rotterdam, Rotterdam, The Netherlands, was searched to identify all patients with a for-cause renal allograft biopsy performed between 2007 and 2014 with the diagnosis suspicious or diagnostic for c-aABMR according to the Banff 2015 criteria.[4] Clinical and demographic data of the patients were collected from the electronic patient files. These included: gender, age at transplantation, donor age and type (living or deceased), primary renal disease, number of renal transplantations (first *vs*. second or higher), the presence or absence of DSAs, estimated GFR at time of biopsy (eGFR), proteinuria at time of biopsy and the cumulative tacrolimus exposure (see below).

DSA testing was performed at the laboratory of immunohematology of the Leiden University Medical Center, which serves as the Eurotransplant reference laboratory. DSAs were considered present when antibodies directed against one or more donor HLA alleles were detected in patient serum samples. Anti-HLA status at time of biopsy was determined using the Luminex Screening Assay [Lifecodes Lifescreen Deluxe (LMX) kit, according to the manufacturer's manual (Immunocor Transplant Diagnostics Inc. Stamford, CT, USA]. If anti-HLA antibodies were found to be present in the screening, they were further typed by use of a Luminex Single Antigen assay, using LAB screen HLA class-I and class-II antigen beads (OneLambda, CanogaPark, GA, USA). It was determined whether these were de novo DSAs based on DSA testing prior to transplantation.

The cumulative tacrolimus exposure was measured by multiplying the tacrolimus through levels after transplantation to time of biopsy with the post transplantation period (cumulative tacrolimus exposure = (C1min + C2min + C3min ... + CXmin/X) x post-transplant time (months)) as previously described by Leal *et al*.[16]

2.1 Histological and immunohistochemical evaluation

Standard H&E, PAS+, Jones and Trichrome sections were re-evaluated according to the Banff 2015 criteria.[4] Immunohistochemical C4d staining was performed on 4 µm slides of formalin-fixed paraffin-embedded (FFPE) tissue with an automated, validated and accredited staining system (Ventana Benchmark ULTRA, Ventana Medical Systems, Tucsen, AZ, USA) using an ultra-view universal DAB detection Kit. In brief, following deparaffinization and heat-induced antigen retrieval

with CC1 (#950-124, Ventana) for 64 minutes, the tissue samples were incubated with a rabbit monoclonal antibody for C4d (SP91, #760-4803, Cell Marque) for 24 minutes at 36°C. Incubation was followed by hematoxylin II counter stain for 8 minutes and then a blue coloring reagent for 8 minutes according to the manufactures instructions (Ventana).

C4d staining in arterioles was semi-quantitatively classified (0-3) as negative (0), small deposits in 1 arteriole (1+), small or large deposits in >1 arteriole (2+) or at least extensive deposits in most arterioles (3+). C4d staining in arteries was scored as negative (0), small deposits in 1 artery (1+), small or large deposits in >1 artery (2+) or at least extensive deposits in most arteries (3+). In the arterioles and arteries, both endothelial and mural staining were counted as positive. In addition, we compared cases with endothelial staining, mural staining and endothelial + mural staining. C4d staining in the PTCs and glomeruli was scored as negative (0%), minimal (<10%), focal (10-50%) or diffuse (>50%) staining.

To investigate if C4d co-localizes with arteriolar hyalinosis (ah), a proof of principal with 3 cases and 3 controls was performed using a C4d immunohistochemical staining as described above. After C4d staining, representative arterioles with ah were photographed and slides were subsequently stained by PAS+. Thereafter, the same area was photographed again to visualize co-localization.

To assess the specificity of C4d deposition by immunohistochemistry in the arterioles, an immunohistochemical staining for IgG was performed in 3 cases and 3 controls using the Ventana Benchmark ULTRA (Ventana Medical Systems Inc.). Four micrometer thick FFPE sections were stained for IgG. In brief, following deparaffinization and heat-induced antigen retrieval with CC1 (PH 9.0) for 36 minutes, slides were incubated with primary antibody IgG (DAKO, A0423, dilution 1:24000) at 37 °C for 32 minutes. Detection was performed with the ultraview kit (cat:760-500, Ventana) followed by incubation with hematoxylin II counter stain for 8 minutes and then a blue coloring reagent for 8 minutes according to the manufactures instructions (Ventana).

2.2   Control group

A matched control group was included to compare arteriolar C4d staining in biopsies from patients with c-aABMR to a group without rejection. To select controls, the pathology database of our center was searched for patients with a renal allograft biopsy in the period 2007- 2014 without evidence of ABMR. This was the same time period as the c-aABMR cases allowing for similar (immunosuppressive) treatment

regimens. Patients were matched to controls in a 1:1 ratio based on the criterion "presence of a for-cause renal allograft biopsy at the same time after transplantation as the case". Controls with a histological diagnosis of hypertensive nephropathy, diabetic nephropathy and calcineurin inhibitor (CNI) nephrotoxicity were also included since ah is often seen in these biopsies, as well as in cases with c-aABMR, making it possible to compare the association between ah and arteriolar C4d staining in both groups.[17-19]

2.3 Native renal biopsies

A total of 18 native renal biopsies was included to compare arteriolar C4d staining in biopsies from patients with c-aABMR to a group of native renal biopsies with a histological diagnosis of diabetic nephropathy, hypertensive nephropathy or CNI nephrotoxicity. C4d immunohistochemistry was additionally performed in these biopsies and both arteriolar C4d staining and ah were scored.

2.4 Statistical analysis

SPSS Statistics version 24.0 was used for all statistical analyses (IBM SPSS Statistics for Windows. Armonk, NY: IBM Corp.). Differences with a (two sided) p-value of less than 0.05 were considered statistically significant. Differences in patient characteristics between cases and matched controls were analyzed by the McNemar's test for categorical variables and the paired sample t-test or Wilcoxon signed rank test for continuous variables. To compare pathological features, including arteriolar C4d scores, in the cases and matched controls, the Wilcoxon signed rank test was used. To compare patient characteristics in the cases and native renal biopsies the Chi-square test was used for categorical variables and the independent sample t-test or Mann Whitney U test for continuous variables. To compare arteriolar C4d scores the Chi-square test was used.

For comparison of the patient characteristics in the c-aABMR subgroups, one-way ANOVA was used for comparison of continuous variables with normal distribution and the Kruskal-Wallis test for continuous variables without normal distribution. Categorical variables were compared using the Chi-square test. Pathological findings were analyzed using the Chi-square test.

To evaluate the prognostic value of arteriolar C4d staining in patients with suspicious/diagnostic c-aABMR, we calculated graft survival rates measured from time of biopsy. Allograft failure was defined as the need to return to dialysis or re-transplantation. Graft survival was compared using Kaplan Meier survival analysis and

log rank test. Univariate and multivariate Cox regression analysis was performed to adjust for other variables associated with graft loss.

2.5   Medical ethics

The study protocol was consistent with professional guidelines and the Declaration of Istanbul; non WMO compliant research is research not residing under the Dutch law on medical research with patients and is regulated by the Dutch Code of Conduct (Federa). Based on this, the study was exempt from approval from the local medical ethics committee.

3.   Results

3.1   Patient characteristics

A total of 46 patients with suspicious/diagnostic c-aABMR diagnosed between 2007 and 2014 was identified. Histological slides were available for 40 of these patients and these were included in this pilot study. Of these, the diagnosis was "suspicious for c-aABMR" in 23 patients (58%) and "diagnostic for c-aABMR" in 17 patients (42%). Patient age ranged between 19 and 72 years (mean 50 ± 15 years). Thirteen patients (33%) were recipients of a deceased donor allograft (mean donor age: 47 ± 13 years). Fourteen patients (35%) were re-transplant recipients. The average eGFR at time of biopsy was 31.2 ± 7.9 mL/min per 1.73 m². DSAs were present in 17 patients (42%). Thirty-three patients (83%) received treatment with tacrolimus. Transplant glomerulopathy (cg>0) was seen in all biopsies with c-aABMR (n=40). In most biopsies, cg3 was observed (80%). In 2 cases, cg1a was diagnosed based on electron microscopy. All biopsies (n=40) had a microvascular inflammation score (ptc + g; MVI) ≥ 2 (median 5; range 3 - 6). C4d positivity in the PTCs was found in 18 patients (45%); <10% in 10 patients (56%), 10-50% in 2 patients (11%) and >50% in 6 patients (33%). Eight patients with C4d staining in the PTCs had a diagnosis of suspicious c-aABMR and 10 patients diagnostic c-aABMR.

In addition, 40 matched controls were selected. The histological diagnoses in the matched controls were T-cell mediated rejection only (TCMR; n=8), hypertensive nephropathy (n=8, of which 3 also showed TCMR), diabetic nephropathy (n=2, of which 1 also showed TCMR), CNI nephrotoxicity (n=3), interstitial fibrosis and tubular atrophy (n=6), focal segmental glomerulosclerosis (n=4, of which 2 also showed TCMR), recurrent IgA nephropathy (n=6, of which 2

also showed TCMR), membranous glomerulopathy (n=1), acute tubular necrosis (n=1) and ascending urinary tract infection (n=1).

Eighteen native renal biopsies with a histological diagnosis of diabetic nephropathy (n=6), hypertensive nephropathy (n=8) and CNI nephrotoxicity (n=4) were included. Of the patients with CNI nephrotoxicity, 2 had a prior lung transplantation, 1 patient had a heart transplantation and 1 a liver transplantation. Patient characteristics of the 3 groups and transplant–related characteristics and pathological features according the Banff Classification 2015 of the c-aABMR and matched control group are shown in Table 1.

Table 1. Clinical characteristics of suspicious/diagnostic c-aABMR cases, matched controls and native renal biopsies.

	c-aABMR cases	matched controls	P	native biopsies	P
n (%)	40	40		18	
Recipient age (years), *mean (SD)*	50±15	55±14	0.08	48±13	0.66
Male (%)	24 (60)	25 (63)	1.00	13 (72)	0.28
Hypertension (%)[1]	30 (75)	28 (70)	0.77	12 (67)	0.36
Diabetes mellitus (%)[2]	12 (30)	13 (33)	1.00	12 (67)	0.01
Deceased donor (%)	13 (31)	15 (38)	0.80	NA	NA
Donor age (years), *mean (SD)*	47±13	54±14	0.02	NA	NA
Re-transplantation (%)	14 (35)	7 (18)	0.14	NA	NA
Time to biopsy (months), *mean (SD)*	72±44	73±44	0.49	NA	NA
eGFR (ml/min/1.73m^2)[3], *mean (SD)*	31.2±7.9	36.1±16.1	0.07	45.6±25.5	0.002
Proteinuria (g/24 h)[3], *median (IQR)*	0.8 (1.2)	0.4 (0.9)	0.02	1.1 (0.5)	0.76
Tacrolimus treatment (%)	33 (83)	38 (95)	1.00	NA	NA
Primary kidney disease					
Hypertensive nephropathy	7	12		8	
Diabetic nephropathy	7	3		6	
PKD	3	7		4	

Table 1. Continued

IgA nephropathy	0	7	0
FSGS	1	5	0
Chronic pyelonephritis	3	0	0
Obstructive nephropathy	1	2	0
Other	16	4	0
Undetermined	2	0	0
Banff Criteria 2015, *median (range)*			
Total inflammation (ti)	3 (0-3)	1 (0-3)	<0.001
Interstitial inflammation (i)	2 (0-3)	0 (0-3)	<0.001
Tubulitis (t)	0 (0-3)	1 (0-3)	0.007
Intimal arteritis (v)	0 (0-2)	0 (0-0)	0.001
Glomerulitis (g)	3 (2-3)	0 (0-3)	<0.001
Peritubular capillaritis (ptc)	2 (0-3)	0 (0-1)	<0.001
Interstitial fibrosis (ci)	2 (0-3)	1 (0-3)	0.009
Tubular atrophy (ct)	1 (0-3)	1 (0-3)	0.38
Vascular intimal thickening (cv)	2 (0-3)	2 (0-3)	0.06
Transplant glomerulopathy (cg)	3 (1-3)	0 (0-1)	<0.001
Arteriolar hyalinosis (ah)	2 (0-3)	2 (0-3)	0.30
Mesangial matrix increase (mm)	3 (0-3)	2 (0-3)	0.008
C4d deposition in PTCs	0 (0-3)	0 (0-0)	<0.001
C4d deposition in GBM	3 (0-3)	0 (0-3)	<0.001
C4d deposition in arterioles	2 (0-3)	1 (0-3)	0.01
C4d deposition in arteries	0 (0-2)	1 (0-3)	0.22

[1]Defined as treatment with antihypertensive drugs.
[2]Defined as treatment with glucose-lowering drugs.
[3]Measurements at time of biopsy.
PKD, polycystic kidney disease; FSGS, focal segmental glomerulosclerosis, PTCs, peritubular capillaries; GBM, glomerular basement membrane.

3.2   Arteriolar C4d staining

Thirty-four c-aABMR cases (85%) showed arteriolar C4d staining in their biopsy compared to 23 of the matched controls (58%) and 14 of the native renal biopsies (78%). A score of ≥2 was observed in 26 c-aABMR cases (65%) compared to 13 matched controls (32.5%) and 6 native renal biopsies (33%). A significant difference in arteriolar C4d staining score was observed between cases and matched controls (p = 0.01) and a trend toward more arteriolar C4d staining in c-aABMR cases compared to native renal biopsies (p = 0.05; Figure 1). Figure 2 shows microscopic examples of arteriolar C4d staining.

In the c-aABMR cases, no significant correlation was found between arteriolar C4d staining and recipient age, donor age or donor type (Table 2). Also, a clinical diagnosis of diabetes mellitus and hypertension was not associated with arteriolar C4d staining. Interestingly, DSAs were detectable in all patients without arteriolar C4d staining (n=6) while only 32% of patients with arteriolar C4d staining had detectable DSAs (p = 0.009). Arteriolar C4d staining was not significantly associated with time after transplantation (p = 0.62).
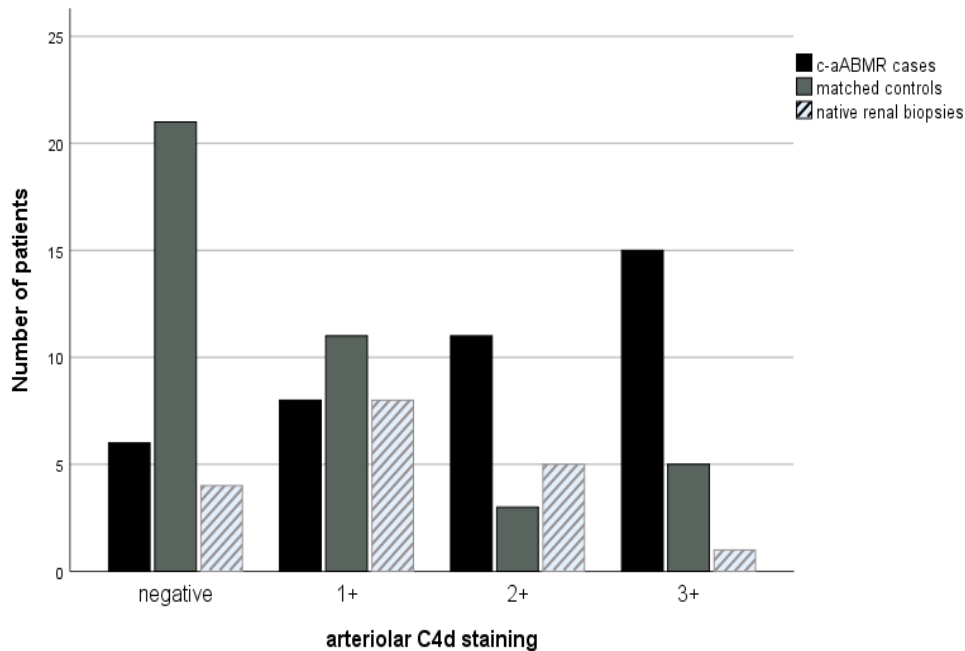

Figure 1. Overview of arteriolar C4d staining scores in the suspicious/diagnostic c-aABMR group, the matched control group and native renal biopsies.

Table 2. Characteristics of the patients with suspicious/diagnostic c-aABMR and subgroups defined by arteriolar C4d staining (negative, 1+, 2+ and 3+) in their kidney allograft biopsy.

	All	C4d 0	C4d 1+	C4d 2+	C4d 3+	P
N	40	6	8	11	15	
Recipient age (years), *mean (SD)*	50±15	58±7	45±11	53±18	47±16	0.31
Male	24	3	5	9	7	0.31
Hypertension[1]	30	5	4	9	12	0.34
Diabetes mellitus[2]	12	1	2	4	5	0.83
Deceased donor	13	3	2	4	4	0.72
Donor age (years), *mean (SD)*	47±13	48±16	44±15	45±13	50±12	0.69
Re-transplantation	14	3	4	2	5	0.43
Time to biopsy (months), *mean (SD)*	72±44	50±27	77±59	77±41	75±43	0.62
PRAs current, *median (IQR)*	0 (4)	0 (8)	1 (4)	0 (3)	0 (0)	0.78
PRAs historical, *median (IQR)*	4 (27)	6.5 (27)	5 (25)	4 (22)	6 (39)	0.81
Detectable DSAs	17	6	1	5	5	0.009
eGFR (ml/min/1.73m^2)[3], *mean (SD)*	31.2±7.9	33.3±8.5	28.4±9.5	32.1±6.4	31.1±8.4	0.68
Proteinuria (g/24 h)[3], *median (IQR)*	0.8 (1.2)	1.1 (5.2)	0.9 (1.3)	0.7 (1.1)	0.7 (1.2)	0.67
Cumulative TAC exposure (ng/mL), *median (IQR)*	537.5 (554.3)	301.7 (564.2)	412.2 (317.3)	661.2 (517.1)	585.2 (695.3)	0.52

[1]Defined as treatment with antihypertensive drugs.
[2]Defined as treatment with anti-diabetic drugs.
[3]Measurements at time of biopsy.
DSAs, donor-specific antibodies; PRAs, panel reactive antibodies; TAC, tacrolimus.

3.3   Associations with other pathologic findings in c-aABMR cases

In 20 of 22 cases without C4d staining in the PTCs, arteriolar C4d staining was observed (90%). However, no negative significant association was found between arteriolar C4d staining score and C4d staining in PTCs (p = 0.07; Table 3). In addition, other C4d staining patterns (in glomeruli and arteries) did not show a significant association with arteriolar C4d staining. Ah was found in 35 biopsies of patients with c-aABMR (88%) and was classified as ah1 in 9 patients (26%), ah2 in 7 patients (20%) and ah3 in 19 patients (54%). No difference in ah score was observed between c-ABMR cases and matched controls (p = 0.30) or between c-aABMR cases and native renal biopsies (p = 0.08). Arteriolar C4d staining was significantly associated with the severity of ah in the cases (p = 0.004) and native renal biopsies (p = 0.024) but not in the matched controls (p = 0.09). Furthermore, c-aABMR cases with arteriolar C4d staining showed significantly more interstitial inflammation (p = 0.007) which was not observed in the matched controls (p = 0.12).

Arteriolar C4d staining in the c-aABMR cases was evaluated in more detail; endothelial C4d staining in the arterioles was observed in 9 cases (27%) and mural arteriolar C4d staining was observed in 10 cases (29%). Fifteen cases showed both endothelial and mural arteriolar C4d staining (44%). The association of the arteriolar C4d staining pattern in c-aABMR cases (endothelial, mural + endothelial, or exclusively mural C4d staining) with other pathological findings according to the Banff Classification 2015 was analyzed and no significant differences were found between these subgroups (Table S1, SDC, http://links.lww.com/TP/B809).

Of the 5 cases without ah, 1 case showed 1+ arteriolar C4d staining, 1 showed 2+ arteriolar C4d staining and 3 showed 3+ arteriolar C4d staining. In contrast, of the 6 cases without arteriolar C4d staining, ah1 was observed in 5 cases and ah3 in 1 case. In cases with ah, arteriolar C4d staining seemed often located at the site of the hyalinosis (Figure 3). To visualize this, C4d immunohistochemistry followed by PAS+ staining was performed in cases as proof of principle showing that arteriolar C4d staining is present within the hyalinosis (Figure 4).

To exclude the possibility of arteriolar C4d staining not being specific (and therefore not reflective of real complement activation) an IgG rabbit polyclonal staining was performed in 3 cases and 3 controls. IgG showed no staining in the arteriolar walls. In particular, no staining was observed at the sites of arteriolar hyalinosis. Nonspecific IgG staining was observed in a heterogeneous fashion; focally in tubular epithelial cells, the Bowman's space and some lumen of the arterioles (Figure S1, SDC, http://links.lww.com/TP/B809).
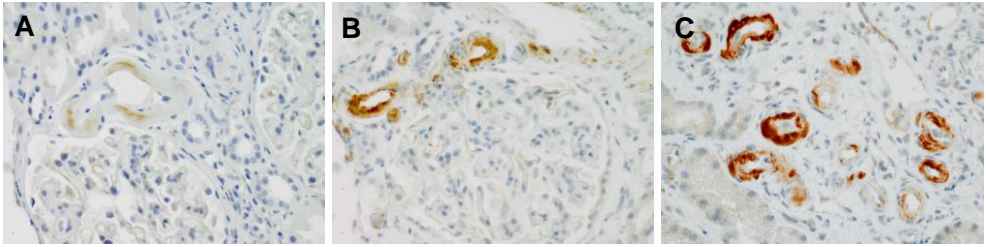
Figure 2. Representative photomicrographs of scoring immunohistochemical arteriolar C4d staining in renal allograft biopsies. (A) score 1+, (B) 2+ and (C) 3+ (magnification 400x).
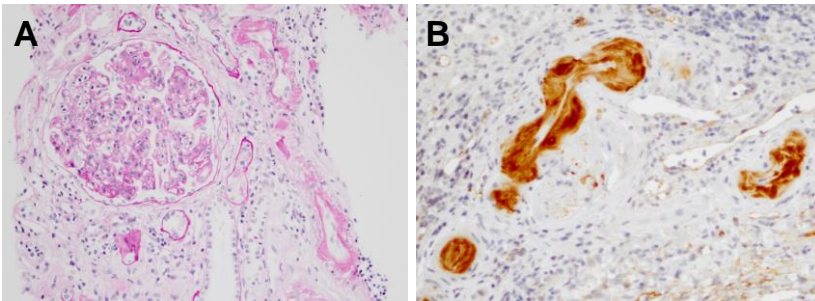

Figure 3. (A) PAS+ staining with an example of severe arteriolar hyalinosis (ah3) (magnification 200x) and (B) 3+ arteriolar C4d staining in arterioles showing severe arteriolar hyalinosis (ah3) (magnification 400x).
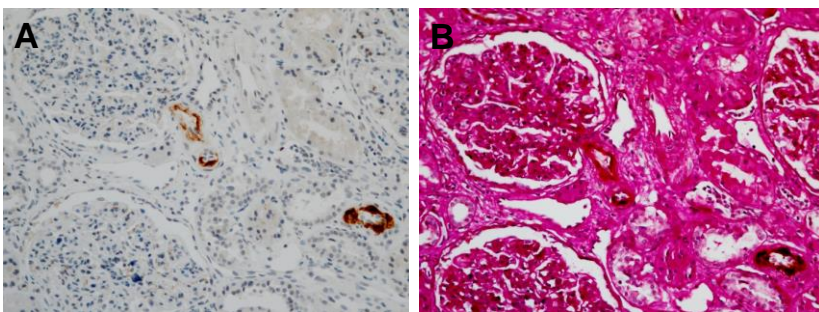

Figure 4. (A) Example of a c-aABMR case with mural arteriolar C4d staining (magnification 200x). (B) Immunohistochemistry for C4d was followed by PAS+ showing arteriolar C4d staining at the site of the hyalinosis (magnification 200x).

Table 3. Association of arteriolar C4d staining scores with other pathological findings in biopsies with suspicious/diagnostic c-aABMR.

Banff Criteria 2015 (n=40)	C4d 0	C4d 1+	C4d 2+	C4d 3+	P
N (%)	6 (15)	8 (20)	11 (27)	15 (38)	
Total inflammation (ti)	2 (0-3)	2 (1-3)	3 (1-3)	3 (0-3)	0.54
Interstitial inflammation (i)	0 (0-3)	1 (1-3)	3 (1-3)	3 (0-3)	0.007
Tubulitis (t)	0 (0-3)	0 (0-1)	0 (0-2)	0 (0-2)	0.53
Intimal arteritis (v)	0 (0-0)	0 (0-1)	1 (0-2)	0 (0-2)	0.10
Glomerulitis (g)	3 (2-3)	3 (2-3)	3 (3-3)	3 (0-3)	0.26
Peritubular capillaritis (ptc)	2 (1-3)	2 (0-3)	2 (0-3)	3 (1-3)	0.58
Interstitial fibrosis (ci)	1 (0-3)	1 (0-3)	1 (0-3)	2 (0-3)	0.27
Tubular atrophy (ct)	1 (1-2)	1 (0-3)	1 (0-1)	2 (1-3)	0.06
Vascular intimal thickening (cv)	1 (0-3)	2 (0-3)	1 (1-3)	3 (0-3)	0.06
Transplant glomerulopathy (cg)	3 (1-3)	3 (1-3)	3 (1-3)	3 (1-3)	0.76
Arteriolar hyalinosis (ah)	1 (1-3)	2 (0-3)	3 (0-3)	3 (0-3)	0.004
Mesangial matrix increase (mm)	3 (0-3)	3 (0-3)	3 (0-3)	3 (0-3)	0.67
C4d deposition in PTCs	2 (0-3)	0 (0-2)	1 (0-3)	0 (0-3)	0.07
C4d deposition in GBM	2 (2-3)	1 (0-3)	3 (0-3)	3 (0-3)	0.35
C4d deposition in arteries	1 (0-1)	0 (0-2)	0 (0-2)	1 (0-2)	0.29

Pathological lesions in the cases with c-aABMR according to the Banff 2015 criteria and the association with arteriolar C4d staining. Median and range of the pathological lesions in the arteriolar C4d subgroups are showed in the table.

PTCs, peritubular capillaries; GBM, glomerular basement membrane.

3.4 Associations of arteriolar C4d staining with other pathologic findings in the entire cohort

In the entire cohort of 80 patients (c-aABMR cases and matched controls), arteriolar C4d staining was observed in 57 patients (71%). No significant association between arteriolar C4d staining and other C4d staining patterns was observed in the entire cohort (Table S2, SDC, http://links.lww.com/TP/B809). Biopsies with arteriolar C4d staining showed significantly more interstitial inflammation (p < 0.001) and a higher score of total inflammation (p = 0.02) and intimal arteritis (p = 0.01). No

significant association was found between ah score and arteriolar C4d staining in the entire cohort (p = 0.07).

3.5   Arteriolar C4d staining and the cumulative tacrolimus exposure

For the calculation of the cumulative tacrolimus exposure a mean of 41 measurements per patient (range 9 - 83) was available in the c-aABMR cases. The median cumulative tacrolimus exposure was 537.5 ng/mL (IQR 554.3 ng/mL). A significant association was observed between severity of ah and cumulative tacrolimus exposure (p = 0.038). No significant association was found between arteriolar C4d staining score and cumulative tacrolimus exposure (p = 0.52). In the entire cohort, a mean of 45 measurements per patient (range 7 - 107) was available and median tacrolimus exposure was 523.4 ng/mL (IQR 492.4 ng/mL). No significant association was observed between ah and cumulative tacrolimus exposure (p = 0.24) or arteriolar C4d staining score and cumulative tacrolimus exposure (p = 0.46).

3.6   Arteriolar C4d staining and transplant outcome in c-aABMR cases

Graft loss was seen in 24 c-aABMR cases (60%) and mean time after biopsy was 42 ± 21 months. No patients died during follow up. Since the groups were small we combined the 4 groups into 2 groups; arteriolar C4d 0/1+ and arteriolar C4d 2+/3+. In the arteriolar C4d 0/1+ group 86% of the grafts failed *vs*. 46% in the arteriolar C4d 2+/3+ group. Graft survival was significantly worse in the group with 0/1+ C4d staining in the arterioles (log rank p = 0.01; Figure 5A). Both C4d staining in the PTCs and DSA status was not significantly associated with graft survival (log rank p = 0.13 and p = 0.22 respectively; Figures 5B and 5C).

Univariate Cox regression analyses demonstrated that interstitial fibrosis was significantly associated with inferior graft survival (hazard ratio 1.559, 95%-CI: 1.069-2.272, p = 0.021), while ah showed a trend toward superior graft survival (hazard ratio 0.760, 95%-CI: 0.538-1.073, p = 0.12). A multivariate Cox regression analysis identified that 2+/3+ arteriolar C4d staining was independently associated with a decreased risk of allograft loss after adjusting for both interstitial fibrosis and ah (hazard ratio 0.260, 95%-CI: 0.104-0.650, p = 0.004; Table 4).

Table 4. Multivariate Cox regression analysis for graft failure.

	HR (95%-CI)	**P**
Arteriolar C4d staining (0/1+ *vs.* 2+/3+)	0.260 (0.104 – 0.650)	0.004
Arteriolar hyalinosis	0.852 (0.582 – 1.247)	0.409
Interstitial fibrosis	1.865 (1.211 – 2.872)	0.005

Multivariate Cox regression analysis using those variables with a p-value <0.15 in a univariate analysis; arteriolar C4d staining, arteriolar hyalinosis and interstitial fibrosis.
HR, hazard ratio; CI, confidence interval

4. Discussion

C4d staining in the PTCs of renal allograft biopsies is a diagnostic criteria for ABMR and correlates with graft dysfunction.[10-12] However, there are limited data about the prevalence of arteriolar C4d staining in c-aABMR. This pilot study demonstrates that arteriolar C4d staining is a common finding in biopsies with suspicious/diagnostic c-aABMR as it was present in 85% of the cases and it seems to be associated with superior graft function over time. In addition, we found that arteriolar C4d staining is significant associated with ah.

The presence of C4d staining outside of the PTCs has only been described in a few publications. Batal *et al.* found C4d positivity in the arterioles in 22 out 48 (46%) paraffin embedded biopsies from patients with a history of DSAs.[20] Kikić *et al.* observed arteriolar C4d staining in 163 out 243 patients (67%) with a for-cause renal allograft biopsy.[21] They found a significant relationship between both arteriolar and glomerular C4d staining and C4d staining in the PTCs and concluded that there might be a relationship between humoral alloimmunity and distinct less established staining patterns.[21] It has been suggested that C4d staining in the glomerulus is associated with transplant glomerulopathy, most likely as a marker of structural capillary wall remodeling.[22-25] We did not observe an association between arteriolar C4d staining and C4d staining in the glomeruli. Through performing additional stainings with IgG we also showed that the deposition of C4d in the arterioles by immunohistochemical staining is specific.
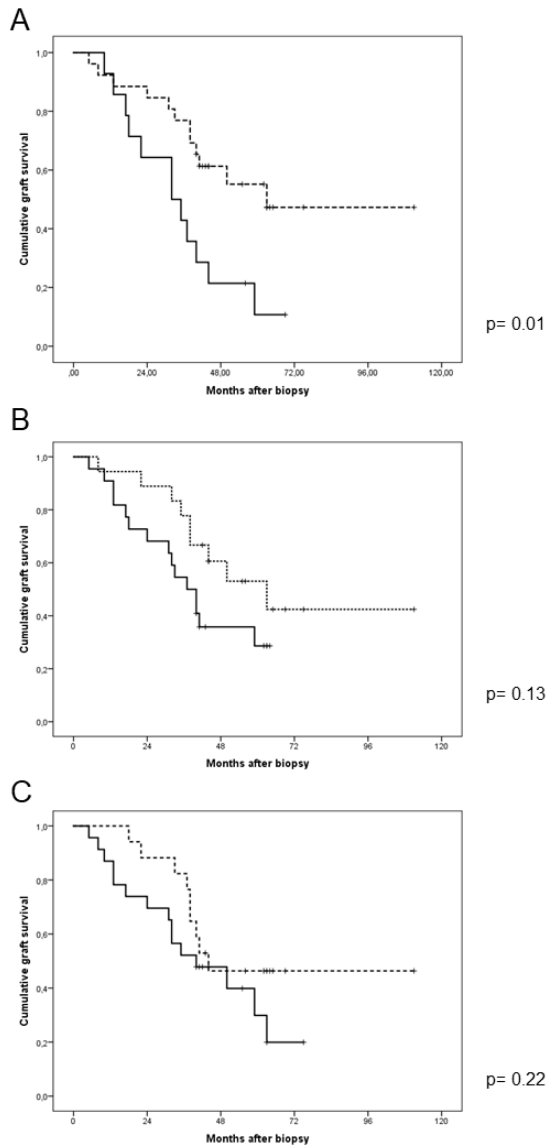
Figure 5. (A) Graft survival in patients with suspicious/diagnostic c-aABMR in the arteriolar C4d 2+/3+ group (n=26; dotted line) and arteriolar C4d 0/1+ group (n=14; continuous line; p=0.01). (B) Graft survival in patients with suspicious/diagnostic c-aABMR with C4d staining in PTCs (n=18; dotted line) and without C4d staining in the PTCs (n=22; continuous line; p=0.13). (C) Graft survival in patients with suspicious/diagnostic c-aABMR with detectable DSAs (n=17; dotted line) and without detectable DSAs (n=13; continuous line; p=0.22).

A matched control group and a cohort of native renal biopsies were included for further comparison. A significant difference in arteriolar C4d score was observed between c-aABMR cases and matched controls and there was a trend toward higher arteriolar C4d staining scores in the c-aABMR group compared to the group with native renal biopsies. 3+ arteriolar C4d staining was observed in 38% of the c-aABMR cases compared to only 6% of the native renal biopsies. The lower sample size in the cohort of native renal biopsies might be an explanation for the fact that no significant difference was reached.

Ah may be caused by any chronic endothelial cell injury and is commonly found in patients with diabetes mellitus and hypertension.[19, 28, 29] In accordance with the study of Batal *et al.* a significant association between arteriolar C4d staining and severity of ah was found in the c-aABMR cases in our study.[20] Arteriolar C4d staining showed no significant association with a clinical diagnosis of hypertension or diabetes mellitus.

As ah is frequently considered to be the consequence of chronic CNI nephrotoxicity, we analyzed the cumulative tacrolimus exposure.[17, 18] A previous report from Einecke *et al.* suggested that ah is rather the consequence of adequate CNI treatment over time than CNI nephrotoxicity.[30] They observed increased risk of graft loss in patients without ah, probably as a result of underimmunosuppression and nonadherence. While ah and cumulative tacrolimus exposure showed a significant association in the c-aABMR cases, no significant correlation between cumulative tacrolimus exposure and arteriolar C4d staining was found, indicating that, unlike ah, arteriolar C4d staining is not tightly associated with cumulative tacrolimus exposure. This significant association between ah and the cumulative tacrolimus exposure was not observed in the entire cohort. An explanation for this finding might be that ah is caused by other factors than tacrolimus exposure in the matched control group, for example diabetic and hypertensive nephropathy.

A small number of patients in our study showed arteriolar C4d staining but no ah and vice versa, indicating that these features are not completely dependent. In cases with ah, arteriolar C4d staining was often observed at the site of the hyalinosis, which was confirmed by performing immunohistochemical staining for C4d followed PAS+. Subsequently, arteriolar C4d staining in the c-aABMR cases was further analyzed by subdividing the staining pattern into endothelial and mural staining, which might reflect two different processes. Endothelial arteriolar C4d staining seems to be related to classical pathway or lectin pathway-associated C4 activation with deposition of C4d on the luminal surface of the endothelium.[7] Mural

arteriolar C4d staining may be caused by leakage of luminal formed C4d into the arteriolar wall due to increased vascular permeability or seepage of plasma into the arteriolar wall with local C4d formation through the activation of either the classical or lectin complement pathway. This mural C4d in the arterioles seems to accumulate at the sites of hyalinosis.[7] However, no significant differences in pathological lesions, including ah, according to the Banff Classification 2015 were observed between the different staining patterns (endothelial, mural and endothelial + mural arteriolar C4d staining).

The correlation of arteriolar C4d staining with other pathologic lesions (besides C4d staining in the glomeruli and PTCs and ah) according to the Banff Classification has not been evaluated before. We showed that interstitial inflammation was significantly associated with arteriolar C4d staining in both the c-ABMR cases and the entire cohort. Furthermore, intimal arteritis and total inflammation were significantly associated with arteriolar C4d staining in the entire cohort.

The Banff classification 2015 was used in this pilot study which allowed us to use the category "suspicious for c-aABMR". Since all biopsies showed histologic evidence of chronic tissue injury and evidence of current / recent antibody interaction with vascular endothelium (MVI≥2), the difference between suspicious and diagnostic c-aABMR in this study was based on the absence or presence of DSAs. In a previous study, Sablik *et al.* observed no difference in histomorphology between biopsies with c-aABMR with and without detectable DSAs.[31] In our study, all 23 patients with suspicious c-aABMR (without detectable DSAs) showed arteriolar C4d staining and in 10 cases (43%) 3+ staining was observed. Interestingly, we noticed that arteriolar C4d staining was significantly more often found in cases without detectable DSAs. In contrast to our study, Kikić *et al.* observed a trend towards more frequent detectable DSAs in patients with arteriolar C4d deposition compared to patients without arteriolar C4d deposition (13% vs 4%; p=0.06).[21]

In contrast to other studies, no significant relationship was shown between C4d staining in the PTCs and inferior graft survival.[9-11, 13] Curve separation was observed but no significance difference in graft survival was reached in this pilot study. There are a few studies showing no differences in graft survival rates irrespective of the presence or absence of C4d staining in PTCs in late allograft biopsies with c-aABMR (after six months after transplantation).[32] We observed that graft survival was better in c-aABMR patients with 2+/3+ arteriolar C4d staining compared to patients with 0/1+ arteriolar C4d staining. In a univariate Cox regression

analysis, as previously described in the literature, we found interstitial fibrosis to be associated with inferior graft outcome.[33, 34] In a multivariate Cox regression analysis, the presence of 2+/3+ arteriolar C4d staining remained independently associated with superior graft outcome, regardless of the presence of interstitial fibrosis and ah. This finding is surprising and we cannot exclude the possibility that it is a confounder or a chance finding resulting from a limiting sample size. Since the c-aABMR group is small, we were not able to analyze this into more detail. Therefore, we cannot draw any conclusions from this observation and more research is needed to assess if arteriolar C4d staining is indeed related to superior graft outcome.

We recognize the limitations associated with this pilot due to the relatively small sample size and therefore no firm conclusions can be drawn. However, we did have complete information about the patient characteristics which made detailed evaluation possible. Furthermore, a matched control group and a cohort of native renal biopsies were included to examine arteriolar C4d staining in these groups and compare the results to the c-aABMR cases.

In conclusion, this pilot study shows that arteriolar C4d staining is a common finding in patients with c-aABMR and that it is significantly associated with the severity of ah. No significant relation was found with C4d staining in the PTCs. This study provides the first insights of arteriolar C4d staining in c-aABMR, however it remains to be confirmed if arteriolar C4d staining is truly specific for antibody-mediated injury and related to superior graft function. These findings make it worthwhile to further investigate the etiology of arteriolar C4d staining in a larger cohort of patients with c-aABMR.

References

1. Sellarés J, de Freitas DG, Mengel M, et al. Understanding the causes of kidney transplant failure: the dominant role of antibody-mediated rejection and nonadherence. *Am J Transplant*. 2012;12(2):388-399.

2. Einecke G, Sis B, Reeve J, et al. Antibody-mediated microcirculation injury is the major cause of late kidney transplant failure. *Am J Transplant*. 2009;9(11):2520-2531.

3. Gaston RS, Cecka JM, Kasiske BL, et al. Evidence for antibody-mediated injury as a major determinant of late kidney allograft failure. *Transplantation*. 2010;90(1):68-74.

4. Loupy A, Haas M, Solez K, et al. The Banff 2015 Kidney Meeting Report: Current Challenges in Rejection Classification and Prospects for Adopting Molecular Pathology. *Am J Transplant*. 2017;17(1):28-41.

5. Feucht HE. Complement C4d in graft capillaries—The missing link in the recognition of humoral alloreactivity. *Am J Transplant*. 2003;3(6):646-652.

6. Feucht HE, Schneeberger H, Hillebrand G, et al. Capillary deposition of C4d complement fragment and early renal graft loss. *Kidney Int*. 1993;43(6):1333-1338.

7. Murata K, Baldwin WM, 3rd. Mechanisms of complement activation, C4d deposition, and their contribution to the pathogenesis of antibody-mediated rejection. *Transplant Rev (Orlando)*. 2009;23(3):139-150.

8. Campbell RD, Gagnon J, Porter RR. Amino acid sequence around the thiol and reactive acyl groups of human complement component C4. *Biochem J*. 1981;199(2):359–370.

9. Regele H, Böhmig GA, Habicht A, et al. Capillary deposition of complement split product C4d in renal allografts is associated with basement membrane injury in peritubular and glomerular capillaries: a contribution of humoral immunity to chronic allograft rejection. *J Am Soc Nephrol*. 2002;13(9):2371-2380.

10. Regele H, Exner M, Watschinger B, et al. Endothelial C4d deposition is associated with inferior kidney allograft outcome independently of cellular rejection. *Nephrol Dial Transplant*. 2001;16(10):2058–2066.

11. Herzenberg AM, Gill JS, Djurdjev O, et al. C4d deposition in acute rejection: An independent long-term prognostic factor. *J Am Soc Nephrol*. 2002;13(1):234–241.

12. Böhmig GA, Exner M, Habicht A, et al. Capillary C4d deposition in kidney allografts: A specific marker of alloantibody-dependent graft injury. *J Am Soc Nephrol*. 2002;13(4):1091-1099.

13. Mauiyyedi S, Pelle PD, Saidman S, et al. Chronic humoral rejection: Identification of antibody-mediated chronic renal allograft rejection by C4d deposits in peritubular capillaries. *J Am Soc Nephrol*. 2001;12(3):574–582.

14. Worthington JE, McEwen A, McWilliam LJ, et al. Association between C4d staining in renal transplant biopsies, production of donor-specific HLA antibodies, and graft outcome. *Transplantation*. 2007;83(4):398-403.

15. Roufosse C, Simmonds N, Clahsen-van Groningen M, et al. A 2018 Reference Guide to the Banff Classification of Renal Allograft Pathology. *Transplantation*. 2018;102(11):1795-1814.

16. Leal R, Tsapepas D, Crew RJ, et al. Pathology of Calcineurin and Mammalian Target of Rapamycin Inhibitors in Kidney Transplantation. *Kidney Int Rep*. 2017; 27;3(2):281-290.

17. Fioretto P, Mauer M. Histopathology of diabetic nephropathy. *Semin Nephrol*. 2007;27(2):195–207.

18. Snanoudj R, Royal V, Elie C, et al. Specificity of histological markers of long-term CNI nephrotoxicity in kidney transplant recipients under low-dose cyclosporine therapy. *Am J Transplant*. 2011;11(12):2635– 2646.

19. Vázquez LC, González AP, Juega J, et al. Nodular Arteriolar Hyalinosis as Histopathologic Hallmark of Calcineurin Inhibitor Nephrotoxicity: Does It Always Have the Same Meaning? *Transplant Proc*. 2015;47(8):2357-2360.

20. Batal I, Girnita A, Zeevi A, et al. Clinical significance of the distribution of C4d deposits in different anatomic compartments of the allograft kidney. *Mod Pathol*. 2008;21(12):1490-1498.

21. Kikić Z, Regele H, Nordmeyer V, et al. Significance of peritubular capillary, glomerular, and arteriolar C4d staining patterns in paraffin sections of early kidney transplant biopsies. *Transplantation*. 2011;91(4):440-446.

22. Sijpkens YW, Joosten SA, Wong MC, et al. Immunologic risk factors and glomerular C4d deposits in chronic transplant glomerulopathy. *Kidney Int*. 2004;65(6):2409-2418.

23. Gasim AH, Chua JS, Wolterbeek R, et al. Glomerular C4d deposits can mark structural capillary wall remodelling in thrombotic microangiopathy and transplant glomerulopathy: C4d beyond active antibody-mediated injury: a retrospective study. *Transpl Int*. 2017;30(5):519-532.

24. Vongwiwatana A, Gourishankar S, Campbell PM, et al. Peritubular capillary changes and C4d deposits are associated with transplant glomerulopathy but not IgA nephropathy. *Am J Transplant*. 2004;4(1):124-129.

25. von der Thusen JH, Maa de Louw R, Cg Bourgondien M, et al. Ultrastructural changes of the glomerular basement membrane...unmasked by C4d staining. *Transpl Int*. 2017;30(9):945-946.

26. Takeda A, Otsuka Y, Horike K, et al. Significance of C4d deposition in antibody-mediated rejection. *Clin Transplant*. 2012;26 Suppl 24:43-48.

27. Corrêa RR, Machado JR, da Silva MV, et al. The importance of C4d in biopsies of kidney transplant recipients. *Clin Dev Immunol*. 2013;2013:678180.

28. Fioretto P, Steffes MW, Sutherland DE, et al. Sequential renal biopsies in insulin-dependent diabetic patients: Structural factors associated with clinical progression. *Kidney Int*. 1995;48(6):1929–1935.

29. Bazzi C, Stivali G, Rachele G, et al. Arteriolar hyalinosis and arterial hypertension as possible surrogate markers of reduced interstitial blood flow and hypoxia in glomerulonephritis. *Nephrology (Carlton)*. 2015;20(1):11-17.

30. Einecke G, Reeve J, Halloran PF. Hyalinosis Lesions in Renal Transplant Biopsies: Time-Dependent Complexity of Interpretation. *Am J Transplant*. 2017;17(5):1346-1357.

31. Sablik KA, Clahsen-van Groningen MC, Looman CWN, et al. Chronic-active antibodymediated rejection with or without donor-specific antibodies has similar histomorphology and clinical outcome - a retrospective study. *Transpl Int*. 2018;31(8):900-908.

32. Lederer SR, Kluth-Pepper B, Schneeberger H, et al. Impact of humoral alloreactivity early after transplantation on the long-term survival of renal allografts. *Kidney Int*. 2001;59(1):334-41.

33. Li X, Zhuang S. Recent advances in renal interstitial fibrosis and tubular atrophy after kidney transplantation. *Fibrogenesis Tissue Repair*. 2014;7:15.

34. Sablik KA, Clahsen-van Groningen MC, Damman J, et al. Banff lesions and renal allograft survival in chronic-active antibody mediated rejection. *Transpl Immunol*. 2019;56:101213.

Author contributions

M.L.H.S. participated in research design, performance of the research, data analysis, interpretation of the results, and writing of the paper; K.A.S. and T.P.P.v.d.B. participated in performance of the research and writing of the paper. D.A.H. and M.G.H.B. participated in writing of the paper and provided intellectual content of critical importance to the work. I.B. participated in research design, writing of the paper and provided intellectual content of critical importance to the work. M.C.C.-v.G. participated in research design, performance of the research, interpretation of the results and writing of the paper.

Conflict of interest

D.A.H. has received lecture and consulting fees from Astellas Pharma and Chiesi Farmaceutici S.p.A., as well as grant support from Astellas Pharma, Bristol Myers-Squibb and Chiesi Farmaceutici S.p.A. (paid to the Erasmus MC). M.C.C.-v.G. received grant support from from Astellas Pharma (paid to the Erasmus MC). The other authors declare no conflicts of interest.

Supplementary files

Table S1. Association of arteriolar C4d staining pattern (endothelial, mural and endothelial + mural C4d staining) with other pathological findings in the c-aABMR cases.

Banff criteria 2015 (n=34)	endothelial	mural	endothelial + mural	P
N (%)	9 (27)	10 (29)	15 (44)	
Total inflammation (ti)	3 (1-3)	3 (1-3)	3 (0-3)	0.126
Interstitial inflammation (i)	2 (1-3)	2 (1-3)	2 (0-3)	0.292
Tubulitis (t)	0 (0-2)	0 (0-2)	0 (0-1)	0.765
Intimal arteritis (v)	0 (0-2)	0 (0-1)	0 (0-2)	0.515
Glomerulitis (g)	3 (2-3)	3 (3-3)	3 (3-3)	0.290
Peritubular capillaritis (ptc)	3 (2-3)	2 (0-3)	3 (1-3)	0.126
Interstitial fibrosis (ci)	1 (0-3)	2 (0-3)	2 (0-3)	0.653
Tubular atrophy (ct)	1 (0-2)	1 (0-3)	1 (1-3)	0.474
Vascular intimal thickening (cv)	2 (0-3)	3 (1-3)	3 (0-3)	0.504
Transplant glomerulopathy (cg)	3 (1-3)	3 (1-3)	3 (1-3)	0.379
Arteriolar hyalinosis (ah)	2 (0-3)	3 (1-3)	2 (0-3)	0.223
Mesangial matrix increase (mm)	3 (0-3)	3 (0-3)	3 (1-3)	0.453
C4d deposition in PTCs	1 (0-3)	0 (0-3)	0 (0-3)	0.969
C4d deposition in GBM	3 (0-3)	2 (0-3)	3 (0-3)	0.286
C4d deposition in arteries	0 (0-2)	0 (0-1)	1 (0-2)	0.140

Pathological lesions in the c-aABMR cases with endothelial, mural and endothelial + mural arteriolar C4d staining. The pathological features were scored according to the Banff 2015 criteria. Median and range of the pathological lesions in the subgroups (endothelial, mural and endothelial + mural arteriolar C4d staining) are showed in the table.

PTCs, peritubular capillaries; GBM, glomerular basement membrane.

Table S2. Association of arteriolar C4d staining scores with other pathological findings in the entire group of 80 patients.

Banff Criteria 2015 (n=80)	C4d 0	C4d 1+	C4d 2+	C4d 3+	P
N (%)	23 (29)	18 (22)	16 (20)	23 (29)	
Total inflammation (ti)	1 (0-3)	2 (0-3)	2 (0-3)	3 (0-3)	0.02
Interstitial inflammation (i)	0 (0-3)	1 (0-3)	1 (0-3)	2 (0-3)	<0.001
Tubulitis (t)	0 (0-3)	0 (0-3)	0 (0-2)	0 (0-3)	0.86
Intimal arteritis (v)	0 (0-0)	0 (0-1)	0 (0-2)	0 (0-2)	0.01
Glomerulitis (g)	0 (0-3)	2 (0-3)	3 (0-3)	3 (0-3)	0.13
Peritubular capillaritis (ptc)	0 (0-3)	0 (0-3)	2 (0-3)	2 (0-3)	0.11
Interstitial fibrosis (ci)	1 (0-3)	1 (0-3)	1 (0-3)	2 (0-3)	0.10
Tubular atrophy (ct)	1 (0-3)	1 (0-2)	1 (0-2)	2 (1-3)	0.05
Vascular intimal thickening (cv)	1 (0-3)	2 (0-3)	2 (0-3)	3 (0-3)	0.08
Transplant glomerulopathy (cg)	0 (0-3)	0 (0-3)	3 (0-3)	2 (0-3)	0.09
Arteriolar hyalinosis (ah)	1 (0-3)	2 (0-3)	3 (0-3)	3 (0-3)	0.07
Mesangial matrix increase (mm)	2 (0-3)	3 (0-3)	3 (0-3)	3 (0-3)	0.23
C4d deposition in PTCs	0 (0-3)	0 (0-2)	0 (0-3)	0 (0-3)	0.07
C4d deposition in GBM	0 (0-3)	0 (0-3)	2 (0-3)	2 (0-3)	0.47
C4d deposition arteries	0 (0-2)	1 (0-3)	0 (0-3)	1 (0-2)	0.34

Pathological lesions in the entire cohort of 80 patients (c-aABMR cases and matched controls) according to the Banff 2015 criteria and the association with arteriolar C4d staining. Median and range of the pathological lesions in the arteriolar C4d subgroups are shown in the table.

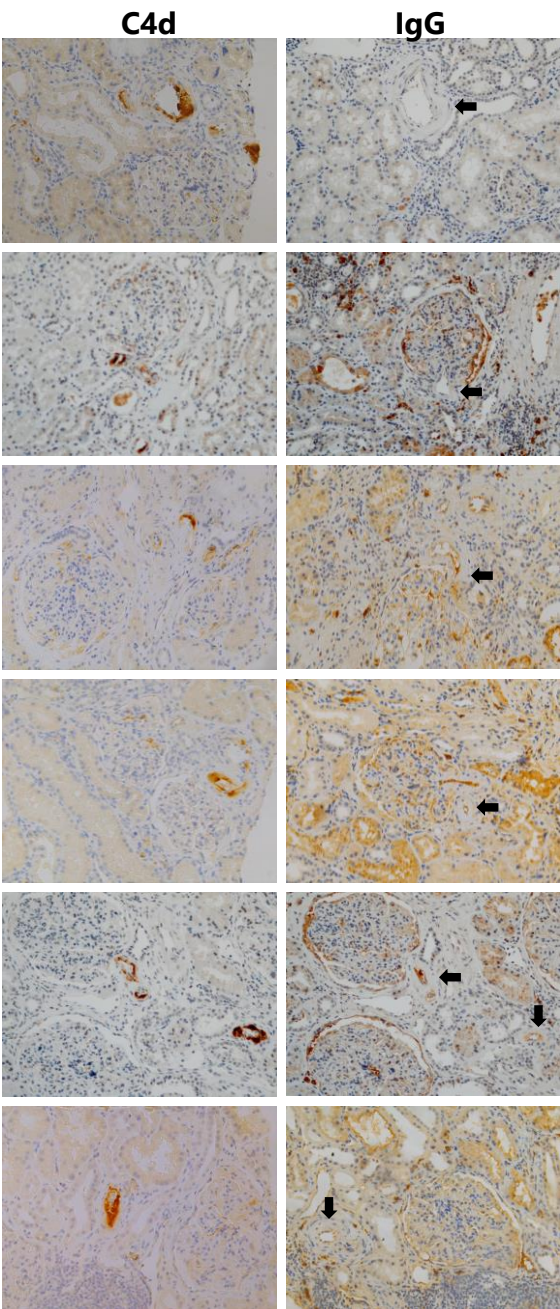art, arteriolar; PTCs, peritubular capillaries; GBM, glomerular basement membrane

Figure S1. Examples of immunohistochemical C4d and IgG staining in 3 c-aABMR cases and 3 matched controls. IgG immunohistochemistry is negative in the arterioles and no staining is observed at the sites of arteriolar hyalinosis (arrows).

CHAPTER 6

**Utility of immunohistochemistry
with C3d in C3 glomerulopathy**

Malou L. H. Snijders[1], Bojou J. van de Wall-Neecke[1], Dennis A. Hesselink[2], Jan U. Becker[3] & Marian C. Clahsen-van Groningen[1]

1. Department of Pathology, Erasmus MC, University Medical Center Rotterdam, Rotterdam, The Netherlands
2. Department of Internal Medicine, Division of Nephrology and Renal Transplantation, Erasmus MC, University Medical Center Rotterdam, Rotterdam, The Netherlands
3. Institute of Pathology, University Hospital of Cologne, Cologne, Germany

Abstract

C3-dominance by immunofluorescence is a defining feature in the diagnosis of C3 glomerulopathy. Most pathologists stain for C3c, which has been reported as a trace/negative even in otherwise clear-cut cases of dense deposit disease. We investigated the usefulness of C3d immunohistochemistry in biopsies with C3 glomerulopathy as an ancillary diagnostic tool. All biopsies from patients diagnosed with C3 glomerulopathy in the period January 2005 to June 2017 in the Erasmus MC, Rotterdam were included (n=14; 10 C3 glomerulonephritis, 4 dense deposit disease). The staining pattern of C3d and C4d by immunohistochemistry was analyzed. As controls, biopsies from patients with immune complex membranoproliferative glomerulonephritis (n=2), infection-associated glomerulonephritis (n=6), pauci-immune crescentic glomerulonephritis (n=7), tubulointerstitial nephritis (n=7) and chronic-active antibody-mediated rejection (n=9) were included. All 14 biopsies with C3 glomerulopathy showed a C3d score of ≥2, including two clear-cut biopsies with C3 glomerulopathy originally showing a trace/negative staining for C3c. In the control group, a C3d score ≥2 was observed in 11 biopsies (35%; 2 with immune complex membranoproliferative glomerulonephritis (100%), 6 with infection-associated glomerulonephritis (100%), 1 with pauci-immune crescentic glomerulonephritis (14%), 1 with tubulointerstitial nephritis (14%) and 1 with chronic-active antibody-mediated rejection (11%)). C4d was positive in 71% of the biopsies with C3 glomerulopathy (10/14). In conclusion, C3d immunohistochemistry is a valuable tool in the diagnosis of C3 glomerulopathy, especially in cases in which C3c immunofluorescence shows a trace/negative. We recommend the use of C3d in addition to C3c in cases suspicious for C3 glomerulopathy.

1.   Introduction

C3 glomerulopathy is a rare type of glomerulonephritis that encompasses both C3 glomerulonephritis and dense deposit disease.[1] C3 glomerulopathy is characterized by C3 deposits in the glomeruli and is caused by uncontrolled activation of the alternative pathway of the complement system.[2, 3] When the alternative complement pathway becomes activated, C3 is split into C3a and C3b by C3 convertase. C3b can react with other components of the complement cascade leading to the formation of the membrane attack complex (C5–C9), which together with C3a induces localized cell injury and inflammation. Degradation of C3b leads to the formation of C3c and the end product C3d.[4-6]

Activation of the alternative complement pathway in patients with C3 glomerulopathy can be caused by mutations in the complement genes, regulatory factors or by acquired defects.[7] For example, specific autoantibodies called C3 nephritic factor, inhibitory autoantibodies against complement factor H as well as inhibitory genetic alterations in the complement factor H gene can impair normal regulation of the alternative complement system.[8-11] Rarely, monoclonal immunoglobulin may cause C3 glomerulopathy.[12]

Renal biopsies from patients with C3 glomerulopathy can reveal various patterns of glomerular injury by light microscopy. In rare cases, no abnormalities are visualized by light microscopy.[3] The main feature of C3 glomerulopathy is the presence of isolated C3 deposits in the glomeruli.[2, 3] In 2013, the definition of C3 glomerulopathy was further defined by the presence of dominant C3 staining with a staining score being at least two orders of magnitude greater than the other stainings (i.e. IgG, IgM, IgA and C1q).[3, 13] Based on electron microscopy findings, C3 glomerulopathy can be further subclassified into C3 glomerulonephritis and dense deposit disease, the prototypical form of C3 glomerulopathy.[2]

In most laboratories, C3 is detected by immunofluorescence on frozen kidney tissue using an antibody against C3c.[3, 14] However, even in clear-cut cases of dense deposit disease, C4d has been shown to be dominant on immunostaining instead of C3c in the experience of others,[15, 16] as well as in our own experience. C4d is a fragment of C4 that can be derived from activation of both the classical and lectin complement pathway.[17] In contrast, the activation of C4 is bypassed in the alternative pathway of complement.[18] After the activation of C4, C4b is generated which is then cleaved into C4d and other fragments such as C4c.[17, 19]

C3d has been suggested to be a more sensitive marker to detect complement activation than the currently used immunofluorescence antibody to C3c.[20] While C3c and other components of the complement system disappear after recovery from cell injury, C3d remains attached to the target cell.[20] Therefore, C3d might be a more robust marker of C3 activation than C3c. Moreover, recent mass spectrometry data have shown that C3b, which also covalently binds surrounding structures, and C3d rather than C3c, accumulate in C3 glomerulopathy.[21]

These observations challenge the traditional use of an antibody against C3c as the sole means of detecting C3 activation and deposition. In the present study we investigated if C3d staining by immunohistochemistry could be a useful complementary tool for detecting C3 deposits in the diagnosis of C3 glomerulopathy, particularly in those cases that are pathogenetically defined but do not meet the consensus criterion of C3-dominance with the traditionally used C3c immunofluorescence.

2. Methods

2.1 Study cohort

The database of the Department of Pathology (Erasmus MC, University Medical Center, Rotterdam, the Netherlands) was searched retrospectively for biopsies from patients diagnosed with C3 glomerulopathy between January 2005 and June 2017. The following clinical data were collected: age, gender, serum creatinine, proteinuria, C-reactive protein and serum C3 and C4 concentrations at the time of biopsy. The presence of antinuclear antigen antibodies, antineutrophil cytoplasmic antibodies, double stranded DNA antibodies, C3 nephritic factor autoantibodies and complement factor H autoantibodies, and genetic mutations in the complement genes was evaluated within 1 month before to 1 month after the first biopsy.

2.2 Cases

A total of 14 biopsies from 11 different patients with C3 glomerulopathy were identified; eight patients were diagnosed with C3 glomerulonephritis and three with dense deposit disease. In two patients, more than one biopsy was performed (Table 1). In patient 11, two biopsies were performed: the first biopsy did not show specific glomerular deposition for C3c by immunofluorescence. Therefore, a second

biopsy was performed 6 weeks later. In patient 8, four biopsies were performed; the first biopsy was a native kidney biopsy that showed C3 glomerulonephritis. Four years later the patient received a kidney transplant with a decline of renal function 2 weeks after transplantation. A total of three allograft biopsies was subsequently performed (2 weeks, 8 months and 13 months after transplantation, respectively) which all showed features of a recurrence of C3 glomerulonephritis. The renal allograft biopsy taken 13 months after transplantation also showed light microscopic features of a borderline acute cellular rejection and was therefore excluded from the present study.

2.3 Controls

Two biopsies from patients with immune complex membranoproliferative glomerulonephritis (both cases of hepatitis C-associated immune complex membranoproliferative glomerulonephritis), six biopsies from patients with infection associated glomerulonephritis, seven biopsies from patients with pauci-immune crescentic glomerulonephritis, seven biopsies from patients with tubulointerstitial nephritis and nine from patients with chronic-active antibody-mediated rejection with transplant glomerulopathy (Banff Lesion Score cg>0) were included as controls.[22]

2.4 Tissue processing

For light microscopy, paraffin-embedded sections were routinely stained with hematoxylin and eosin, periodic acid-Schiff, Jones and Trichrome, according to the standardized diagnostic protocols for renal biopsy processing. Immunofluorescence staining for IgG, IgA, IgM, C3c, C1q, kappa and lambda on fresh snap-frozen renal tissue was routinely performed immediately after renal biopsy in all cases. Immunofluorescence was performed on 5 μm sections of fresh snap-frozen tissue, which were air dried on adhesive glass slides and pretreated with acetone for 10 min. Fluorescein-tagged polyclonal rabbit antihuman antibodies to IgG, IgA, IgM, C3c, C1q, kappa and lambda were all performed on a VENTANA BenchMark ULTRA according to the BenchMark Ultra protocol. For C3c, incubation with anti-C3c-FITC conjugated (Ventana 760–2686) for 24 min at 36 °C was performed. Immunofluorescence results, including C3c, were collected retrospectively from the biopsy reports. Electron microscopy was performed in all cases to differentiate between C3 glomerulonephritis and dense deposit disease.

For the purpose of the present study, immunohistochemical C3d staining was performed on 2–3 μm sections of formalin-fixed paraffin-embedded tissue. Tissue sections were dried overnight at 58 °C and subsequently deparaffinized, rehydrated and subjected to antigen retrieval using Lab Vision™ PT Module™ Deparaffinization and Heat-Induced Epitope Retrieval Solutions at pH 8. The tissue samples were incubated with the polyclonal antibody against C3d (#403A-76, Cell Marque) at 97 °C for 20 min and dilution 1:50. The detection system was used as recommended by the manufacturer.

Immunohistochemical C4d staining was performed on 4 μm slides of formalin-fixed paraffin-embedded tissue with an automated, validated and accredited staining system (Ventana Benchmark ULTRA, Ventana Medical Systems, Tucsen, AZ, USA) using an ultra-view universal DAB detection kit. In brief, following deparaffinization and heat induced antigen retrieval with CC1 (#950-124, Ventana) for 64 min, the tissue samples were incubated with C4d (SP91, #760-4803, Cell Marque) for 24 min at 36 °C. C3d and C4d immunohistochemistry were scored on a scale from 0 to 3+ by two pathologists (MS and JUB) who were blinded to patient information.

We ruled out the entity of masked IgG kappa deposits recently described by Larsen *et al.* by staining all biopsies for kappa-light chains by immunohistochemistry after proteinase treatment of paraffin sections.[23, 24] Five biopsies from patients with C3 glomerulopathy showed positivity for kappa (36%); three biopsies showed 2+ staining (21%) and two biopsies 1+ staining (14%). 3+ staining for kappa was not observed in any of the biopsies with C3 glomerulopathy, effectively ruling out this entity in all biopsies.

Table 1. Clinical characteristics of patients with C3 glomerulopathy.

Patient	Biopsy	Gender	Age	Creatinine (µmol/L)	Proteinuria (g/L)	CRP (mg/L)	Serum C3 (g/L)	Serum C4 (g/L)	ANA	ANCA	Anti-dsDNA (IU/mL)	C3NeF	CFH	Genetic defect
1	1	F	15	315	6.00	25.2	0.95	0.18	neg	neg	neg	neg	neg	no
2	2	F	16	74	5.51	0.3	0.04	0.05	pos	neg	5.6	pos	+/-	yes*
3	3	F	76	944	0.36	24.0	1.2	0.32	pos	neg	1.4	NA	NA	NA
4	4	M	37	146	3.44	0.3	0.72	0.25	neg	NA	0.6	neg	+/_	no
5	5	M	56	103	1.88	0.7	0.49	0.07	neg	NA	0.5	NA	neg	no
6	6	F	8	72	5.75	0.3	0.30	0.09	neg	neg	neg	neg	neg	no
7	7	M	25	1087	11.76	2.4	0.98	0.24	neg	neg	NA	NA	NA	NA
8	8.1	M	14	92	3.55	1.0	0.30	0.20	pos	neg	neg	neg	neg	no
	8.2	M	17	172	0.37	14.0	0.23	0.22	pos	neg	NA	neg	neg	no
	8.3	M	18	192	3.73	0.8	0.57	0.41	pos	neg	neg	neg	neg	no
9	9	M	5	85	0.45	16.0	0.90	0.54	neg	neg	NA	neg	neg	no
10	10	F	13	75	2.84	0.3	0.23	0.15	pos	neg	neg	pos	neg	no
11	11.1	F	16	1456	8.29	21.0	0.54	0.33	pos	neg	NA	neg	neg	no
	11.2	F	16	1154	0.24	2.2	0.77	0.18	pos	neg	0.8	neg	neg	no

ANA antinuclear antigen autoantibodies, ANCA antineutrophil cytoplasmic antibodies, anti-dsDNA double-stranded DNA antibodies, CFH complement factor H autoantibodies, CRP C-reactive protein, C3GN C3 glomerulonephritis, C3NeF C3 nephritic factor autoantibodies, DDD dense deposit disease.
*A heterozygous mutation of unknown significance was found in the C3 gene ((c.691A > C p.(Ser231Arg)).

3.   Results

Patient characteristics are given in Table 1. The mean age at the time of diagnosis was 26 ± 22 years (range 5–76 years). Six patients (55%) were male. The mean serum creatinine concentration at the time of diagnosis was 412 ± 151 μmol/L. The degree of proteinuria at the time of biopsy was highly variable and ranged from 0.4 to 11.8 g/L (mean proteinuria 4.5 ± 3.4 g/L). Nephrotic-range proteinuria was present in 6 of 11 patients. C-reactive protein was relatively low in all patients (mean 10.1 mg/L, range 0.30–25.2 mg/L; reference range < 10 mg/L). Mean serum C3 at the time of diagnosis was 0.51 g/L (range 0.04–0.98 g/L; reference range: 0.65–1.65 g/L) and a low serum C3 (< 0.65 g/L) was observed in six patients. Mean serum C4 at the time of diagnosis was 0.22 g/L (range 0.05–0.54 g/L; reference range: 0.16–0.6 g/L); a decreased serum C4 was observed in four patients. Antinuclear antigen antibodies were found in five patients (45%); none of the patients tested positive for antineutrophil cytoplasmic antibodies. Evaluation of the alternative complement pathway was performed in nine patients. C3 nephritic factor autoantibodies were present in two patients (patients 2 and 10; Table 1). In one patient (patient 2) a heterozygous mutation with unknown significance was found in the C3 gene ((c.691A > C p.(Ser231Arg)). Complement factor H autoantibodies were dubiously positive in two patients (patients 2 and 4).

3.1   Glomerular C3c staining by IF

A staining score of 2+ or 3+ for C3c by immunofluorescence was observed in 12 biopsies from patients with C3 glomerulopathy (ten biopsies showed 3+ staining and two biopsies 2+ staining). In two biopsies (patients 2 and 11) C3c by immunofluorescence showed negative to 1+ staining only (Figure 1). C3c by immunofluorescence was also dominant with 3+ in all biopsies with infection-associated glomerulonephritis.

3.2   Immunohistochemical glomerular C3d staining

All 14 biopsies with C3 glomerulopathy were positive for C3d: 11 biopsies showed 3+ staining for C3d and three biopsies showed 2+ staining for C3d (Figure 2). A score of 2+ and 3+ was observed in the two biopsies showing 1+ and negative C3c staining by immunofluorescence, respectively (Table 2).

In the control group, C3d immunohistochemistry was positive in 22 of 31 biopsies; 2+ or 3+ C3d staining was observed in 11 of 31 biopsies (35%): two biopsies

with immune complex membranoproliferative glomerulonephritis (100%), six biopsies with infection-associated glomerulonephritis (100%), one biopsy with pauci-immune crescentic glomerulonephritis (14%), one biopsy with tubulointerstitial nephritis (14%) and one biopsy with chronic-active antibody-mediated rejection (11%). A score of 1+ for C3d was seen in 11 of 31 biopsies (35%): four biopsies with pauci-immune crescentic glomerulonephritis (57%), one biopsy with tubulointerstitial nephritis (14%), six biopsies with chronic-active antibody-mediated rejection (67%). The immunohistochemical findings are shown in Table 3.

Table 2. Overview of C3c staining score by immunofluorescence and C3d staining by immunohistochemistry in biopsies from patients with C3 glomerulopathy.

Patient	Biopsy	Diagnosis	C3c IF	C3d IHC
1	1	C3GN	3	3
2	2	C3GN	0	3
3	3	C3GN	3	3
4	4	C3GN	3	3
5	5	C3GN	2	3
6	6	C3GN	3	3
7	7	C3GN	3	2
8	8.1	C3GN	3	3
	8.2	C3GN	NA[a]	3
	8.3	C3GN	3	3
9	9	DDD	3	3
10	10	DDD	3	3
11	11.1	DDD	1	2
	11.2	DDD	2	2

C3GN C3 glomerulonephritis, DDD dense deposit disease, NA not available

[a] No glomeruli present in the snap frozen renal biopsy

3.3 Consensus criteria for C3 glomerulopathy

Ten of 14 biopsies fulfilled the consensus criteria for C3 glomerulopathy based on C3c immunofluorescence staining alone (8/10 C3 glomerulonephritis and 2/4 dense deposit disease).[3] These ten biopsies showed dominant C3c staining by immunofluorescence and electron-dense deposits without substructure by electron microscopy.

Based on both C3c immunofluorescence and C3d immunohistochemistry, 12 of 14 biopsies (10/10 C3 glomerulonephritis, 2/4 dense deposit disease) fulfilled the criteria for C3 glomerulopathy. In patient 2, the diagnosis of C3 glomerulopathy could only be made after C3d immunohistochemistry staining because C3c immunofluorescence was negative while C3d immunohistochemistry showed 3+ staining. This patient showed characteristic ribbon-like electron-dense deposits in the thickened glomerular basement membrane by electron microscopy. One of the three biopsies performed in patient 8 did not contain glomeruli in the snap-frozen tissue and therefore the diagnosis of C3 glomerulopathy could not be made on this biopsy based on C3c immunofluorescence. However, C3d immunohistochemistry on the formalin-fixed paraffin-embedded slide showed 3+ staining in this biopsy. In patient 11, the diagnosis of C3 glomerulopathy could not be made according to the consensus criteria using both C3c immunofluorescence and C3d immunohistochemistry. However, electron microscopy showed glomerular basement membrane thickening with dense osmiophilic intramembranous electron deposits diagnostic of dense deposit disease. In this patient, two biopsies were performed, showing 1+ and 2+ staining for C3c immunofluorescence respectively, whereas both biopsies showed 2+ staining for C3d immunohistochemistry, raising the C3 staining to codominant. C1q showed 2+ staining in both biopsies.

3.4   Immunohistochemical glomerular C4d staining

C4d staining was positive in 10 of 14 biopsies with C3 glomerulopathy (71%); six biopsies showed 3+ staining (43%), three biopsies 2+ staining (21%) and one biopsy 1+ staining (7%) (Figure 3). In addition, both biopsies with immune complex membranoproliferative glomerulonephritis showed 3+ staining for C4d (100%). Only 2/6 biopsies with infection-associated glomerulonephritis showed ≥2+ staining for C4d (33%), the other four were negative. Three biopsies with pauci-immune crescentic glomerulonephritis showed 2+ staining (43%), while the other four were negative for C4d (57%). All seven biopsies with tubulointerstitial nephritis were negative for C4d. In biopsies with chronic active antibody-mediated rejection, one showed 3+ staining (11%), one showed 2+ staining (11%), four showed 1+ staining (45%) and three biopsies were negative (33%).
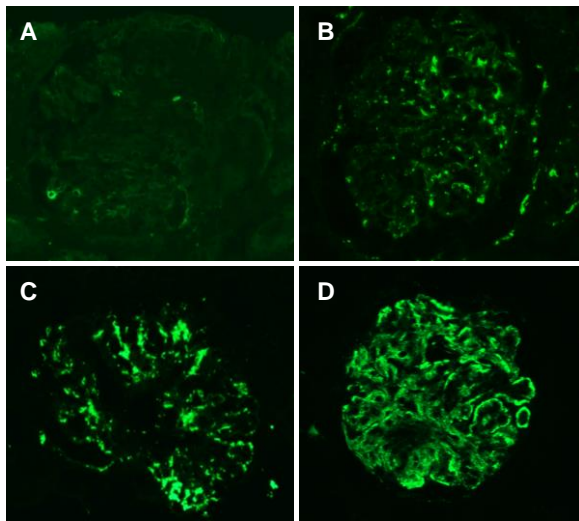
Figure 1. Examples of C3c by immunofluorescence in biopsies from patients with C3 glomerulopathy (negative (A; biopsy 2), 1+ (B; biopsy 11.1), 2+ (C; biopsy 5) and 3+ (D; biopsy 8.3).
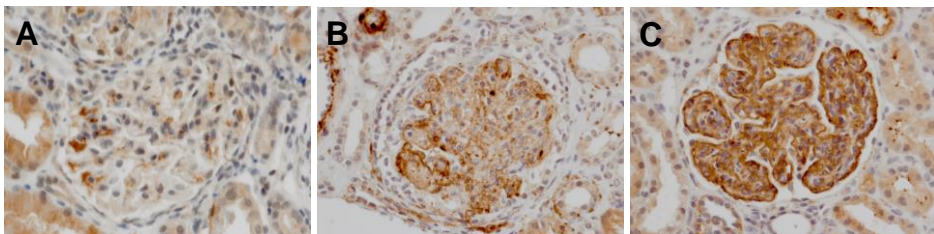

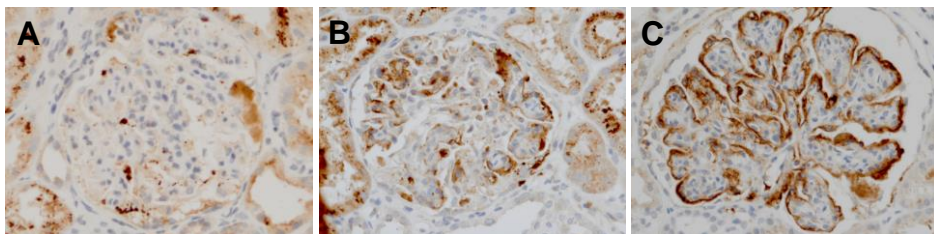Figure 2. Examples of C3d immunohistochemistry 1+ (A; biopsy 23), 2+ (B; biopsy 11.1) and 3+ (C; biopsy 2).

Figure 3. Examples of C4d immunohistochemistry 1+ (A; biopsy 4), 2+ (B; biopsy 2) and 3+ (C; biopsy 11.2).

Table 3. Immunohistochemical staining with C3d, C4d and kappa in biopsies from patients with C3 glomerulonephritis, dense deposit disease, immune complex membranoproliferative glomerulonephritis, infection-associated glomerulonephritis, pauci-immune glomerulonephritis, tubulointerstitial nephritis and chronic-active antibody-mediated rejection.

Patient	Biopsy	Diagnosis	C3d	C4d	kappa
1	1	C3GN	3	3	0
2	2	C3GN	3	2	0
3	3	C3GN	3	0	2
4	4	C3GN	3	1	0
5	5	C3GN	3	3	0
6	6	C3GN	3	2	0
7	7	C3GN	2	3	0
8	8.1	C3GN	3	3	0
	8.2	C3GN	3	2	2
	8.3	C3GN	3	0	1
9	9	DDD	3	0	0
10	10	DDD	3	3	2
11	11.1	DDD	2	0	0
	11.2	DDD	2	3	1
12	12	ICMGNP	3	3	1
13	13	ICMGNP	3	3	2
14	14	IAGN	3	3	0
15	15	IAGN	3	2	0
16	16	IAGN	3	0	0
17	17	IAGN	3	0	0
18	18	IAGN	3	0	0
19	19	IAGN	3	0	0
20	20	PCGN	1	0	1
21	21	PCGN	0	0	1
22	22	PCGN	1	2	0
23	23	PCGN	1	0	0
24	24	PCGN	2	2	3
25	25	PCGN	1	2	0

Table 3. Continued

26	26	PCGN	0	0	0
27	27	TIN	0	0	0
28	28	TIN	0	0	0
29	29	TIN	0	0	0
30	30	TIN	0	0	0
31	31	TIN	2	0	0
32	32	TIN	0	0	0
33	33	TIN	1	0	0
34	34	c-aABMR	0	3	0
35	35	c-aABMR	1	1	0
36	36	c-aABMR	1	0	0
37	37	c-aABMR	0	0	1
38	38	c-aABMR	1	1	0
39	39	c-aABMR	1	1	1
40	40	c-aABMR	1	2	0
41	41	c-aABMR	2	1	0
42	42	c-aABMR	1	0	0

c-aABMR chronic-active antibody-mediated rejection, C3GN C3 glomerulonephritis, DDD dense deposit disease, IAGN infection-associated glomerulonephritis, ICMGNP immune complex membranoproliferative glomerulonephritis, PCGN pauci-immune glomerulonephritis, TIN tubulointerstitial nephritis.

4. Discussion

C3 glomerulopathy is a disease entity defined by dysregulation of the alternative complement pathway.[2, 3] This results in the deposition of complement C3 fragments in the glomerulus which is currently detected using immunofluorescence with an antibody to C3c.[3] However, cases of dense deposit disease, the prototypical form of C3 glomerulopathy, with C4d-dominance (C4-dense deposit disease) not fulfilling the consensus criteria, have been observed.[16, 25] C3d is one of the final degradation products of C3 and is more stable in vivo than C3c, because C3d remains attached to the tissue site after recovery of injury leaving a visible footprint.[20] Therefore, we hypothesized that C3d would be a more sensitive and robust immunostaining marker for the diagnosis of C3 glomerulopathy than C3c.

We observed at least 2+ staining for C3d in all 14 biopsies with C3 glomerulopathy. Interestingly, two biopsies with C3 glomerulopathy, in which C3c staining by immunofluorescence was negative/sparse, showed ≥2+ staining with C3d by immunohistochemistry (patients 2 and 11), enabling the reclassification as at least C3-codominant. In patient 11, two biopsies were performed in which the diagnosis of C3 glomerulopathy, according to the consensus criteria, could still not be made after C3d immunohistochemistry since both C3d immunohistochemistry and C1q immunofluorescence showed 2+ staining in both biopsies.[3] However, electron microscopy showed glomerular basement membrane thickening with dense osmiophilic intramembranous deposits characteristic for dense deposit disease. So even after the use of C3d immunohistochemistry we are left with cases that, as either codominant or as only dominant by one magnitude do not fulfill the consensus criteria for C3 glomerulopathy. These findings raise the question whether the current consensus criteria are sensitive enough.

In patient 2, C4d immunohistochemistry was also performed at the time of diagnosis. Sethi *et al.* recently described three cases with C3 glomerulopathy in which no or only sparse C3c staining was observed by immunofluorescence and introduced a new entity called C4 glomerulopathy characterized by mesangial electron-dense deposits and bright staining for C4d with either immunohistochemistry or immunofluorescence and absent to a trace staining for C3 and immunoglobulins.[15, 16] In patient 2, C4d immunohistochemistry showed 2+ staining and therefore the diagnosis of C4 glomerulopathy was made at that time. However, C3d staining by immunohistochemistry showed 3+ staining and therefore this case might in fact represent a case of C3 glomerulopathy. Of course, we cannot rule out with absolute certainty a role for abnormal C1 or lectin pathway activation in this patient. However, positive C3 nephritic factor autoantibodies and a genetic mutation in the C3 gene were found, arguing for the diagnosis of C3 glomerulopathy in this particular case. Just relying on the traditional C3c immunofluorescence along with C4d staining, cases might be misdiagnosed as C4 glomerulonephritis or C4 dense deposit disease. C3d immunohistochemistry could be helpful in avoiding this mistake and to demonstrate a histopathological correlate to C3 activation.

In a study by Sethi *et al*, the use of C4d was evaluated to distinguish C3 glomerulopathy from immune complex membranoproliferative glomerulonephritis.[26] They observed ≥2+ C4d staining in 89% (16/18) of the biopsies with immune complex membranoproliferative glomerulonephritis, while C4d staining was found in only 20% (6/30) of the biopsies with C3 glomerulopathy

showing only a trace or 1+ staining. Based on these results, they suggested that negative glomerular staining for C4d can serve as a marker for C3 glomerulopathy. In contrast, we observed C4d immunohistochemical staining in 10/14 biopsies with C3 glomerulopathy (71%), suggesting that C4d staining is in fact often observed in patients with C3 glomerulopathy. In line with our findings, Bouatou *et al.* concluded that C4d staining is of limited value for the discrimination between C3 glomerulopathy and immune complex membranoproliferative glomerulonephritis.[27]

We observed the presence of both ≥2+ staining for C3 (either C3c or C3d) and C4d in a total of nine biopsies with C3 glomerulopathy (64%) showing evidence of a complement-mediated glomerular disease driven by both the alternative and classical/lectin pathway. This finding has been described previously in a single case of dense deposit disease by Vankalakunt *et al.*[28] Singh *et al.* performed an observational study including 27 dense deposit disease cases and 14 C3 glomerulonephritis cases. They observed C4d staining of variable intensity with ≥2+ staining in 48% of dense deposit disease cases and 21% of C3 glomerulonephritis cases.[29] It has been hypothesized that in these cases the alternative complement pathway is upregulated in addition to activation of the classical or lectin pathway caused by infection, auto-immune disease or monoclonal gammopathy.[18] We stained for kappa after protease digestion on all biopsies and excluded monoclonal gammopathy in all C3 glomerulopathy cases in our study, effectively ruling out monoclonal gammopathy-associated forms of glomerulonephritis and the peculiar entity of masked kappa deposits recently described.[23, 24] The possibility of an infection as a trigger for C3 glomerulopathy in some of the patients reported here could not be totally excluded.[30] However, the rather low C-reactive protein concentration at the time of biopsy and the clinical findings in all patients argues against this.

The "typical" work-up for patients with suspicion for C3 glomerulopathy includes testing for antinuclear antigen antibodies, antineutrophil cytoplasmic antibodies, double-stranded DNA antibodies and exclusion of infections with hepatitis B and C, and HIV, as well as monoclonal gammopathy. In addition, patients are tested for serum complement C3, C4 and C1q, autoantibodies against complement factor H, C3 nephritic factor, C4 nephritic factor, terminal complement complex, Bb, C3bc, C3bBbP, Factor H, Factor I, Factor B and abnormalities in complement protein encoding or regulating genes.

Abnormalities in the alternative complement pathway are observed in most patients with C3 glomerulopathy.[31, 32] In contrast to other studies, no abnormalities

in the alternative complement pathway were observed in the majority of C3 glomerulopathy patients in our study. This may be explained by the small cohort size or the fact that alternative complement pathway abnormalities were only thoroughly evaluated in 9 out 11 patients (82%).

Limitations of this proof-of-principle study are the small cohort size and the fact that this was a retrospective study and therefore some clinical data were not available. However, a relatively large control group was included to compare immunohistochemical C3d staining results in renal biopsies from patients with C3 glomerulopathy to biopsies from patients with such diverse diagnoses as immune complex membranoproliferative glomerulonephritis, infection-associated glomerulonephritis, pauci-immune crescentic glomerulonephritis, tubulointerstitial nephritis and chronic-active antibody-mediated rejection. As expected, biopsies from patients with immune complex membranoproliferative glomerulonephritis and infection associated glomerulonephritis showed 3+ staining for C3d immunohistochemistry. Biopsies with tubulointerstitial nephritis, pauci-immune crescentic glomerulonephritis and chronic-active antibody-mediated rejection were negative or showed only 1+ staining for C3d immunohistochemistry in most of the cases. C3 glomerulopathy can show overlapping histomorphologic features with pauci-immune crescentic glomerulonephritis and chronic-active antibody-mediated rejection which can make it difficult to distinguish between these entities by light microscopy.[33-35] Dominant C3d staining by immunohistochemistry may support the diagnosis of C3 glomerulopathy in these cases.

Based on the findings in the present study, we recommend the use of C3d immunohistochemistry in addition to C3c immunofluorescence in all cases with membranoproliferative glomerulonephritis. In addition, both clinical suspicion and electron microscopy findings indicative of dense deposit disease could be of guidance to recommend the use of C3d immunohistochemistry, especially in those cases in which C3c immunofluorescence shows a trace/negative. Furthermore, C3d immunohistochemistry can be of value in those cases with a trace/negative C3c immunofluorescence and positive C4d staining, since these cases could be incorrectly labeled as C4d-dominant glomerulopathy. Also, in those cases where frozen renal tissue is not available, C3d immunohistochemistry could be used in common practice (in combination with C3c immunohistochemistry when this is available). For example, in our study no glomeruli were present in a snap-frozen renal biopsy from patient 8 (biopsy 8.2). This is a problem in cases with a strong suspicion for C3 glomerulopathy. C3c immunofluorescence has been reported to not be

reliable by salvage technique on formalin-fixed paraffin-embedded tissue by some laboratories.[36] In those situations, C3d immunohistochemistry can be performed on the formalin fixed paraffin-embedded tissue.

In conclusion, C3d immunohistochemistry shows at least codominant staining in all biopsies with C3 glomerulopathy and could especially be helpful in those C3 glomerulopathy cases with absent or a trace C3c staining by immunofluorescence. Therefore, we recommend the use of C3d in addition to C3c on all biopsies suspicious for C3 glomerulopathy. Our results about the usefulness of C3d need validation in large, multicenter studies employing cluster-analysis approaches as has been suggested recently.[37]

References

1. Barbour TD, Pickering MC, Terence Cook H. Dense deposit disease and C3 glomerulopathy. *Semin Nephrol*. 2013;33:493–507.

2. Fakhouri F, Frémeaux-Bacchi V, Noël LH, Cook HT, Pickering MC. C3 glomerulopathy: a new classification. *Nat Rev Nephrol*. 2010;6:494–9.

3. Pickering MC, D'Agati VD, Nester CM, Smith RJ, Haas M, Appel GB, et al. C3 glomerulopathy: consensus report. *Kidney Int*. 2013;84:1079–89.

4. Noris M, Remuzzi G. Glomerular diseases dependent on complement activation, including atypical hemolytic uremic syndrome, membranoproliferative glomerulonephritis, and C3 glomerulopathy: core curriculum 2015. *Am J Kidney Dis*. 2015;66:359–75.

5. Noris M, Remuzzi G. Overview of complement activation and regulation. *Semin Nephrol*. 2013;33:479–92.

6. Thurman JM, Holers VM. The central role of the alternative complement pathway in human disease. *J Immunol*. 2006;176:1305–10.

7. Zipfel PF, Skerka C, Chen Q, Wiech T, Goodship T, Johnson S, et al. The role of complement in C3 glomerulopathy. Mol Immunol. 2015;67:21–30.

8. Sethi S, Nester CM, Smith RJH. Membranoproliferative glomerulonephritis and C3 glomerulopathy: resolving the confusion. *Kidney Int*. 2012;81:434–41.

9. Salvadori M, Bertoni E. Complement related kidney diseases: recurrence after transplantation. *World J Transpl*. 2016;6:632–45.

10. de Córdoba SR, de Jorge EG. Translational mini-review series on complement factor H: genetics and disease associations of human complement factor H. *Clin Exp Immunol*. 2008;151:1–13.

11. Józsi M, Reuter S, Nozal P, et al. Autoantibodies to complement components in C3 glomerulopathy and atypical hemolytic uremic syndrome. *Immunol Lett*. 2014;160:163–71.

12. Sethi S, Fervenza FC, Rajkumar SV. Spectrum of manifestations of monoclonal gammopathy-associated renal lesions. *Curr Opin Nephrol Hypertens*. 2016;25:127–37.

13. Hou J, Markowitz GS, Bomback AS, et al. Toward a working definition of C3 glomerulopathy by immunofluorescence. *Kidney Int*. 2014;85:450–6.

14. West CD, Witte DP, McAdams AJ. Composition of nephritic factor-generated glomerular deposits in membranoproliferative glomerulonephritis type 2. *Am J Kidney Dis*. 2001;37:1120–30.

15. Sethi S, Quint PS, O'Seaghdha CM, et al. C4 Glomerulopathy: a disease entity associated with C4d deposition. *Am J Kidney Dis*. 2016;67:949–53.

16. Sethi S, Sullivan A, Smith RJ. C4 dense-deposit disease. *N Engl J Med*. 2014;370:784–6.

17. Murata K, Baldwin WM 3rd. Mechanisms of complement activation, C4d deposition, and their contribution to the pathogenesis of antibody mediated rejection. *Transpl Rev (Orlando)*. 2009;23:139–50.

18. Angioi A, Fervenza FC, Sethi S, et al. Diagnosis of complement alternative pathway disorders. *Kidney Int*. 2016;89:278–88.

19. Mortensen S, Kidmose RT, Petersen SV, Szilágyi Á, Prohászka Z, Andersen GR. Structural basis for the function of complement component C4 within the classical and lectin pathways of complement. *J Immunol*. 2015;194:5488–96.

20. Schulze M, Pruchno CJ, Burns M, Baker PJ, Johnson RJ, Couser WG. Glomerular C3c localization indicates ongoing immune deposit formation and complement activation in experimental glomerulonephritis. *Am J Pathol*. 1993;142:179–87.

21. Sethi S, Vrana JA, Fervenza FC, et al. Characterization of C3 in C3 glomerulopathy. *Nephrol Dial Transpl*. 2017;32:459–65.

22. Haas M, Loupy A, Lefaucheur C, et al. The Banff 2017 Kidney Meeting Report: revised diagnostic criteria for chronic active T cell-mediated rejection, antibody-mediated rejection, and prospects for integrative endpoints for next-generation clinical trials. *Am J Transpl*. 2018;18:293–307.

23. Larsen CP, Boils CL, Cossey LN, Sharma SG, Walker PD. Clinicopathologic features of membranous-like glomerulopathy with masked IgG kappa deposits. *Kidney Int Rep*. 2016;1:299–305.

24. Larsen CP, Ambruzs JM, Bonsib SM, et al. Membranous-like glomerulopathy with masked IgG kappa deposits. *Kidney Int*. 2014;86:154–61.

25. Ali A, Schlanger L, Nasr SH, Sethi S, Gorbatkin SM. Proliferative C4 dense deposit disease, acute thrombotic microangiopathy, a monoclonal gammopathy, and acute kidney failure. *Am J Kidney Dis*. 2016;67:479–82.

26. Sethi S, Nasr SH, De Vriese AS, Fervenza FC. C4d as a diagnostic tool in proliferative GN. *J Am Soc Nephrol*. 2015;26:2852–9.

27. Bouatou Y, Kers J, Chevalier-Florquin MSN, et al. Diagnostic accuracy of immunofluorescence versus immunoperoxidase staining to distinguish immune complex mediated glomerulonephritis and C3 dominant glomerulopathy. *Histopathology*. 2018;72:601–8.

28. Vankalakunti M, Augustine R, Jangamani R, et al. Dense deposit disease involving C3 and C4d deposits. *Indian J Nephrol*. 2018;28:61–4.

29. Singh G, Singh SK, Nalwa A, et al. Glomerular C4d staining does not exclude a C3 glomerulopathy. *Kidney Int Rep*. 2019;4:698–709.

30. Sethi S, Fervenza FC, Zhang Y, et al. Atypical postinfectious glomerulonephritis is associated with abnormalities in the alternative pathway of complement. *Kidney Int*. 2013;83:293–9.

31. Iatropoulos P, Noris M, Mele C, et al. Complement gene variants determine the risk of immunoglobulin associated MPGN and C3 glomerulopathy and predict long-term renal outcome. *Mol Immunol*. 2016;71:131–42.

32. Noris M, Donadelli R, Remuzzi G. Autoimmune abnormalities of the alternative complement pathway in membranoproliferative glomerulonephritis and C3 glomerulopathy. *Pedia Nephrol*. 2019;34:1311–23.

33. Singh L, Singh G, Bhardwaj S, Sinha A, Bagga A, Dinda A. Dense deposit disease mimicking a renal small vessel vasculitis. *J Am Soc Nephrol.* 2016;27:59–62.

34. Ito N, Ohashi R, Nagata M. C3 glomerulopathy and current dilemmas. *Clin Exp Nephrol.* 2017;21:541–51.

35. Remport A, Ivanyi B, Mathe Z, Tinckam K, Mucsi I, Molnar MZ. Better understanding of transplant glomerulopathy secondary to chronic antibody-mediated rejection. *Nephrol Dial Transpl.* 2015;30:1825–33.

36. Nasr SH, Galgano SJ, Markowitz GS, Stokes MB, D'Agati VD. Immunofluorescence on pronase-digested paraffin sections: a valuable salvage technique for renal biopsies. *Kidney Int.* 2006;70:2148–51.

37. Iatropoulos P, Daina E, Curreri M, Piras R, Valoti E, Mele C, et al. Cluster analysis identifies distinct pathogenetic patterns in C3 glomerulopathies/immune complex-mediated membranoproliferative GN. *J Am Soc Nephrol.* 2018;29:283–94.

Conflict of interest

Ethical approval

The study protocol was consistent with international ethical and professional guidelines (the Declaration of Helsinki and the International Conference on Harmonization Guidelines for Good Clinical Practice). The study was approved by the local medical ethics committee (MEC-2016-350).

CHAPTER 7

Summary and Discussion

Kidney transplantation is the treatment of choice for patients with end stage renal disease.[1] Long-term transplant survival is determined by different variables including donor and recipient conditions, duration of cold and warm ischemia, degree of human leucocyte antigens (HLA) matching, ischemia-reperfusion injury (IRI) and acute and chronic rejection.[2, 3] Improvement of immunosuppressive drug regimens, as well as pre-transplantation screening, have provided better donor-recipient matching and reduced the chances of developing rejection. However, acute rejection and late graft failure remain common and difficult obstacles.[4] Up to 50% of all renal allografts are lost within 10 years after transplantation.[5] Better understanding of the various factors that contribute to allograft failure can provide insight into which patients are at risk for inferior graft outcome. This can result in the development of new treatment options leading to longer transplant survival rates, as well as an increase in the quality of life. The scope of this thesis was to evaluate potentially important pathological features in renal transplant biopsies in the post-transplantation period.

Histological and immunohistochemical features are important in the evaluation of renal allograft biopsies, but the presence of specific proteins and molecular markers in renal allograft tissue can also give deeper insight to predict which patients are at risk for future graft loss. For both diagnostics and future research purposes, it is vital that renal tissue is stored in a fashion that maximizes tissue preservation.[6, 7] The most common embedding medium in which biopsy samples are snap-frozen is optimal cutting temperature (OCT) compound, a cryopreservative medium composed of polyethylene glycol (PEG), polyvinyl alcohol (PVA) and nonreactive ingredients. OCT stabilizes tissue allowing easy positioning of tissue samples in the microtome and provides a smooth cutting surface resulting in good quality of the tissue sections.[8]

The analysis of complete sets of proteins in a given tissue sample can be performed by mass spectrometry (MS).[9] MS analyses of OCT embedded tissue is difficult due to the presence of polymers in the OCT. The interference of these polymers in the MS analysis can cause suppression of ion formation and the presence of high polymer peaks of OCT in the mass spectra may hide other smaller peaks.[8, 9] These polymers are difficult to remove from the MS columns as they have a strong interaction with them. A portion of the polymers may even bind irreversibly which affect the separation performance and the lifetime of the columns considerably.

Therefore, the OCT has to be removed from the tissue samples before MS analysis is performed, which is a complex and time-consuming procedure.[8, 10-12]

In **Chapter 2** the use of Cryo-Gel as embedding compound for snap-freezing of renal biopsies, as a replacement for OCT, was evaluated. In this study, fresh renal samples were snap-frozen using Cryo-Gel, OCT and without embedding compound. In addition, samples from other tissue (spleen, skin, liver and colon) were analyzed. Cryo-Gel embedded tissue showed good morphological preservation, no interference with immunohistochemical or immunofluorescent investigations and a good quality of extracted RNA and DNA was observed. Polymers in the OCT embedded samples disturbed the signal in the MS, which was not observed in the Cryo-Gel embedded samples. Although the chemical compounds of Cryo-Gel are confidential, we assume that Cryo-Gel does not contain polymers like those in OCT compound.

The polymers in OCT compound mainly suppress lower abundant signals which can only be observed using a mass spectrometer with high speed. In our study, protein analyses were obtained on an older type of mass spectrometer which is slower compared to the newest generation of mass spectrometers. This could be a potential explanation for the fact that no difference in the amount of identified proteins was observed, even while the polymer signal was clearly present in the acquired spectra. Based on the findings in the present study, it was concluded that Cryo-Gel is a preferable alternative for OCT compound for both diagnostic and research purposes of renal biopsies when MS is (possibly) required.

In **Chapter 3** the incidence of calcium oxalate (CaOx) deposition in the renal transplant biopsy within 3 months after transplantation as a cause of impaired graft function and its influence on graft survival was evaluated. CaOx deposition was observed in 26/149 biopsies (17%). Risk factors for CaOx deposition as described in literature are a high concentration of oxalic acid in the urine, damage to renal tubular cells, volume depletion and oliguria that leads to low tubular flow.[13, 14] After renal transplantation, a large amount of oxalate is excreted. When the urine becomes supersaturated with oxalate, CaOx crystals are formed which can deposit in the renal tubules and cause damage to the renal tubular cells.[15, 16]

In the present study, patients with CaOx deposition were significantly more often treated with dialysis before transplantation. This can be explained by the fact that the newly transplanted kidney is exposed to higher pre-transplant oxalic acid concentrations in patients dependent on dialysis compared to those with impaired

but functioning kidneys. Delayed graft function (DGF) was more common in patients with CaOx in their biopsies and the presence of CaOx was associated with a significantly lower estimated glomerular filtration rate at the time of biopsy. Also, graft survival was significantly worse in patients with CaOx deposition.

The exact relationship between CaOx deposition and DGF in the renal allograft is challenging. CaOx can cause direct injury to the tubular cells which may promote the pathogenesis of DGF in the post-transplantation period.[17, 18] However, it is also possible that injury to the tubular epithelial cells and low tubular flow as a result of DGF facilitate CaOx deposition. This all can lead to a vicious circle of damage to the renal allograft. Following this injury, impaired tubular repair can lead to tubulo-interstitial fibrosis resulting in loss of function of the kidney transplant.[19-21] Bagnasco *et al.* showed increased tubulo-interstitial scarring in biopsies with CaOx compared to those without in the analysis of repeating renal allograft biopsies.[22] Based on these findings, the systematic examination of all for-cause renal allograft biopsies by polarized light for CaOx deposition is strongly advised.

The relationship between plasma oxalic acid levels pre-transplantation and the risk for CaOx deposition was not evaluated in the present study, since plasma oxalic acid levels pre-transplantation were not available. However, it would be interesting to investigate this because it could identify those patients that may benefit from preventive treatment to reduce plasma oxalic acid levels pre- and post-renal transplantation. A low oxalate diet (40-50 mg/day) and/or intensive hemodialysis treatment in the direct pre- and post-transplant phase, to lower the serum oxalate acid levels as much as possible and thereby reducing the risk of CaOx deposition in the renal allograft, should be considered in these patients.[23]

The innate immune system has been shown to play an important role in the pathogenesis of renal transplant related injury. In **Chapter 4** the mRNA expression of TLRs, complement and apoptosis-related genes was examined in renal allograft biopsies from patients with acute rejection and paired pre-implantation biopsies. In the pre-implantation biopsies, the expression of the complement genes C2 and C3 and the BAX:BCL2 ratio was higher in deceased donor kidneys compared to living donor kidneys. This is most likely the result of extensive IRI in deceased donor kidneys which initiates the activation of the innate immune system.[24] High C2 and C3 expression levels and a high BAX:BCL2 ratio might serve as early warning for IRI, before the renal transplant function deteriorates. Interestingly, no difference in the expression of TRLs was observed between pre-implantation biopsies from living and

deceased donors. This could indicate that the TLR pathway is not as important as the complement pathway in the occurrence of IRI.

IRI is considered the main cause of DGF. Interestingly, all recipients who developed DGF had received a renal allograft from a deceased donor. While a high BAX:BCL2 ratio in pre-implantation biopsies has been associated with an increased risk of DGF by others, none of the markers investigated was predictive for DGF in the present study.[25]

Paired pre-implantation and acute rejection biopsies were available for 75 patients. TRL1-TLR3, TLR6-TLR10 and C2 showed higher expression levels in the acute rejection biopsies than in the pre-implantation biopsies, while the complement regulators CD46, CD55 and CD59 were slightly decreased during acute rejection. Additionally, we analyzed if the upregulation of TRLs during acute rejection could be ascribed to the infiltration of inflammatory cells in the renal biopsy. Therefore, the mRNA expression levels of CD163, CD68, CD20 and CD3e were evaluated. The TRLs each correlated with one or more inflammatory cell markers, except for TRL2, TLR3 and TLR5. Also, C2 and C3 expression levels and the BAX:BCL2 ratio significantly correlated with the expression of macrophage makers (CD68, CD163). These findings show that the altered gene expression of TRLs and complement factors during an acute rejection may at least partly be the result of infiltrating inflammatory cells. TLR2 and TLR3 expression levels were increased at the time of acute rejection but did not show a correlation with inflammatory markers. This suggests that TLR2 and TLR3 are dominantly expressed in the renal parenchyma itself, as has been described in a previous study.[26]

Relatively high TLR4 expression and a high BAX:BCL2 ratio during acute rejection were shown to be independent risk factors for adverse outcome after transplantation in patients with a deceased donor kidney. Furthermore, a donor age of >50 years was shown to be a significant independent risk factor for allograft loss. None of the investigated genes in the pre-implantation biopsies was associated with graft loss.

The findings presented in this study show that activation of the innate immune system occurs both at time of graft implantation and during acute rejection. Inhibition of complement pathways may act as a therapeutic target to protect the renal transplant from effects of IRI, especially in patients with a deceased donor renal allograft. Monitoring the TRL4 expression levels and BAX:BCL2 ratio during acute rejection may be of additional value in predicting future renal allograft outcome.

During antibody-mediated rejection, the interaction between B cell responses and the classical complement pathway activation is demonstrated by positive C4d staining in the peritubular capillaries (PTCs).[27] The significance of C4d staining in other structures of the renal allograft, like the glomeruli and arterioles, is not clear. In **Chapter 5** the importance of arteriolar C4d staining by immunohistochemistry (IHC) in patients with suspicious and diagnostic chronic active antibody-mediated rejection (c-aABMR) was analyzed. Arteriolar C4d staining was observed in 85% of the biopsies from patients with c-aABMR and was less common in the control groups (renal allograft biopsies without rejection and a group of native renal biopsies). It was excluded that arteriolar C4d staining is a form of nonspecific staining through performing additional staining with IgG IHC. Arteriolar C4d staining showed no significant association with C4d staining in the PTCs or C4d staining in the glomeruli. Also, a C4d staining score of ≥2 in the arterioles was independently associated with superior graft outcome in a multivariate Cox regression analysis.

In patients with c-aABMR, arteriolar C4d staining was significantly associated with the severity of arteriolar hyalinosis (ah). In cases with ah, arteriolar C4d staining was often observed at the site of hyalinosis. Subsequently, arteriolar C4d staining in the c-aABMR cases was further analyzed by subdividing the staining pattern into endothelial and mural staining, which might reflect two different processes. Endothelial arteriolar C4d staining is related to classical pathway or lectin pathway-associated C4 activation with deposition of C4d on the luminal surface of the endothelium.[27] Mural arteriolar C4d staining is more likely to be caused by leakage of luminally formed C4d into the arteriolar wall or seeping of plasma into the arteriolar wall due to increased vascular permeability with local C4d formation through the activation of either the classical or lectin complement pathway.[27] Mural C4d in the arterioles seems to accumulate at the sites of hyalinosis.

Due to the relatively small sample size, the findings in this pilot study do not allow for any definitive conclusions about the finding of C4d staining in arterioles in the setting of c-aABMR, but it is a useful starting point for further research. Larger studies are needed to examine in more detail if arteriolar C4d staining is truly related to antibody-mediated injury.

C3 glomerulopathy is a rare renal disease caused by excessive activation of the alternative complement pathway resulting in deposition of complement factor C3 in glomeruli.[28, 29] A renal biopsy is required to evaluate the presence of these

depositions and to confirm the diagnosis. C3-dominance by immunofluorescence (IF) is a defining feature in the diagnosis of C3 glomerulopathy. However, clear-cut cases with C3 glomerulopathy not fulfilling the consensus criteria have been observed.[30, 31] In **Chapter 6** the usefulness of C3d IHC in biopsies with C3 glomerulopathy as an ancillary diagnostic tool was evaluated. C3d IHC was analyzed in 14 biopsies with C3 glomerulopathy which all showed a C3d staining score of ≥2. In 4 biopsies, the diagnosis of C3 glomerulopathy according to the consensus criteria could not be made, as dominant C3c staining by IF was not observed. Interestingly, in 2 of these biopsies C3c IF was negative/sparse, while dominant staining with C3d by IHC (with a score of ≥2) was observed, thus confirming the diagnosis C3 glomerulopathy. In the remaining 2 biopsies, the diagnosis C3 glomerulopathy, according to the consensus criteria, could still not be made after the use of C3d IHC, since both C3d and C1q showed 2+ staining in both biopsies. So even after the use of C3d IHC we are left with cases that do not fulfill the consensus criteria for C3 glomerulopathy.

Deposition of C4 and its breakdown products (*e.g.* C4d) in the kidney result from activation of the classical and/or lectin pathway.[27] It has been suggested that C4d could be used to distinguish C3 glomerulopathy from immune complex membranoproliferative glomerulonephritis.[32] Sethi *et al.* described that negative glomerular staining for C4d can serve as a marker for C3 glomerulopathy.[32] However, this could not be confirmed in the present study as glomerular C4d staining by IHC was observed in 10 of 14 biopsies with C3 glomerulopathy (71%). In line with our findings, Bouatou *et al.* concluded that C4d staining is of limited value for the discrimination between C3 glomerulopathy and immune complex membranoproliferative glomerulonephritis.[33]

The presence of both ≥2+ staining for C3 (either C3c or C3d) and C4d IHC was observed in 64% of the biopsies, showing evidence of a complement-mediated glomerular disease driven by both the alternative and classical and/or lectin pathway. It has been hypothesized that in these cases the alternative complement pathway is upregulated in addition to activation of the classical or lectin pathway caused by infection, auto-immune disease or monoclonal gammopathy.[34] The possibility of an infection as a trigger for C3 glomerulopathy in some of the patients reported could not be completely excluded. The presence of kappa light chains as observed in monoclonal gammopathy can remain masked when performing IF on fresh frozen renal biopsies. Therefore, kappa staining was performed on formalin fixed paraffin embedded renal biopsies after protease digestion which effectively ruled out

monoclonal gammopathy-associated forms of glomerulonephritis in all C3 glomerulopathy cases.[35, 36]

This study shows that the current consensus criteria are not conclusive in a minority of the cases with C3 glomerulopathy. The use of C3d IHC in addition to C3c IF is recommended in all cases suspicious for C3 glomerulopathy, especially in those cases in which C3c IF is negative/sparse.

The results presented in this thesis show specific histological characteristics and immunohistochemical and molecular markers in renal (transplant) biopsies that could be helpful in diagnostics and are associated with renal transplant outcome. The identification of these features in kidney tissue help us to better understand the pathogenesis of kidney diseases and could lead to new diagnostic and prognostic markers and subsequent superior (tailored) therapeutic regimens.

References

1. Abecassis M, Bartlett ST, Collins AJ, et al. Kidney transplantation as primary therapy for end-stage renal disease: a National Kidney Foundation/Kidney Disease Outcomes Quality Initiative (NKF/KDOQITM) conference. *Clin J Am Soc Nephrol.* 2008;3(2):471-80.

2. Koo EH, Jang HR, Lee JE, et al. The impact of early and late acute rejection on graft survival in renal transplantation. *Kidney Res Clin Pract.* 2015;34(3):160-4.

3. Kaplan B, Srinivas TR, Meier-Kriesche HU. Factors associated with long-term renal allograft survival. *Ther Drug Monit.* 2002;24(1):36-9.

4. Meier-Kriesche HU, Schold JD, Srinivas TR, Kaplan B. Lack of improvement in renal allograft survival despite a marked decrease in acute rejection rates over the most recent era. *Am J Transplant.* 2004;4:378-383.

5. Coemans M, Süsal C, Döhler B, et al. Analyses of the short- and long-term graft survival after kidney transplantation in Europe between 1986 and 2015. *Kidney Int.* 2018;94(5):964-973.

6. Riegman PH, van Veen EB. Biobanking residual tissues. *Hum Genet.* 2011;130(3):357-68.

7. Zatloukal K, Hainaut P. Human tissue biobanks as instruments for drug discovery and development: impact on personalized medicine. *Biomark Med.* 2010;4(6):895-903.

8. Vrana M, Goodling A, Afkarian M, Prasad B. An Optimized Method for Protein extraction from OCT-embedded human kidney tissue for protein quantification by LC-MS/MS proteomics. *Drug Metab Dispos.* 2016;44(10):1692-6.

9. Schwartz SA, Reyzer ML, Caprioli RM. Direct tissue analysis using matrix-assisted laser desorption/ionization mass spectrometry: practical aspects of sample preparation. *J Mass Spectrom.* 2003;38;699–708.

10. Shah P, Zhang B, Choi C, et al. Tissue Proteomics Using Chemical Immobilization and Mass Spectrometry. *Anal Biochem.* 2015;469;27–33.

11. Weston LA, Hummon AB. Comparative LC-MS/MS analysis of optimal cutting temperature (OCT) compound removal for the study of mammalian proteomes. *Analyst.* 2013;138, 6380-4.

12. Palmer-Toy DE, Krastins B, Sarracino DA, Nadol JB Jr, Merchant SN. Efficient method for the proteomic analysis of fixed and embedded tissues. *J Proteome Res.* 2005;4;2404-11.

13. Coe FL, Parks JH, Asplin JR. The Pathogenesis and Treatment of Kidney Stone. *N Engl J Med.* 1992; 327:1141-1152.

14. Khan SR. Renal tubular damage/dysfunction: key to the formation of kidney stones. *Urol Res.* 2006;34(2):86-91.

15. Elgstoen KB, Johnsen LF, Woldseth B, Morkrid L, Hartmann A. Plasma oxalate following kidney transplantation in patients without primary hyperoxaluria. *Nephrol Dial Transplant.* 2010;25:2341–2345.

16. Hoppe B, Beck BB, Milliner DS. The primary hyperoxalurias. *Kidney Int* 2009;75:1264-1271.

17. Schepers MS, van Ballegooijen ES, Bangma CH, Verkoelen CF. Crystals cause acute necrotic cell death in renal proximal tubule cells, but not in collecting tubule cells. *Kidney Int.* 2005;68: 1543–1553.

18. Schepers MS, van Ballegooijen ES, Bangma CH, Verkoelen CF. Oxalate is toxic to renal tubular cells only at supraphysiologic concentrations. *Kidney Int.* 2005;68(4):1660-9.

19. Paul LC. Chronic allograft nephropathy—a model of impaired re-pair from injury. *Nephrol Dial Transplant.* 2000;15:149–151.

20. Racusen L, Solez K, Colvin R. Fibrosis and atrophy in renal allo-grafts: interim repost and new directions. *Am J Transplant* 2002;2:203–206.38. .

21. Joosten SA, Van Kooten C, Sijpkens YW, De Fijter JW, Paul LC. The pathobiology of chronic allograft nephropathy: immune-mediated damage and accelerated aging. *Kidney Int.* 2004;65:1556–1559.

22. Bagnasco SM, Mohammed BS, Mani H, et al. Oxalate deposits in biopsies from native and transplanted kidneys, and impact on graft function. *Nephrol Dial Transplant.* 2009;24(4):1319-25.

23. Roodnat JI, de Mik-van Egmond AME, Visser WJ, et al. Kidney Transplantation in Patients With Enteric (Secondary) Hyperoxaluria. *Transplant Direct.* 2017;3(12):e331.

24. Naesens M, Li L, Ying L, et al. Expression of complement components differs between kidney allografts from living and deceased donors. *J Am Soc Nephrol.* 2009;20(8):1839-51.

25. Goncalves-Primo A, Mourão TB, Andrade-Oliveira V, et al. Investigation of apoptosis-related gene expression levels in preimplantation biopsies as predictors of delayed kidney graft function. *Transplantation.* 2014;97(12):1260-5.

26. Dessing MC, Bemelman FJ, Claessen N, Ten Berge IJ, Florquin S, Leemans JC. Intragraft Toll-like receptor profiling in acute renal allograft rejection. *Nephrol Dial Transplant.* 2010;25(12):4087-92.

27. Murata K, Baldwin WM. Mechanisms of complement activation, C4d deposition, and their contribution to the pathogenesis of antibody-mediated rejection. *Transplant Rev (Orlando).* 2009;23(3):139-50.

28. Fakhouri F, Frémeaux-Bacchi V, Noël LH, Cook HT, Pickering MC. C3 glomerulopathy: a new classification. *Nat Rev Nephrol.* 2010;6:494-9.

29. Pickering MC, D'Agati VD, Nester CM, et al. C3 glomerulopathy: consensus report. *Kidney Int.* 2013;84:1079-89.

30. Sethi S, Quint PS, O'Seaghdha CM, et al. C4 Glomerulopathy: A Disease Entity Associated With C4d Deposition. *Am J Kidney Dis.* 2016;67:949-53.

31. Sethi S, Sullivan A, Smith RJ. C4 dense-deposit disease. *N Engl J Med.* 2014;370:784–6.

32. Sethi S, Nasr SH, De Vriese AS, Fervenza FC. C4d as a diagnostic tool in proliferative GN. *J Am Soc Nephrol.* 2015;26:2852-9.

33. Bouatou Y, Kers J, Chevalier-Florquin MSN, et al. Diagnostic accuracy of immunofluorescence versus immunoperoxidase staining to distinguish immune complex-

mediated glomerulonephritis and C3 dominant glomerulopathy. *Histopathology.* 2018;72:601-608.

34. Angioi A, Fervenza FC, Sethi S. et al. Diagnosis of complement alternative pathway disorders. *Kidney Int.* 2016;89:278-88.

35. Larsen CP, Boils CL, Cossey LN, Sharma SG, Walker PD. Clinicopathologic Features of Membranous-Like Glomerulopathy With Masked IgG Kappa Deposits. *Kidney Int Rep.* 2016;1:299–305.

36. Larsen CP, Ambruzs JM, Bonsib SM, et al. Membranous-like glomerulopathy with masked IgG kappa deposits. *Kidney Int.* 2014;86:154–161.

CHAPTER 8

Future Perspectives

Adapted from

Molecular analysis of renal allograft biopsies: where do we stand and where are we going?

Malou L. H. Snijders[1], Hilal Varol[1], Marieke van der Zwan[2], Jan U. Becker[3], Dennis A. Hesselink[2, 4], Carla C. Baan[2, 4], Jan H. von der Thüsen[1] & Marian C. Clahsen-van Groningen[2, 4]

1. Department of Pathology, Erasmus MC, University Medical Center Rotterdam, Rotterdam, The Netherlands.
2. Department of Internal Medicine, Division of Nephrology and Transplantation, Erasmus MC, University Medical   Center Rotterdam, Rotterdam, The Netherlands.
3. Institute of Pathology, University Hospital of Cologne, Cologne, Germany.
4. Rotterdam Transplant Group, Erasmus MC, University Medical Center Rotterdam, Rotterdam, The Netherlands.

A renal core biopsy for histological evaluation is the gold standard to investigate renal (transplant) biopsies.[1] However, histological interpretation of renal biopsies is subjective and differential diagnostic dilemmas remain a problem. Histology of rejection for example, can show a wide range of features and subjective interpretations of lesions may cause interobserver variation, despite the standardization of the histopathological features to diagnose rejection in the Banff Classification.[2, 3] Molecular analysis may provide more clarity in renal transplant biopsies in which histological features are difficult to classify. Several publications have stressed the importance of combining current histological diagnostic practice with molecular analysis in renal transplant biopsies.[4-7] The upregulation of specific molecular markers can improve diagnostics and predict renal transplant outcome more accurately than histological features. The Banff Foundation for Organ Transplantation is encouraging research to incorporate molecular analysis in the classification of kidney diseases.[8]

Over time, different molecular techniques have been used to identify genes involved in allograft rejection.[9] In recent years, molecular analysis using microarray expression analysis has garnered considerable interest. Advantages of these techniques are that small amounts of renal tissue are needed and the possibility to measure the expression of tens of thousands of genes simultaneously.[10] A suitable platform to perform microarray analysis is the novel nCounter analysis system from NanoString. With the use of NanoString methodology, mRNA target molecules can be measured directly and therefore no reverse transcription step is required, which is innovative compared to other microarray platforms.[11] It uses molecular barcodes in which up to 770 unique transcripts can be detected in one hybridization reaction. Only small amounts of RNA from formalin-fixed paraffin-embedded (FFPE) biopsies are needed (100 ng) and the analysis can be performed within two days, parallel and complementary to histology.[11]

1.   Molecular analysis in diagnosing acute TCMR

Acute T cell-mediated rejection (TCMR) is characterized by infiltration of effector T cells and macrophages in the renal transplant. In acute TCMR, donor human leucocyte antigens (HLA) expressed on antigen presenting cells (*e.g.* dendritic cells and macrophages) and donor cells activate effector T cells in secondary lymphoid tissues resulting in clonal expansion of these cells.[12] Activated effector T

cells migrate to the allograft, exit the microcirculation and enter the interstitium, where they trigger an inflammatory response with upregulation of interferon-gamma (IFNγ).[13] IFNγ plays an important role in the establishment of the typical phenotype of TCMR, because it induces expression of different genes in the kidney allograft, including chemokines such as CCL5, CXCL9, CXCL10, CXCL11 and major histocompatibility complex class I and II.[13] The transcripts which contribute to the profile for TCMR are mostly related to effector T cells (CTLA4, ICOS, BTLA, CD96, LAG3, SIRPG, LCP2, DUSP2, CD8A), macrophages (CD84, SLAMF8, ADAMDEC1), B cells (CD274, BTLA), and IFNγ related transcripts (ANKRD22, FCGR1B, SLAMF8).[4] Figure 1A shows a schematic picture of the histological features in acute TCMR and the involved genes.

Acute TCMR is histologically diagnosed by scoring interstitial inflammation, tubulitis and vasculitis.[14, 15] Renal transplant biopsies with histological inflammation and tubulitis below the thresholds for a diagnosis of acute TCMR are diagnosed as borderline rejection, which denotes possible TCMR. Only 30% of these patients will eventually develop an acute TCMR but solely based on histology it cannot be determined which patients will develop acute TCMR and therefore will benefit from treatment.[16-18] Molecular phenotyping may have the potential to reclassify borderline cases into TCMR and nonrejection, thereby eliminating the need for the category of borderline rejection.[19, 20]

The significance of isolated v-lesions, defined as intimal arteritis that occurs with minimal concurrent tubulointerstitial inflammation, is also problematic.[21] According to the Banff Classification, isolated v-lesions are to be classified as an acute TCMR vascular type (aTCMR2A) or are considered an activity marker for ABMR.[22-24] However, many biopsies classified as having acute TCMR by histology on the basis of v-lesions alone have no evidence of a molecular TCMR.[4, 25] Molecular profiling of transplant biopsies could therefore be of additional value in cases with an isolated v-lesion and guide in personalized treatment regimens.

Another obstacle is the diagnosis of TCMR in biopsies with BK virus nephropathy. The histology of BK virus nephropathy includes interstitial inflammation and tubulitis which can be confused with acute TCMR.[26] Furthermore, the reduction of immunosuppressive drugs after a diagnosis of BK virus nephropathy can trigger an acute TCMR.[27] Positive molecular TCMR scores in biopsies with BK virus nephropathy without a histological diagnosis of TCMR may provide evidence that some of these patients have concurrent TCMR.[28]

2.   Molecular analysis in diagnosing active ABMR

In active antibody-mediated rejection (ABMR), the activation of B cells and plasma cells result in the formation of donor specific antibodies (DSAs), which bind to the endothelium in the microcirculation. The pathogenesis of endothelial damage involves the direct action of DSAs and complement factors.[29] Also, the presence of NK cells in the glomerular or peritubular capillaries can mediate endothelial injury by triggering of CD16a Fc receptors.[30] The CD16a Fc receptors engage the Fc portions of DSAs on the endothelium which in turn activates the release of IFNγ and cytokines, causing an injury response in the endothelium.[30] These patterns of acute cellular injury can result in a relatively rapid decline in renal allograft function.

The gene expression profiles in ABMR display three molecular pathways: natural killer (NK) cell-associated transcripts (SH2D1B, GNLY, FGFBP2, CD160), endothelial cell-associated transcripts (DARC, ROBO4, CDH5, CDH13, COL13A1) and IFNγ-induced transcripts (phospholipase PLA1A and chemokine CXCL11).[30-33] Hidalgo *et al.* identified 23 transcripts associated with DSAs, the so called DSA-specific transcripts (DSASTs), which are primarily expressed in NK cells (CX3CR1, MYBL1, FGFBP2, KLRF1, SH2D1B, GNLY) and the endothelium (CDH13, CDH5, COL13A1, MALL, PLAT, ROBO4, SOX7, TEK, ICAM2).[30] Figure 1B shows a schematic picture of the histological features in active ABMR and the involved genes.

The histologic diagnosis of ABMR is problematic because its appearance is heterogeneous and has a remarkable dynamic range, from subtle with mild acute tubular necrosis, to fulminant with microvascular inflammation (MVI) and hemorrhage.[6] Furthermore, there is strong evidence that DSAs can induce histological and molecular features similar to that of ABMR in the absence of C4d deposition, which has led to the inclusion of C4d negative ABMR in the 2013 Banff Classification.[24] The evaluation of the expression of endothelial cell transcripts could serve as a marker for endothelial injury in C4d negative cases and might predict allograft loss better than C4d staining itself.[32-34] It has been proposed that ABMR could be diagnosed in the absence of C4d positivity if there are DSAs, microvascular inflammation or molecular findings such as endothelial cell-associated transcripts.[32] Likewise, the clinical significance of C4d positive biopsies without evidence of rejection is unknown.[35, 36] Molecular analysis in these biopsies has the potential to identify patients with a higher risk of developing ABMR.
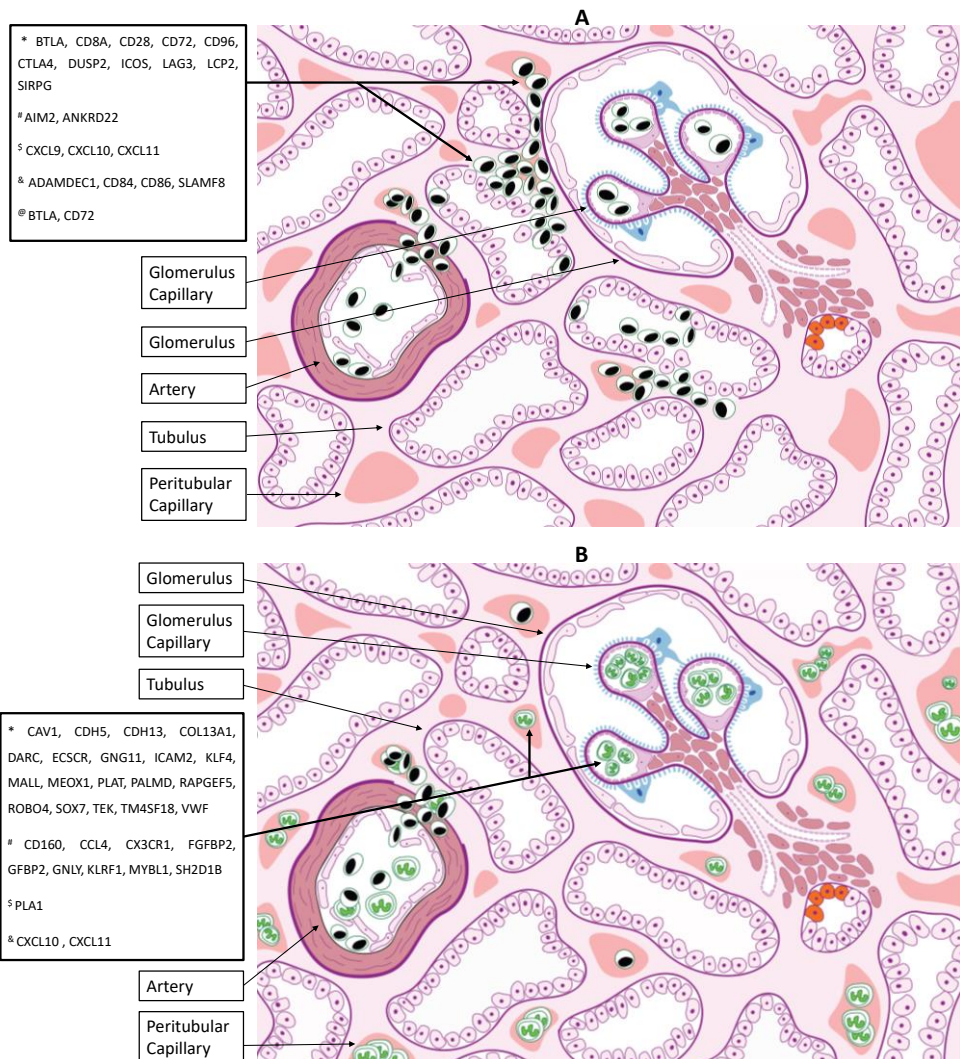
A

* BTLA, CD8A, CD28, CD72, CD96, CTLA4, DUSP2, ICOS, LAG3, LCP2, SIRPG

AIM2, ANKRD22

$ CXCL9, CXCL10, CXCL11

& ADAMDEC1, CD84, CD86, SLAMF8

@ BTLA, CD72

Glomerulus Capillary

Glomerulus

Artery

Tubulus

Peritubular Capillary

B

Glomerulus

Glomerulus Capillary

Tubulus

* CAV1, CDH5, CDH13, COL13A1, DARC, ECSCR, GNG11, ICAM2, KLF4, MALL, MEOX1, PLAT, PALMD, RAPGEF5, ROBO4, SOX7, TEK, TM4SF18, VWF

CD160, CCL4, CX3CR1, FGFBP2, GFBP2, GNLY, KLRF1, MYBL1, SH2D1B

$ PLA1

& CXCL10 , CXCL11

Artery

Peritubular Capillary

Figure 1. Schematic representations of the histological features of acute TCMR and active ABMR and the involved genes. A) Activated effector T cells* cross the capillary endothelium and enter the interstitium where they cause upregulation of IFNγ-associated transcripts# and chemokines$. Histology shows infiltration of the interstitium and tubules by T cells and macrophages&, dendritic cells and B cells@ which induce local injury through direct effects on the renal parenchyma, tubular epithelium and arteries. B) DSAs cause direct injury to the capillary endothelium resulting in upregulation of endothelial cell-associated transcripts*. DSAs can also cause indirect injury via complement activation and recruitment of NK-cells# with Fc receptors resulting in the upregulation of IFNγ-associated transcripts$ and cytokines&. This all induces microvascular inflammation (glomerulitis and peritubular capillaritis) including neutrophils and mononuclear cells.

The requirement of the detection of DSAs to diagnose ABMR is another debatable subject.[37-39] Evidence of ABMR in the absence of anti-HLA antibodies suggests the presence of non-anti–HLA antibodies.[40] Current standard DSA testing methods do not detect all antibodies that are potentially causing the injury as non-anti-HLA antibodies are not included in these tests. The expression of transcripts associated with DSAs may be useful in those cases with histological features of ABMR but without C4d positivity of PTCs and without detectable DSAs.

3.   Molecular markers predicting allograft outcome

Better insight in the early pathogenesis of chronic damage by evaluating gene expression in renal allograft biopsies performed in the first weeks or months after transplantation could offer a way to identify those patients who are at risk of future allograft loss. Microarray analysis on renal allograft biopsies is able to detect subtle levels of inflammation that are below the diagnostic threshold of histological diagnosis as defined by the current Banff Classification months before histologic lesions appear.[41] This allows for early interventions that slow the progression of kidney failure. The Paris Transplant Group has recently developed the integrative Box (iBox) system; a multidimensional prognostic score to predict transplant patients' individual risks of allograft loss. Allograft parameters including patient characteristics, transplant characteristics, renal allograft histology, treatment and prospective anti-HLA DSA measurements are integrated in this scoring system.[7, 42] Inclusion of molecular transcripts and novel predictive markers in this scoring system could be of added value in identifying those patients who are at risk of future allograft loss.

4.   Molecular classifier scores

Molecular classifiers could be helpful in diagnosing rejection in renal allograft biopsies. These classifiers are derived via machine learning algorithms evaluating those genes that distinguish rejection from other diagnoses. The Edmonton group has built an molecular classifier system for both TCMR and ABMR in which a score between 0 and 1 for each biopsy is used, reflecting the probability of the diagnosis of rejection in the tissue.[43] The TCMR score is based on 403 for-cause renal allograft biopsies diagnosed according to the Banff Classification by

three different pathologists and was considered positive for TCMR above a cut-off of 0.1.[4] High scores correspond with histological unanimity among the three pathologists. Discrepancies were primarily observed in those cases where histology resulted in diagnostic difficulties (*e.g.* histological borderline rejection, isolated v-lesions).

The Edmonton group also developed a molecular ABMR score that correlates with the presence of microvascular inflammation and DSAs.[6, 7] A score exceeding 0.2 was selected as positive for ABMR. Positive scores were compared with the conventional diagnosis of ABMR (histology plus serology) showing diagnostic agreement in 85% of the cases. High ABMR scores were associated with unanimity among pathologists and were observed in both C4d-positive and C4d-negative ABMR. In addition, the molecular score was shown to be an independent predictor of allograft survival.[6]

5.   Issues in molecular analysis of renal allograft biopsies

Discrepancies between molecular scores and conventional histological diagnosis are an area of investigation. The lack of a robust gold standard, caused by controversies in the histological diagnosis and poor reproducibility in the setting of rejection, is a major problem in the development and validation of a molecular classifier score. Machine learning classifiers are expected to be more accurate than single genes or unweighted gene sets. A disadvantage of the developed molecular classifier scores is that they are platform specific and therefore they cannot easily be used on other platforms. Furthermore, the developed molecular classifier scores have been performed on a relatively small number of patients (maximal a few hundreds of patients) and literature does not give clear transparency about the specific genes included in the molecular classifier scores for TCMR and ABMR. At the moment, it is not clear which genes discriminate the best between rejection and non-rejection and it remains a question how many genes should be included in the molecular test. The optimal molecular test is able the identify the type of rejection (TCMR or ABMR), but can also distinguish between other types of kidney injury.

It is also important to realize that the analysis of pure TCMR and pure ABMR represent extremes of a rejection continuum with different degrees of inflammation resulting in different gene expression levels. Furthermore, it is likely that many biopsies simply labeled as ABMR have concurrent TCMR.[44] Both the molecular ABMR and TCMR score are using arbitrary cut-offs, but the actual score seems more

accurately expressed as a continuum. For the use of molecular analysis in renal allograft diagnostics, it is important to be able to give an accurate assessment of where we are on the spectrum and to place cut-offs for those diagnostic categories that require treatment.

Molecular classifier scores and cut-offs for rejection (and treatment decisions) would ideally be based on large-scale multicenter studies. For the development of a multicentered validated classifier score it is important to 1) further define the molecular phenotypes of TCMR and of ABMR, 2) create a reliable machine learning classifier score, and 3) to use a freely accessible, affordable diagnostic platform.

The recently introduced Banff Human Organ Transplant Panel (B-HOT panel) is a panel of 770 genes in which genes known to be involved in transplant rejection, tissue damage and even genes for viruses are included. This gene panel has been created through a collaboration between NanoString and the Banff Foundation for Allograft Pathology. The B-HOT panel can be run on the widely available nCounter platform from NanoString. Through the use of this 770-gene panel and the development of a data sharing platform, the Banff community aims to validate the B-HOT panel on a multicenter level. This panel could give us the ability to optimize the molecular diagnostic classification of renal transplant biopsies.

6.   **Concluding remarks**

The use of molecular analysis can improve the diagnosis of rejection in renal allograft biopsies. Upregulation of specific transcripts might help to predict rejection even before the injury is visible by light microscopy, which can help nephrologists to determine which patients are at risk of rejection and predict possible future allograft loss. This is especially important since long-term immunosuppression is associated with severe side effects and knowing which patient should receive further therapy could specify treatment to the needs of the individual patient. Molecular profiling of kidney transplant biopsies has the potential to be more precise and more reproducible than traditional histological evaluation in the diagnostic setting. The combination of conventional approaches (histology, serology and clinical data) and molecular analysis will most likely offer the best diagnostic approach in the evaluation of renal transplant biopsies (Figure 2). Large-scale, multicenter validation using an affordable and reliable platform will be the next step to prove that molecular

diagnostics can be broadly implemented in the diagnostics of renal transplant biopsies. With this we are on our way to significantly improve not only diagnostics but also personalized therapeutic regimens and long-term transplant outcome.
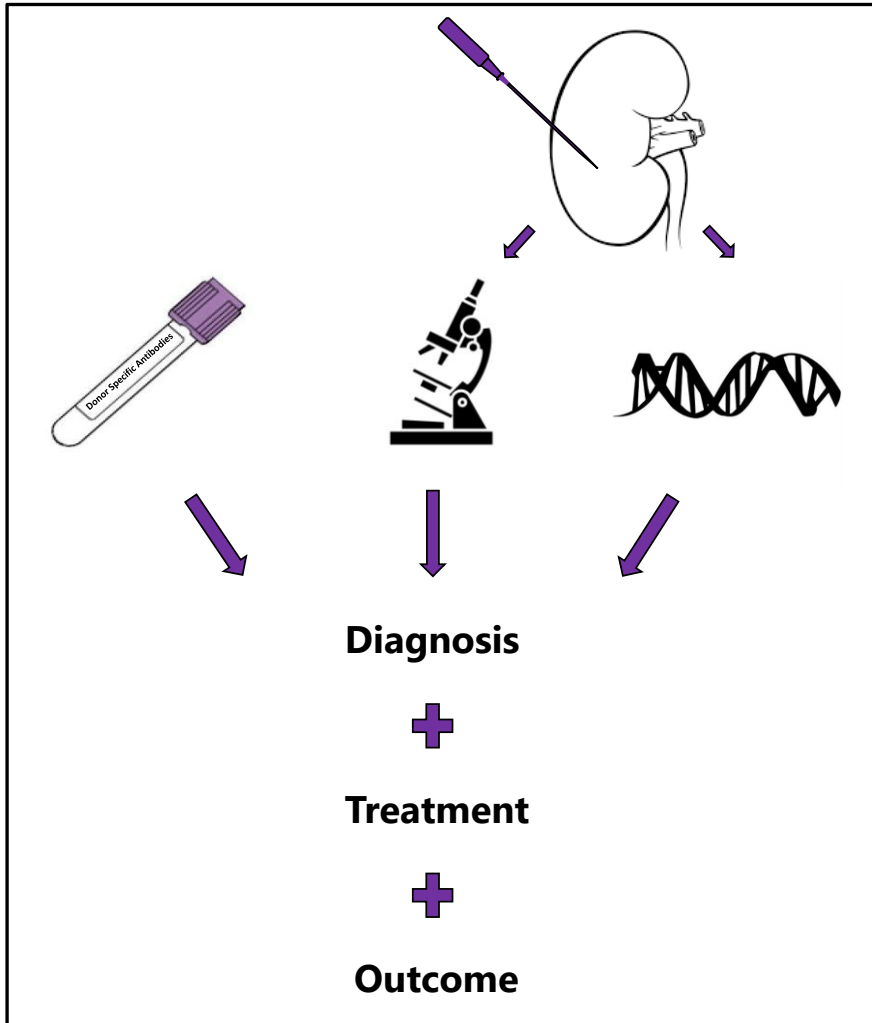

Figure 2. The combination of serology, histology and molecular evaluation offers new strategies in the handling and assessment of renal allograft biopsies and could improve diagnostics, treatment regimens and long-term transplant outcome.

References

1. Brachemi S, Bollée G. Renal biopsy practice: What is the gold standard? *World J Nephrol.* 2014;3(4):287–294.2.

2. Marcussen N, Olsen TS, Benediktsson H, Racusen L, Solez K. Reproducibility of the Banff classification of renal allograft pathology. Inter- and intraobserver variation. *Transplant.* 1995;60:1083–1089.

3. Furness PN, Taub N, Assmann KJ, et al. International variation in histologic grading is large, and persistent feedback does not improve reproducibility. *Am J Surg Pathol.* 2003;27;805–810.

4. Reeve J, Sellarés J, Mengel M, et al. Molecular diagnosis of T cell-mediated rejection in human kidney transplant biopsies. *Am J Transplant.* 2013;13(3):645–655.

5. Halloran PF, Pereira AB, Chang J, et al. Potential impact of microarray diagnosis of T cell-mediated rejection in kidney transplants: The INTERCOM study. *Am J Transplant.* 2013;13(9):2352–2363.

6. Sellarés J, Reev J, Loupy A, et al. Molecular diagnosis of antibody-mediated rejection in human kidney transplants. *Am J Transplant*. 2013;13(4):971–983.

7. Halloran PF, Pereira AB, Chang J, et al. Microarray diagnosis of antibody-mediated rejection in kidney transplant biopsies: an international prospective study (INTERCOM). *Am J Transplant*. 2013;13(11):2865–2874.

8. Haas M, Loupy A, Lefaucheur C, et al. The Banff 2017 Kidney Meeting Report: Revised diagnostic criteria for chronic active T cell-mediated rejection, antibody-mediated rejection, and prospects for integrative endpoints for next-generation clinical trials. *Am J Transplant*. 2018;18(2):293-307.

9. Henger A, Schmid H, Kretzler M. Gene expression analysis of human renal biopsies: recent developments towards molecular diagnosis of kidney disease. *Curr Opin Nephrol Hypertens.* 2004;13(3):313-8.

10. Menon MC, Keung KL, Murphy B, O'Connell PJ. The Use of Genomics and Pathway Analysis in Our Understanding and Prediction of Clinical Renal Transplant Injury. *Transplantation.* 2016;100(7):1405-14.

11. Geiss GK, Bumgarner RE, Birditt B, et al. Direct multiplexed measurement of gene expression with color-coded probe pairs. *Nat Biotechnol*. 2008;26(3):317-25.

12. Ingulli E. Mechanism of cellular rejection in transplantation. *Pediatr Nephrol.* 2010;25(1): 61–74.

13. Famulski KS, Einecke G, Reeve J, et al. Changes in the transcriptome in allograft rejection: IFN-c induced transcripts in mouse kidney allografts. *Am J Transplant.* 2006;6:1342–1354.

14. Katsuma A, Yamakawa T, Nakada Y, Yamamoto I, Yokoo T. Histopathological findings in transplanted kidneys. *Renal Replacement Therapy*. 2017;3:6.

15. Lusco MA, Fogo AB, Najafian B, Alpers CE. AJKD Atlas of Renal Pathology: Acute T-Cell-Mediated Rejection. *Am J Kidney Dis.* 2016;67(5):e29-30.

16. Dahan K, Audard V, Roudot-Thoraval F, et al. Renal allograft biopsies with borderline changes: Predictive factors of clinical outcome. *Am J Transplant.* 2006;6:1725–1730.

17. Seron D, Moreso F, Bover J, et al. Early protocol renal allograft biopsies and graft outcome. *Kidney Int.* 1997;51:310–316.

18. Mengel M, Chang J, Kayser D, et al. The molecular phenotype of six-week protocol biopsies from human renal allografts: Reflections of prior injury but not future course. *Am J Transplant.* 2011;11:708–718.

19. de Freitas DG, Sellarés J, Mengel M, et al. The nature of biopsies with "borderline rejection" and prospects for eliminating this category. *Am J Transplant.* 2012;12(1):191-201.

20. Desvaux D, Schwarzinger M, Pastural M, et al. Molecular diagnosis of renal-allograft rejection: correlation with histopathologic evaluation and antirejection-therapy resistance. *Transplantation.* 2004;78(5):647-53.

21. Rabant M, Boullenger F, Gnemmi V, et al. Isolated v-lesion in kidney transplant recipients: Characteristics, association with DSA, and histological follow-up. *Am J Transplant.* 2018;18(4):972-981.

22. Sis B, Bagnasco SM, Cornell LD, et al. Isolated endarteritis and kidney transplant survival: a multicenter collaborative study. *J Am Soc Nephrol.* 2015;26(5):1216-27.

23. Solez K, Colvin RB, Racusen LC, et al. Banff 07 classification of renal allograft pathology: updates and future directions. *Am J Transplant.* 2008;8(4):753-60.

24. Haas M, Sis B, Racusen LC, et al. Banff 2013 meeting report: inclusion of c4d-negative antibody-mediated rejection and antibody-associated arterial lesions. *Am J Transplant.* 2014;14(2):272-83.

25. Salazar ID, Merino López M, Chang J, Halloran PF. Reassessing the Significance of Intimal Arteritis in Kidney Transplant Biopsy Specimens. *J Am Soc Nephrol.* 2015;26(12):3190-8.

26. Ahuja M, Cohen EP, Dayer AM, et al. Polyoma virus infection after renal transplantation. Use of immunostaining as a guide to diagnosis. *Transplantation.* 2001;71(7):896-9.

27. Menter T, Mayr M, Schaub S, Mihatsch MJ, Hirsch HH, Hopfer H. Pathology of resolving polyomavirus-associated nephropathy. *Am J Transplant.* 2013;13(6):1474-83.

28. Halloran PF, Reeve JP, Pereira AB, Hidalgo LG, Famulski KS. Antibody-mediated rejection, T cell-mediated rejection, and the injury-repair response: new insights from the Genome Canada studies of kidney transplant biopsies. *Kidney Int.* 2014;85(2):258-64.

29. Djamali A, Kaufman DB, Ellis TM, Zhong W, Matas A, Samaniego M. Diagnosis and management of antibody-mediated rejection: current status and novel approaches. *Am J Transplant.* 2014;14(2):255-71.

30. Hidalgo LG, Sellares J, Sis B, Mengel M, Chang J, Halloran PF. Interpreting NK cell transcripts versus T cell transcripts in renal transplant biopsies. *Am J Transplant.* 2012;12:1180–1191.

31. Hidalgo LG, Sis B, Sellares J, et al. NK cell transcripts and NK cells in kidney biopsies from patients with donor-specific antibodies: Evidence for NK cell involvement in antibody-mediated rejection. *Am J Transplant.* 2010;10:1812–1822.

32. Sis B, Jhangri G, Bunnag S, Allanach K, Kaplan B, Halloran PF. Endothelial gene expression in kidney transplants with alloantibody indicates antibody-mediated damage despite lack of C4d staining. *Am J Transplant*. 2009;9:2312–2323.

33. Reeve J, Einecke G, Mengel M, et al. Diagnosing rejection in renal transplants: A comparison of molecular- and histopathology-based approaches. *Am J Transplant*. 2009;9:1802–1810.

34. Sis B, Halloran PF. Endothelial transcripts uncover a previously unknown phenotype: C4d-negative antibody-mediated rejection. *Curr Opin Organ Transplant*. 2010;15:42–8.

35. Dominy KM, Willicombe M, Al Johani T, et al. Molecular Assessment of C4d-Positive Renal Transplant Biopsies Without Evidence of Rejection. *Kidney Int Rep*. 2018;4(1):148-158.

36. Kikić Ž, Kainz A, Kozakowski N, et al. Capillary C4d and Kidney Allograft Outcome in Relation to Morphologic Lesions Suggestive of Antibody-Mediated Rejection. *Clin J Am Soc Nephrol*. 2015;10(8):1435-43.

37. Senev A, Coemans M, Lerut E, et al. Histological picture of antibody-mediated rejection without donor-specific anti-HLA antibodies: Clinical presentation and implications for outcome. *Am J Transplant*. 2019;19(3):763-780.

38. Sablik KA, Clahsen-van Groningen MC, Looman CWN, et al. Chronic-active antibody-mediated rejection with or without donor-specific antibodies has similar histomorphology and clinical outcome - a retrospective study. *Transpl Int*. 2018;31(8):900-908.

39. Halloran PF, Merino Lopez M, Barreto Pereira A. Identifying subphenotypes of antibody-mediated rejection in kidney transplants. *Am J Transplant*. 2016;16(3):908-20.

40. Cardinal H, Dieudé M, Hébert MJ. The Emerging Importance of Non-HLA Autoantibodies in Kidney Transplant Complications. *J Am Soc Nephrol*. 2017;28(2):400-406.

41. Naesens M, Khatri P, Li L, et al. Progressive histological damage in renal allografts is associated with expression of innate and adaptive immunity genes. *Kidney Int*. 2011;80:1364–1376.

42. Loupy A, Aubert O, Orandi B, et al. A Multidimensional Prognostic Score and Nomogram to Predict Kidney Transplant Survival: The Integrative Box (iBox) System. *Am J Transplant*. 2017;17:342-342.

43. Viglietti D, Loupy A, Aubert O, et al. Dynamic Prognostic Score to Predict Kidney Allograft Survival in Patients with Antibody-Mediated Rejection. *J Am Soc Nephrol*. 2018;29(2):606-619.

44. Liu P, Tseng G, Wang Z, Huang Y, Randhawa P. Diagnosis of T-cell-mediated kidney rejection in formalin-fixed, paraffin-embedded tissues using RNA-Seq-based machine learning algorithms. *Hum Pathol*. 2019;84:283-290.

CHAPTER 9

Nederlandse Samenvatting

De belangrijkste functie van de nieren is het verwijderen van afvalstoffen uit het lichaam door uitscheiding via de urine. Daarnaast zorgen de nieren voor het op peil houden van de water-zoutbalans in het bloed. Door schade aan de nieren kan de nierfunctie achteruit gaan, met als gevolg dat afvalstoffen zich in het lichaam ophopen en de water-zoutbalans verstoord raakt. In het laatste stadium van chronische nierschade is er sprake van eindstadium nierfalen en is behandeling met dialyse of transplantatie noodzakelijk om in leven te blijven. Bij het verrichten van een niertransplantatie wordt een gezonde nier van iemand anders in de patiënt met slecht werkende nieren geïmplanteerd. Het probleem hierbij is dat het niertransplantaat door de ontvanger als lichaamsvreemd wordt gezien, waardoor het afweersysteem wordt geactiveerd en de nieuwe nier wordt afgestoten. Om dit te voorkomen moet het afweersysteem van de ontvanger onderdrukt worden met afweer onderdrukkende medicatie, genaamd immunosuppressiva.

Door de ontwikkeling van steeds betere immunosuppressiva is de kans op afstoting de afgelopen jaren sterk gedaald. Echter, zowel acute als chronische afstoting blijven een veel voorkomend probleem en leiden tot schade aan het niertransplantaat. Circa 50% van de niertransplantaten faalt binnen 10 jaar na de transplantatie. Een beter begrip van de verschillende factoren die geassocieerd zijn met transplantaatfalen - op zowel korte als lange termijn - is essentieel om effectieve behandelingen te ontwikkelen die de achteruitgang van de niertransplantaatfunctie kunnen vertragen of voorkomen. Het verrichten van een nierbiopt wordt beschouwd als de gouden standaard om de achteruitgang van de nierfunctie te analyseren en is tevens een belangrijk hulpmiddel bij het onderzoeken van mogelijke risicofactoren voor transplantaatfalen. Het doel van dit proefschrift is om potentieel belangrijke kenmerken in niertransplantaatbiopten te identificeren en de associatie met het risico op transplantaatfalen te evalueren.

1.   Cryo-Gel voor vriezen van nierbiopten

Nierbiopten kunnen zowel op microscopisch niveau (histologie, immunohistochemie) als op eiwit niveau en moleculair niveau worden onderzocht op specifieke kenmerken die een rol spelen bij het risico op (toekomstig) transplantaatfalen. Voor zowel diagnostiek als toekomstige onderzoeksdoeleinden is het van belang dat het nierweefsel wordt opgeslagen op een manier die de weefselconservering maximaliseert. Voor het vriezen van het nierweefsel wordt

meestal optimal cutting temperature (OCT) compound als inbedmedium gebruikt. Echter, het verrichten van eiwitanalyse middels massaspectometrie is lastig bij weefsels die ingebed zijn in OCT. Dit komt doordat OCT polymeren bevat die de massaspectometrie uitslagen kunnen vertroebelen. In **Hoofdstuk 2** werd het nieuwe inbedmedium Cryo-Gel voor het vriezen van nierbiopten onderzocht. Er werd aangetoond dat Cryo-Gel geschikt is als inbedmedium. Bij het verrichten van massaspectometrie werd een goed signaal waargenomen, zonder vertroebeling door polymeren, zoals gezien wordt bij OCT. Op basis van deze bevindingen kan worden geconcludeerd dat het inbedmedium Cryo-Gel de voorkeur heeft boven OCT voor het vriezen van nierbiopten, met name wanneer massaspectometrie (mogelijk) verricht zal worden.

2.   Calcium oxalaat deposities

Vrij recent werd gesuggereerd dat de histologische aanwezigheid van calciumoxalaat (CaOx) een mogelijke oorzaak is van de achteruitgang in de nierfunctie in de vroege post-transplantatieperiode. Oxaalzuur is het eindproduct van verschillende metabole routes en wordt voornamelijk uitgescheiden via de nieren. Wanneer de nierfunctie daalt, zal minder oxaalzuur via de urine worden uitgescheiden met als gevolg dat de plasmaconcentratie van oxaalzuur stijgt. Dit is de reden dat hoge plasma oxaalzuurconcentraties worden waargenomen bij patiënten met eindstadium nierfalen. Behandeling met dialyse is niet voldoende om deze hoge oxaalzuurconcentraties te doen dalen. Na niertransplantatie zal een grote hoeveelheid oxaalzuur worden uitgescheiden door de 'nieuwe' nier. De urine zal hierdoor verzadigd raken met oxaalzuur, waardoor dit neerslaat in de vorm van calciumoxalaat (CaOx) kristallen die zich kunnen ophopen in de niertubuli en hieraan schade kunnen veroorzaken.

In **Hoofdstuk 3** werden CaOx deposities aangetoond in 17% van de niertransplantatiebiopten afgenomen binnen 3 maanden na transplantatie. Patiënten met CaOx deposities in hun nierbiopt werden significant vaker behandeld met dialyse voor transplantatie. Dit kan worden verklaard door het feit dat hogere plasma oxaalzuurconcentraties worden gezien bij dialyse patiënten dan bij patiënten met een verminderde nierfunctie waarbij dialyse nog niet noodzakelijk is. Bij deze laatste groep patiënten zal de resterende nierfunctie ervoor zorgen dat een deel van het oxaalzuur via de nieren wordt uitgescheiden.

Een verminderde nierfunctie in de vroege post-transplantatieperiode kwam vaker voor bij patiënten met CaOx deposities in hun nierbiopt. Bovendien werd gezien dat de overleving van het transplantaat significant slechter is bij patiënten met CaOx deposities in hun nierbiopt. De exacte relatie tussen CaOx deposities en verminderde nierfunctie in de vroege post-transplantatieperiode blijft lastig te achterhalen. CaOx deposities kunnen directe schade aan de niertubuli veroorzaken, waardoor de nierfunctie achteruit gaat. Het is echter ook mogelijk dat reeds ontstane schade aan de niertubuli ten tijde van de verminderde nierfunctie het neerslaan van CaOx deposities vergemakkelijkt. Dit alles kan leiden tot een vicieuze cirkel van schade aan het niertransplantaat met uiteindelijk functieverlies van het transplantaat. Op basis van deze bevindingen is het systematisch beoordelen van nierbiopten op de aanwezigheid van CaOx deposities sterk geadviseerd.

3.   Genexpressie levels van het aangeboren immuunsysteem

Het aangeboren immuunsysteem - waaronder 'toll-like' receptoren, complement en apoptose gerelateerde genen - speelt een belangrijke rol bij het ontstaan van schade in niertransplantaties. In **Hoofdstuk 4** werd de mRNA expressie van deze genen onderzocht in nierbiopten die net voor transplantatie en op het moment van acute afstoting genomen zijn. In de nierbiopten afgenomen net voor transplantatie, was de mRNA expressie van de complement factoren C2 en C3 en de apoptose (geprogrammeerde celdood) gerelateerde BAX:BCL2 ratio hoger in biopten van postmortale donornieren dan in biopten van levende donornieren. Activatie van het aangeboren immuunsysteem kan onder andere ontstaan door ischemische-reperfusie schade, wat vaak wordt gezien in postmortale donornieren. Het onderdrukken van complement en apoptose gerelateerde genen zou bescherming kunnen bieden tegen ischemische-reperfusie schade, met name in niertransplantaties afkomstig van postmortale donoren.

Gedurende acute afstoting speelt activatie van het aangeboren immuunsysteem een belangrijke rol. De meeste 'toll-like' receptoren en complement factor C2 toonden hogere expressie levels in de nierbiopten met acute afstoting dan in de nierbiopten afgenomen net voor transplantatie. Deze verhoogde expressie bleek grotendeels gerelateerd aan influx van ontstekingscellen in het niertransplantaat. Bovendien werd gezien dat relatief hoge 'toll-like' receptor 4 expressie levels en een hoge BAX:BCL2 ratio tijdens acute afstoting onafhankelijke

risicofactoren zijn voor transplantaatfalen in de groep patiënten met een postmortale donornier.

De bevindingen gepresenteerd in deze studie tonen aan dat activering van het aangeboren immuunsysteem zowel vlak voor transplantatie als tijdens een acute rejectie plaatsvindt. Het onderdrukken van complement en apoptose gerelateerde markers kan als therapeutisch doelwit fungeren om het niertransplantaat te beschermen tegen de effecten van ischemische-reperfursie schade. Bovendien kan monitoren van de 'toll-like' receptor 4 expressie en BAX:BCL2 ratio tijdens acute afstoting van prognostische waarde zijn bij het voorspellen van transplantaatuitkomst.

4.   Arteriolaire C4d in antilichaam gemedieerde afstoting

C4d aankleuring in het endotheel van de peritubulaire capillairen is een belangrijk kenmerk van antilichaam gemedieerde afstoting. De betekenis van C4d aankleuring in andere structuren van de nier, zoals de glomeruli en arteriolen, bij patiënten met antilichaam gemedieerde afstoting is niet duidelijk. In **Hoofdstuk 5** werd de significantie van C4d aankleuring in de arteriolen bij patiënten met chronisch actieve antilichaam gemedieerde afstoting onderzocht. Arteriolaire C4d aankleuring was aanwezig in 85% van de nierbiopten met chronisch actieve antilichaam gemedieerde afstoting en werd significant minder vaak gezien in de controlegroepen (niertransplantaten zonder antilichaam gemedieerde afstoting en een groep van natieve nierbiopten). Bovendien werd gezien dat sterke (score ≥2) arteriolaire C4d aankleuring onafhankelijk geassocieerd is met betere transplantaatoverleving in een multivariate Cox-regressie analyse.

Arteriolaire C4d aankleuring was geassocieerd de ernst van arteriolaire hyalinose. In casus met arteriolaire hyalinose werd de arteriolaire C4d aankleuring vaak waargenomen op de plaats van de hyalinose. Deze casus werden verder geanalyseerd door het aankleuringspatroon van C4d onder te verdelen in endotheliale en murale aankleuring. Deze verschillende aankleuringspatronen zouden op verschillende processen kunnen duiden; endotheliale aankleuring van C4d in de arteriolen is gerelateerd aan complement activatie met afzetting van C4d aan de luminale zijde van het endotheel. Murale aankleuring van C4d wordt daarentegen waarschijnlijk veroorzaakt door lekkage van de luminaal afgezette C4d in de wand van de arteriolen of door het lekken van plasma in de wand van de

arteriolen als gevolg van verhoogde permeabiliteit van het endotheel met lokale C4d afzetting ter plaatse.

Deze pilot studie geeft de eerste inzichten in arteriolaire C4d aankleuring in chronisch actieve antilichaam gemedieerde afstoting. Echter, de vraag of arteriolaire C4d aankleuring echt specifiek is voor chronisch actieve antilichaam gemedieerde schade blijft bestaan en maakt het de moeite waard om dit verder te onderzoeken in een groter patiënten cohort.

5.   C3d immunohistochemie in C3 glomerulopathie

C3 glomerulopathie is een zeldzame nierziekte die wordt veroorzaakt door overmatige activering van de alternatieve route van het complementsysteem. Dit resulteert in de depositie van complement factor C3 in de glomeruli van de nieren. Volgens de consensus criteria is een nierbiopt noodzakelijk om de aanwezigheid van deze C3 deposities aan te tonen; dominante aankleuring met C3c immunofluorescentie ten opzichte van de andere kleuringen (IgA, IgG, IgM en C1q) wordt namelijk beschouwd als karakteristiek kenmerk voor de diagnose C3 glomerulopathie. Echter, in een aantal evidente gevallen van C3 glomerulopathie kan niet aan de consensus criteria worden voldaan. Hierdoor ontstaat de vraag of de huidige consensus criteria toereikend zijn en of andere markers wellicht van toegevoegde waarde kunnen zijn.

In **Hoofdstuk 6** werd de meerwaarde van C3d immunohistochemie in biopten met C3 glomerulopathie geëvalueerd. In totaal werden 14 nierbiopten met C3 glomerulopathie onderzocht, welke allemaal matige tot sterke aankleuring met C3d toonden. In 4 van de biopten kon de diagnose C3 glomerulopathie – volgens de consensus criteria - niet worden gesteld, doordat geen dominante aankleuring met C3c bij immunofluorescentie werd gezien. In 2 van deze biopten was C3c aankleuring nihil/negatief, terwijl met C3d immunohistochemie sterke en dominante aankleuring werd gezien, waardoor de diagnose alsnog bevestigd werd. In de 2 overgebleven biopten toonden zowel C3d als C3c matige aankleuring. Dit betrof echter geen dominante aankleuring, aangezien ook C1q matige aankleuring liet zien en hierdoor kon de diagnose C3 glomerulopathie niet worden gesteld.

Concluderend kan gesteld worden dat C3d immunohistochemie van toegevoegde waarde is bij het diagnosticeren van C3 glomerulopathie, vooral in de gevallen waar geen of geringe aankleuring wordt gezien met C3c. Echter, ook na het

gebruik van C3d immunohistochemie is er een klein percentage waarbij de consensus criteria voor het stellen van de diagnose C3 glomerulopathie niet toereikend zijn.

De resultaten gepresenteerd in dit proefschrift tonen histologische, immunohistochemische en moleculaire kenmerken in nier(transplantaat)biopten die van toegevoegde waarde kunnen zijn binnen de diagnostiek en geassocieerd zijn met de uitkomst van niertransplantaties. Het identificeren van deze markers helpt ons de pathogenese van nierziekten beter te begrijpen en kan tot nieuwe diagnostische en prognostische markers leiden en uiteindelijk de ontwikkeling van op maat gemaakte therapeutische behandelingen bevorderen.

Appendices

Curriculum Vitae
List of publications
PhD portfolio
Acknowledgements (Dankwoord)

Curriculum Vitae

Malou Snijders werd geboren op 30 september 1989 te 's-Gravenhage. In 2008 behaalde zij haar gymnasium diploma aan College het Loo in Voorburg. In hetzelfde jaar startte zij met haar studie Geneeskunde aan het Leids Universitair Medisch Centrum (LUMC). Zij volgde haar wetenschapsstage en oudste coschap op de afdeling radiotherapie en haar keuzecoschap op de afdeling oncologie in het HMC Westeinde. Na het afronden van haar studie startte zij in april 2015 met de opleiding tot patholoog in het Erasmus MC te Rotterdam. In november 2016 begon zij naast haar specialisatie tot patholoog met een promotieonderzoek binnen de nefropathologie onder supervisie van dr. M.C. Clahsen-van Groningen en dr. D.A. Hesselink. Sinds 1 januari 2020 is zij werkzaam in het Amsterdam UMC, locatie AMC, als fellow patholoog met als deelspecialisaties de gynaecopathologie, mammapathologie en cytologie.

List of publications

Snijders MLH, Varol H, van der Zwan M, Becker JU, Hesselink DA, Baan CC, von der Thüsen JH and Clahsen-van Groningen MC. Molecular analysis of renal allograft biopsies: where do we stand and where are we going? *Transplantation. 2019 doi: 10.1097/TP.0000000000003220.*

Snijders MLH, Sablik KA, Hesselink DA, Betjes MGH, Batal I and Clahsen-van Groningen MC. Clinical relevance of arteriolar C4d staining in patients with chronic-active antibody-mediated rejection: A pilot study. *Transplantation. 2020;104(5):1085-1094.*

Snijders MLH, van de Wall-Neecke BJ, Hesselink DA, Becker JU and Clahsen-van Groningen MC. Utility of immunohistochemistry with C3d in C3 glomerulopathy. *Mod Pathol. 2020;33(3):431-439.*

Snijders MLH, Zajec M, Walter LAJ, de Louw RMAA, Oomen MHA, Arshad S, van den Bosch TPP, Dekker LJM, Doukas M, Luider TM, Riegman PHJ, van Kemenade FJ and Clahsen-van Groningen MC. Cryo-Gel embedding compound for renal biopsy biobanking. *Sci Rep. 2019;9(1):15250.*

Snijders MLH, Hesselink DA, Clahsen-van Groningen MC, Roodnat JI. Oxalate deposition in renal allograft biopsies within 3 months after transplantation is associated with allograft dysfunction. *PLoS One. 2019;14(4):e0214940.*

Yang J, **Snijders MLH**, Haasnoot GW, van Kooten C, Mallat M, de Fijter JW, Clahsen-van Groningen MC, Claas FHJ, Eikmans M. Elevated intragraft expression of innate immunity and cell deathrelated markers is a risk factor for adverse graft outcome. *Transpl Immunol. 2018;48:39-46.*

Struikmans H, **Snijders M**, Mast ME, Fisscher U, Franssen JH, Immink MJ, Marinelli A, Merkus J, Petoukhova A, Speijer G, Koper P. Single dose IOERT versus whole breast irradiation: Cosmetic results in breast-conserving therapy. *Strahlenther Onkol. 2016 Oct;192(10):705-13.*

PhD Portfolio

Name PhD student: M.L.H. Snijders
Department: Pathology
Research School: Molecular Medicine
PhD period: November 2016 – March 2020
Promotor: Prof. dr. F. J. van Kemenade
Co-promotors: Dr. M. C. Clahsen-van Groningen
                      and Dr. D. A. Hesselink

Title	Year	Workload (ECTS)
General courses		
Basis Introduction course on SPSS	2018	1.0
GraphPad Prism Version 6	2018	1.0
BROK course	2018	1.5
Integrity course	2018	0.3
Survival analyses course	2018	0.5
Microscopic Image Analysis: From Theory to Practice	2018	0.8
Workshops and seminars		
BOP cursus moleculaire pathologie	2016	1.0
BOP cursus pathofysiologie	2016	1.0
BOP cursus immunologie en ontsteking	2016	1.0
BOP cursus oncologie	2016	1.0
DOO Medische ethiek	2017	0.3
DOO Ziekenhuismanagement	2017	0.6
DOO Teach the Teacher II	2018	0.3
DOO Inspirerend Leiderschap	2018	0.3
Stralingscursus 5B	2018	1.5
Winterschool, Driebergen	2018	1.5
Veldhuizen cursus FNA hals, Amsterdam	2018	0.3
Nanostring seminar, Amsterdam	2019	0.3
Workshop Talentwaarderend opleiden	2019	0.3
Diagnostic Histopathology of Breast Disease Course	2019	2.5

The Columbia Renal Biopsy Course, New York	2019	1.5
Nepropathology educational meeting, Rotterdam	2019	1.0

Presentations

Oral presentation Bootcongres, NTV, Zeist	2017	1.0
Poster presentation Banff Meeting, Barcelona	2017	0.5
Oral presentation European Society for Organ Transplantation (ESOT), Barcelona	2017	1.0

(Inter)national conferences

Pathologendagen, Zeist	2016	0.6
Bootcongres NTV, Zeist	2017	0.6
Banff Meeting, Barcelona	2017	1.0
Bootcongres NTV, Rotterdam	2018	0.6

Internships

Short fellowship nephropathology, Cologne	2018	3.0

Teaching

Supervision vaardighedenonderwijs pathologie	2016-2019	4.0
Supervision of two medical students	2018	2.0

Acknowledgement (Dankwoord)